Generalized Schrieffer-Wolff Theory: An Effective Liouvillian Approach to Superconducting Qubit Readout

Auteur : Massoz, Fanny
Promoteur(s) : Damanet, François
Faculté : Faculté des Sciences
Diplôme : Master en sciences physiques, à finalité approfondie
Année académique : 2025-2026
URI/URL : http://hdl.handle.net/2268.2/25607

FACULTY OF SCIENCE
DEPARTMENT OF PHYSICS

Generalized Schrieffer-Wolff Theory: An Effective Liouvillian Approach to Superconducting Qubit Readout

Author: Fanny MASSOZ

Supervisor: François DAMANET

Master's thesis submitted in the partial fulfillment of the requirements for the Master's degree in Physical Science.

Academic year 2025-2026

This page intentionally left blank.

Acknowledgments

This work is the result of far more than individual effort, and I wish to express my profound gratitude to all those who, in one way or another, contributed to its completion.

I would like to begin by expressing my deepest gratitude to my supervisor, Dr. François Damanet, for his invaluable guidance. Over the course of the year, our many exchanges proved to be a constant source of direction, whether through his insightful technical advice or more personal reflections. I have no doubt that the lessons drawn from these conversations will continue to be valuable to me well beyond the scope of this thesis, accompanying me throughout my academic and professional journey.

Additionally, I am grateful to Théo Lejeune, whose thoughtful discussions proved instrumental in the progress of this work. His sharp advice throughout the development of this project was greatly appreciated, and I am particularly grateful for the remarkable care and dedication he brought to the proofreading of this thesis.

My gratitude also goes to the members of the reading committee, Prof. T. Bastin, Prof. A. Silhanek, and Prof. G. Lumay, who kindly accepted to review and assess this thesis.

On a more personal note, I wish to thank my family and friends, whose constant presence and support throughout the course of my studies have been an immeasurable source of strength.

Last but not least, I wish to thank Thibault, whose patience and unwavering encouragement have been a constant source of comfort throughout this work.

Contents

Introduction

Over the past decades, as certain computational problems remain out of reach for even the most powerful classical computers, quantum computing has emerged as a promising alternative that exploits quantum mechanical effects to process information. Indeed, it offers the prospect of accelerating a wide range of computational tasks and improving their efficiency [1]. Among the various platforms proposed for the physical realization of quantum bits, *superconducting qubits* have emerged as one of the leading candidates, owing to their relatively accessible fabrication techniques and the significant progress achieved in recent years [2]. The measurement of superconducting qubits is commonly performed within the framework of circuit quantum electrodynamics (cQED), where ongoing experimental and theoretical efforts aim to enhance both the fidelity and the speed of qubit readout [3]. This thesis focuses on *dispersive readout*, in which the qubit is coupled to a *resonator* or *cavity*, whose dissipation into a transmission line allows, within a given parameter regime, for the probing of the qubit state without destroying it, thereby realizing a so-called *quantum non-demolition* (QND) measurement. More specifically, mathematical tools for analyzing such systems are presented.

The dispersive readout of superconducting qubits is generally modeled by applying a unitary *Schrieffer-Wolff transformation* to the qubit-cavity Hamiltonian. This transformation corresponds to a form of perturbation theory that yields an effective Hamiltonian describing the system dynamics. Dissipation is then accounted for by deriving a *master equation* for the qubit [4, 5], that is, an equation of motion for the qubit that incorporates the effects of its environment, obtained from a second-order perturbative treatment. This approach becomes heavy and technically challenging when attempting to go beyond second-order perturbative corrections as shown for example by Roberta Palacino in the context of dissipative phase transitions [6]. Yet further order perturbation terms are crucial in an attempt to accurately describe the so-called non-*Markovian* effects, i.e., environment back-action on the system dynamics induced by the finite memory of the environment, which are significant in superconducting circuits. The core motivation of this thesis is to develop a more fundamental and systematic framework to include dissipation more accurately when modeling these systems.

This work adapts and applies a generalization of the Schrieffer-Wolff transformation to dissipative systems, originally developed by E.M. Kessler [7]. Unlike the standard method, this generalized transformation is applied directly onto the *Liouvillian* superoperator $\mathcal{L}$ entering the master equation governing the dynamics of the *density operator*, which describes the state of the system. This allows for a systematic, order-by-order expansion of the Liouvillian itself, incorporating the dissipative evolution directly into the perturbative treatment and making higher-order corrections considerably more straightforward to implement than in standard perturbation theory.

This thesis is organized as follows. Chapter 1 first introduces the theoretical framework of open quantum systems, covering the density operator formalism, master equations, and the spectral theory of Liouvillians. Chapter 2 then presents the superconducting qubit readout architecture and the commonly used model, pointing out its limitations and motivating the need

for more accurate approaches. Thereafter, Chapter 3 presents the generalized Schrieffer-Wolff formalism for dissipative systems, establishing the perturbative expansion of the effective Liouvillian. Equipped with this formalism, Chapter 4 constitutes the original contribution of this thesis by applying it to a qubit coupled to a damped resonator and comparing the higher-order corrections with exact numerical results. Additionally, the validity conditions of the expansion beyond those originally introduced are discussed. Finally, as a perspective for future work, Chapter 5 extends the model to include a coherent drive on the resonator.

Throughout this thesis, three types of highlighted boxes are used to structure the presentation. *Theoretical Concept* boxes, framed in orange, serve as reminders of theoretical notions required in the text and with which the reader may not be fully familiar. *Key Result* boxes, framed in pink, highlight the central results derived in this thesis and *Chapter Summary* boxes provide a concise recapitulation of the main points covered at the end of each chapter.

Theoretical Concept

Key Result

Chapter Summary

Chapter 1

Open Quantum Systems

Open quantum systems correspond to quantum systems that are not perfectly isolated from their surroundings. Indeed, in contrast with closed systems, open systems exchange energy and information with an external environment, thus leading to a need for a formulation beyond the standard Schrödinger equation.

The aim of this chapter is to introduce the mathematical tools used throughout this thesis to describe such systems. For this purpose, we first present the density operator, a generalization of the notion of a quantum state, in Section 1.1. Then, we establish the Redfield master equation in Section 1.2, which describes the reduced dynamics of a quantum system weakly coupled to an external environment. Next, Section 1.3 presents the Lindblad master equation, which provides a general framework for characterizing Markovian dynamics in open quantum systems. In the last three sections, we introduce the vectorization formalism in Section 1.4, discuss some spectral properties of the Liouvillians in Section 1.5 and close this chapter by discussing the adjoint master equation in Section 1.6. Together, these tools form the theoretical basis for the treatment of dissipative quantum systems in the rest of this work.

1.1 Density Operator

In the following, we present the density operator along with its main properties. Although it is defined in a general framework, this operator is particularly useful for describing open quantum systems.

Consider a system whose state is not known with certainty, but is known to have a probability p_i of being in the state $|\psi_i\rangle$, where the probabilities satisfy $0 \leq p_i \leq 1$ and $\sum_i p_i = 1$. In contrast to a *pure state*, where the system is described by a single well-defined ket vector $|\psi\rangle$, the ensemble $\{p_i, |\psi_i\rangle\}$ describes a *mixed state*, which reflects the statistical uncertainty in the system's state. In this context, the *density operator*, acting on the Hilbert space of the system, is defined as

$$\hat{\rho} = p_i \sum_i |\psi_i\rangle\langle\psi_i| \,, \tag{1.1}$$

where $|\psi_i\rangle$ might depend on time, implying that $\hat{\rho}$ would be time-dependent as well [8]. Let us note that the density matrix for a pure state $|\psi\rangle$ is thus defined as

$$\hat{\rho} = |\psi\rangle\langle\psi| \,, \tag{1.2}$$

since, in this case, the system has a probability $p = 1$ to be in the state $|\psi\rangle$.
The density operator admits a matrix representation and is thus commonly referred to as the density matrix. In the remainder of this thesis, the two terms will be used without distinction.

Moreover, choosing an arbitrary orthonormal basis $\{|\phi_n\rangle\}$ of the Hilbert space $\mathcal{H}$ of the system, the density operator admits the decomposition

$$\hat{\rho} = \sum_{ij} \rho_{ij} |\phi_i\rangle\langle\phi_j| \text{ with } \rho_{ij} = \langle\phi_i| \hat{\rho} |\phi_j\rangle , \tag{1.3}$$

where ρ_{ij} are the matrix coefficients of the density matrix in this basis. The diagonal elements ρ_{ii} are called *populations*, while off-diagonal elements are called *coherences*. Due to the properties of $\hat{\rho}$, its elements satisfy $\rho_{ii} \geq 0$ and $\rho_{ij} \in \mathbb{C} : \rho_{ij} = \rho^*_{ji}$.

Several key properties of $\hat{\rho}$, relevant to this work, can be established directly from its definition (1.1) [9], namely:

- $\hat{\rho}$ is hermitian: $\hat{\rho}^\dagger = \hat{\rho}$.
- $\hat{\rho}$ is of trace 1: $\mathrm{Tr}\hat{\rho} = 1$.
- $\hat{\rho}$ is a positive operator: $\langle\phi| \hat{\rho} |\phi\rangle \geq 0 \quad \forall |\phi\rangle \in \mathcal{H}$, where $\mathcal{H}$ is the system Hilbert space.
- The expectation value of an arbitrary observable $\hat{O}$ in the state $\hat{\rho}$ is

$$\langle\hat{O}\rangle_{\hat{\rho}} = \mathrm{Tr}\left[\hat{\rho}\hat{O}\right] . \tag{1.4}$$

Moreover, the time evolution of a closed quantum system is dictated by the *Liouville-von Neumann equation* (LvN)

$$\boxed{\dot{\hat{\rho}}(t) = -\frac{i}{\hbar}\left[\hat{H}, \hat{\rho}(t)\right] ,} \tag{1.5}$$

where $\hbar$ is the reduced Planck constant and $\hat{H}$ is the Hamiltonian of the system. This equation is perfectly equivalent to Schrödinger's equation and corresponds to a unitary evolution[1].

Reduced density operator

Let us consider a bipartite system whose Hilbert space is $\mathcal{H} = \mathcal{H}_A \otimes \mathcal{H}_B$. The density operator describing the system is $\hat{\rho}_{AB}$. If the set $\{|a_n\rangle\}$ $(n = 1, ..., \dim(\mathcal{H}_A))$ is a basis of $\mathcal{H}_A$ and $\{|b_m\rangle\}$ $(m = 1, ..., \dim(\mathcal{H}_B))$ is a basis o $\mathcal{H}_B$, then $\{|a_n\rangle \otimes |b_m\rangle \equiv |a_n, b_m\rangle\}$ forms a basis of the total Hilbert space $\mathcal{H}$. In this context, the *reduced density operator* of subsystem A is defined as the operator

$$\hat{\rho}_A : \mathcal{H}_A \to \mathcal{H}_A, \tag{1.6}$$

defined through

$$\langle a_i| \hat{\rho}_A |a_j\rangle = \sum_k \langle a_i, b_k| \hat{\rho}_{AB} |a_j, b_k\rangle . \tag{1.7}$$

In practice, this is written as

$$\hat{\rho}_A \equiv \mathrm{Tr}_B \left[\hat{\rho}_{AB}\right] , \tag{1.8}$$

where $\mathrm{Tr}_B[\cdot]$ is known as the *partial trace* over system B[2]. A similar definition can of course be introduced for the partial trace over subsystem A giving the reduced density operator of subsystem B

$$\hat{\rho}_B : \mathcal{H}_B \to \mathcal{H}_B, \tag{1.9}$$

[1] That is the state $\hat{\rho}_0$ of the system at time t_0 is related to the state $\hat{\rho}(t)$ of the system at time t by a unitary operator $U(t, t_0) = \exp\left(-\frac{i}{\hbar}H(t - t_0)\right)$ which depends only on the times t_0 and t, i.e., $\hat{\rho}(t) = U(t, t_0)\rho_0 U^\dagger(t, t_0)$[8].

[2] The trace over the total bipartite system is defined as $\mathrm{Tr}[\hat{\rho}_{AB}] = \sum_{n,m} \langle a_n, b_m| \hat{\rho}_{AB} |a_n, b_m\rangle$. This illustrates the terminology *partial trace*.

defined through

$$\langle b_i| \hat{\rho}_B |b_j\rangle = \sum_k \langle a_k, b_i| \hat{\rho}_{AB} |a_k, b_j\rangle , \tag{1.10}$$

and written as

$$\hat{\rho}_B \equiv \mathrm{Tr}_A [\hat{\rho}_{AB}] . \tag{1.11}$$

1.2 Redfield Master Equation

In this section, we derive an equation of motion governing the reduced dynamics of a quantum system weakly coupled to an external environment, known as the Redfield master equation. To this end, let us consider a quantum mechanical system S coupled to a *bath* B, also called *environment* or *reservoir*. The Hamiltonian of the total system "system + bath" is assumed to be of the form

$$H = H_S + H_B + V, \tag{1.12}$$

where H_S and H_B designate the free Hamiltonian of the system and the bath respectively, while V corresponds to the interaction Hamiltonian between the two.

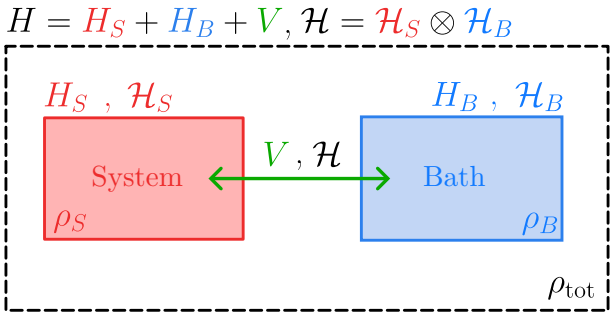

Figure 1.1: Illustration of the generic open quantum system formalism. A system with Hilbert space $\mathcal{H}_S$ and described by a Hamiltonian H_S is coupled to a bath with Hilbert space $\mathcal{H}_B$ and described by a Hamiltonian H_B, through an interaction Hamiltonian V defined in the total Hilbert space $\mathcal{H} = \mathcal{H}_S \otimes \mathcal{H}_B$. The state of the total system "system + bath" is given by ρ_{tot}. In addition the states of the system and the bath are represented by the corresponding density matrices ρ_S and ρ_B corresponding to $\rho_S = \mathrm{Tr}_B[\rho_{\mathrm{tot}}]$ and $\rho_B = \mathrm{Tr}_A[\rho_{\mathrm{tot}}]$, respectively.

In the previous section, we stated that the Liouville von-Neumann (LvN) equation (1.5) gave an equation of motion for the density matrix in the context of closed quantum systems. In this section we want to derive what is called a *master equation*, i.e., an equation of motion that describes the dynamics of the reduced density matrix of an open quantum system. However, working in the interaction picture is more straightforward and we begin thus by writing LvN (1.5) in the interaction picture (with the convention $\hbar = 1$):

$$\dot{\rho}_{\mathrm{tot},I}(t) = -i [V_I(t), \rho_{\mathrm{tot},I}(t)] , \tag{1.13}$$

where the hat notation for operators has been omitted. This convention will be adopted throughout the remainder of this work, except when explicitly needed for clarity.

Theoretical Concept 1.1. Rotating frame, Interaction and Heisenberg pictures

In the Schrödinger picture, the time evolution of the density matrix $\rho_{\mathrm{tot}}(t)$ is governed by the total Hamiltonian $H = H_S + H_B + V$. However, there exist multiple equivalent descriptions of the dynamics obtained by transferring the time dependence from the density matrix to the operators.

To this end, rotating frames are defined by arbitrary unitary operators $R(t) = e^{-i\tilde{H}t/\hbar}$, which transform the state vector $|\psi\rangle$, operators O and Hamiltonian H of the system according to the following relations [10]

$$|\psi_{RF}(t)\rangle = R^\dagger(t)\,|\psi(t)\rangle \;\Rightarrow\; \rho_{RF}(t) = |\psi_{RF}(t)\rangle\langle\psi_{RF}(t)| = R^\dagger(t)\rho(t)R(t), \tag{1.14}$$

$$O_{RF}(t) = R^\dagger(t)O(t)R(t), \tag{1.15}$$

$$H_{RF}(t) = i\hbar\dot{R}^\dagger(t)R(t) + R^\dagger(t)H(t)R(t). \tag{1.16}$$

For instance, in the case of the *interaction picture*, the rotating frame is defined with respect to $\tilde{H} = H_S + H_B$ and the time evolution of the density matrix will be generated by V through[3]

$$\dot{\rho}_{\text{tot},I}(t) = -\frac{i}{\hbar}\left[H_I(t), \rho_{\text{tot},I}(t)\right] = -\frac{i}{\hbar}\left[V_I(t), \rho_{\text{tot},I}(t)\right], \tag{1.17}$$

while the operators dynamics will be dictated by $\tilde{H} = H_S + H_B$ through Eq. (1.15).

Additionally, the *Heisenberg picture* corresponds to a representation in which the density matrix is no longer time-dependent, while the entire time evolution is carried by the operators.

Finally, expectation values of operators are invariant under a change of frame/picture. Indeed, recalling the expression of the expectation value of an operator given in Section 1.1, using $RR^\dagger = \mathbb{1}$ and the cyclic property of the trace, we get[4]

$$\text{Tr}\left[\hat{\rho}_{RF}\hat{O}_{RF}\right] = \text{Tr}\left[R^\dagger\hat{\rho}RR^\dagger\hat{O}R\right] = \text{Tr}\left[R^\dagger\hat{\rho}\mathbb{1}\hat{O}R\right] = \text{Tr}\left[\hat{\rho}\hat{O}RR^\dagger\right] = \text{Tr}\left[\hat{\rho}\hat{O}\right].$$

Integrating Eq. (1.13) leads to

$$\rho_{\text{tot},I}(t) = \rho_{\text{tot},I}(0) - i\int_0^t \left[V_I(\tau), \rho_{\text{tot},I}(\tau)\right]d\tau. \tag{1.18}$$

Written in this form, the LvN provides a natural starting point for deriving approximate solutions within a perturbative framework [11]. Indeed, substituting Eq. (1.18) into Eq. (1.13), tracing over the bath and dropping the indices I regarding the interaction picture yields

$$\boxed{\dot{\rho}_S(t) = -\int_0^t \text{Tr}_B\left[V(t), \left[V(\tau), \rho_{\text{tot}}(\tau)\right]\right]d\tau,} \tag{1.19}$$

assuming that $\text{Tr}_B\left[V(t), \rho_{\text{tot}}(0)\right] = 0$ without loss of generality [11]. ρ_S and $\rho_{\text{tot}} = \rho_S \otimes \rho_B$ correspond to the reduced density matrix of the system and the total density matrix of the bipartite system "system + bath" respectively, in the interaction picture.

[3] In the specific case of interaction picture, Eq. (1.16) yields $H_I(t) = -\tilde{H}e^{i\tilde{H}t}e^{-i\tilde{H}t} + e^{i\tilde{H}t}(\tilde{H} + V)e^{-i\tilde{H}t}$. By linearity, and recalling that $e^{\pm i\tilde{H}t}$ commutes with $\tilde{H}$, we get $H_I(t) = V_I(t)$.

[4] The cyclic property of the trace states that the operators inside a trace can be cyclically permuted without changing the value of the trace. For instance, we have

$$\text{Tr}\left[\hat{A}\hat{B}\hat{C}\right] = \text{Tr}\left[\hat{B}\hat{C}\hat{A}\right] = \text{Tr}\left[\hat{C}\hat{A}\hat{B}\right],$$

with three arbitrary operators $\hat{A}$, $\hat{B}$, $\hat{C}$. This property extends naturally to products involving more than three operators.

Born approximation

Eq. (1.19) is still an exact equation. Indeed, no approximation has been made. However, it is common to consider a *weak coupling* between the environment and the system implying that the state of the environment is weakly affected by the state of the system and their interaction. Hence, in this approximation, the state $\rho_B(t)$ of the bath at time t is not significantly influenced by the state of the total system $\rho_{\text{tot}}(t)$. This translates mathematically to

$$\rho_{\text{tot}}(t) \approx \rho_S(t) \otimes \rho_B, \tag{1.20}$$

where ρ_B is assumed to be time-independent, since the impact of the system on the bath can be neglected [11]. This is commonly referred to as the *Born approximation*.
Substituting Eq. (1.20) into the exact equation (1.19) governing the dynamics leads to

$$\boxed{\dot{\rho}_S(t) = -\int_0^t \text{Tr}_B[V(t), [V(\tau), \rho_S(\tau) \otimes \rho_B]]d\tau.} \tag{1.21}$$

Markov approximation

Another assumption is generally made regarding the system in order to further simplify Eq. (1.21). Indeed, the so-called *Markov approximation* assumes that the state of the system ρ_S does not depend on the state of the system at previous times. It is mathematically represented by [11]

$$\rho_S(\tau) \approx \rho_S(t). \tag{1.22}$$

This can be seen as the system having no memory since its state at a given time t does not depend on previous states at times $t_i < t$. Inserting this second approximation into Eq. (1.21) gives the so-called *Redfield equation*

$$\boxed{\dot{\rho}_S(t) = -\int_0^t \text{Tr}_B[V(t), [V(\tau), \rho_S(t) \otimes \rho_B]]d\tau.} \tag{1.23}$$

Markovian master equation

Although in Eq. (1.23), the Markov approximation accounts for the state of the system to be "memory-less", the time derivative of the density operator still depends on the chosen initial state $\rho_S(t = 0)$ [11]. In order to remove this dependence, we perform the change of variables $\tau \to t - \tau$ in the integral of Eq. (1.23), together with the extension of the upper integration limit to infinity [12]. Ultimately, we arrive at the following equation describing the reduced dynamics of the system [11]

$$\dot{\rho}_{S,I}(t) = -\int_0^\infty \text{Tr}_B[V_I(t), [V_I(t-\tau), \rho_{S,I}(t) \otimes \rho_{B,I}]]d\tau, \tag{1.24}$$

where the subscript I labeling the interaction picture has been reintroduced for clarity. The latter equation is called a *Markovian master equation* because all memory effects were erased from the dynamics. Nonetheless, with a slight abuse of terminology, we will refer to Eq. (1.24) as Redfield as well. Moreover, the approximations used in order to derive it are collectively referred to as the *Born-Markov approximation*.

It can be shown that the Born-Markov approximation only requirement is the following clear

separation of time scales: the system state must evolve significantly only over a relaxation time τ_R much longer than the correlation time τ_B of the bath over which the bath "forgets" information received from the system, i.e., $\tau_B \ll \tau_R$ [13]. Furthermore, τ_B corresponds to the typical decay time of the so-called *bath correlation functions*, related to the isolated dynamics of the damped bath, which will be introduced later in Theoretical Concept 4.1.

1.3 Lindblad Master Equation

In 1976, Gorini, Kossakowski, Sudarshan and Lindblad (GKSL) demonstrated in [14, 15] that the general form of the generator of a Markovian quantum evolution, defined through $\dot{\rho}_S = \mathcal{L}\rho_S$, takes the (GKSL) form:

$$\dot{\rho}_S = -i\left[H_S + H_{LS}, \rho_S\right] + \sum_k \gamma_k \left(L_k \rho_S L_k^\dagger - \frac{1}{2}\left\{L_k^\dagger L_k, \rho_S\right\}\right) \equiv \mathcal{L}[\rho_S], \tag{1.25}$$

where the explicit time dependence of the density matrix has been omitted for readability, L_k are known as jump operators, H_{LS} is the Lamb-Shift Hamiltonian, i.e., a Hamiltonian contribution to the dynamics of the system coming from its interaction with the environment, and the notation $\{A, B\} = AB + BA$ represents the anticommutator between two arbitrary operators A and B [16]. This equation can be obtained from Eq. (1.24) by performing a further approximation called the *secular approximation* and by returning to the Schrödinger picture. The secular approximation consists in averaging to zero terms which oscillates much faster than the typical timescale of the system τ_S and is valid if $\tau_S \ll \tau_R$, i.e., the typical intrinsic timescale of the system is small compared to the relaxation time τ_R of the system due to its interaction with the environment [11]. Moreover, $\mathcal{L}$ is a superoperator[5] or *map* called the *Liouvillian* or *Lindbladian*. Sometimes Eq. (1.25), is written as

$$\dot{\rho}_S = -i\left[H_S + H_{LS}, \rho_S\right] + \mathcal{D}(L_k)[\rho_S], \tag{1.26}$$

highlighting the separation between the unitary evolution given by the commutator with the Hamiltonians, and the dissipative part reexpressed as the action of a superoperator $\mathcal{D}$, called the *dissipator*, which depends on the jump operators L_k and acts on the density matrix of the system ρ_S.

1.4 Vectorization Formalism

In the previous section, it has been shown that the dynamics of an open quantum system is governed by a Liouvillian superoperator. However, while the density operator is naturally represented by a matrix, the explicit representation of a superoperator is less intuitive. The present section addresses this issue by vectorizing the density operator. Indeed, mapping the density matrix to a column vector enables the Liouvillian to be represented as a matrix. To this end, let us consider a quantum system associated with a finite-dimensional Hilbert space $\mathcal{H}$, with $\dim \mathcal{H} = N$. The set $\mathcal{B}(\mathcal{H})$ of linear operators acting on $\mathcal{H}$

$$\hat{A} : \mathcal{H} \to \mathcal{H},\ |\psi\rangle \to \hat{A}\,|\psi\rangle \quad \forall\, |\psi\rangle \in \mathcal{H}, \tag{1.27}$$

forms a Hilbert space when equipped with the so-called Hilbert-Schmidt inner product [17]

$$\left(\hat{A}, \hat{B}\right) = \mathrm{Tr}\left[\hat{A}^\dagger \hat{B}\right] \in \mathbb{C}. \tag{1.28}$$

[5]The term *superoperator* reflects the fact that $\mathcal{L}$ acts linearly on operators, just as an ordinary operator acts linearly on vectors. The dissipator introduced later is likewise a superoperator.

Its elements can therefore be represented as column vectors, just as $|\psi\rangle$ is represented by a column vector in an orthonormal basis $\{|\phi_n\rangle : n = 1, \dots, N\}$ of $\mathcal{H}$ [18].
Hence, if the matrix representation of $\hat{A}$ is given by

$$A = \begin{pmatrix} a_{11} & \dots & a_{1N} \\ \vdots & & \vdots \\ a_{N1} & \dots & a_{NN} \end{pmatrix} \quad \text{with} \quad A_{ij} = \langle \phi_i | \hat{A} | \phi_j \rangle ,$$

then its vectorized form is[6]

$$|A\rangle\!\rangle = \begin{pmatrix} a_{11} \\ \vdots \\ a_{1N} \\ \vdots \\ a_{NN} \end{pmatrix} . \tag{1.29}$$

With this notation, Eq. (1.28) is reexpressed as

$$\langle\!\langle A|B\rangle\!\rangle = \begin{pmatrix} a_{11}^* & \dots & a_{1N}^* & \dots a_{NN}^* \end{pmatrix} \begin{pmatrix} b_{11} \\ \vdots \\ b_{1N} \\ \vdots \\ b_{NN} \end{pmatrix} = \mathrm{Tr}\left[\hat{A}^\dagger \hat{B}\right] . \tag{1.30}$$

Formally, we have that

$$\hat{A} = \sum_{ij} A_{ij} |\phi_i\rangle\langle\phi_j| \tag{1.31}$$

is mapped to

$$\boxed{|A\rangle\!\rangle = \sum_{ij} A_{ij} |\phi_i\rangle \otimes |\phi_j\rangle ,} \tag{1.32}$$

where $|A\rangle\!\rangle$ is thus a ket vector of the Hilbert space $\mathcal{H} \otimes \mathcal{H}$ of dimension N^2 [17].
Furthermore, since a density matrix $\hat{\rho} = \sum_{ij} \rho_{ij} |\phi_i\rangle\langle\phi_j|$ is an element of $\mathcal{B}(\mathcal{H})$, the formalism just introduced can be extended to it. Hence, the density operator $\hat{\rho}$ acting on $\mathcal{H}$ is mapped to a ket vector of the Hilbert space $\mathcal{H} \otimes \mathcal{H}$.
Under this vectorization, a superoperator acting on $\mathcal{B}(\mathcal{H})$, i.e.,

$$\mathcal{S} : \mathcal{B}(\mathcal{H}) \to \mathcal{B}(\mathcal{H}), \ \hat{A} \to \mathcal{S}[\hat{A}], \tag{1.33}$$

such as the Liouvillian, is represented by an $N^2 \times N^2$ matrix acting on vectorized operators of $\mathcal{B}(\mathcal{H})$. In fact, we have

$$\boxed{|\, \mathcal{S}[\hat{A}] \,\rangle\!\rangle = S|A\rangle\!\rangle,} \tag{1.34}$$

where S is an $N^2 \times N^2$ matrix acting on the vectorized operator $|A\rangle\!\rangle$.
As a conclusion, an operator of $\mathcal{B}(\mathcal{H})$ can be mapped to a vector of $\mathcal{H} \otimes \mathcal{H}$. Correspondingly, a superoperator acting on $\mathcal{B}(\mathcal{H})$, such as the Liouvillian can be mapped to an $N^2 \times N^2$ matrix[7].

[6] It should be noted that there exist two conventions, namely row-major ordering, used in this thesis, and column-major ordering, where vectorization consists in stacking the columns of the matrix representation to form a vector rather than stacking the rows.

[7] Going a step further, one often introduces the more abstract Choi-Jamiołkowski isomorphism. First introduced in [19, 20], it maps superoperators acting on $\mathcal{B}(\mathcal{H})$ to operators acting on $\mathcal{H} \otimes \mathcal{H}$, thus defined on $\mathcal{L}(\mathcal{H} \otimes \mathcal{H})$ and admitting a matrix representation. In particular, completely positive and trace preserving maps such as the

In practice, the vectorization framework yields

$$|A\rho B\rangle\rangle = (A \otimes B^T)|\rho\rangle\rangle, \tag{1.35}$$

with A and B, arbitrary matrices, $\otimes$ the Kronecker product[8] and T denotes the transpose. From this, it is possible to write the vectorized form of the Liouvillian appearing in Eq. (1.25) as

$$\mathcal{L} = -i\left(H \otimes \mathbb{1} - \mathbb{1} \otimes H^T\right) + \sum_k \gamma_k \left(L_k \otimes L_k^* - \frac{1}{2} L_k^\dagger L_k \otimes \mathbb{1} - \frac{1}{2}\mathbb{1} \otimes L_k^T L_k^*\right). \tag{1.36}$$

Furthermore, the vectorized Lindblad master equation (1.25) is expressed as

$$\boxed{|\dot{\rho}\rangle\rangle = \mathcal{L}|\rho\rangle\rangle,} \tag{1.37}$$

where $|\rho\rangle\rangle$ denotes the vectorized density matrix and $\mathcal{L}$ is the matrix representation (1.36) of the Liouvillian. Note that the same notation are used for the Liouvillian superoperator and its matrix representation acting on the vectorized density matrix. The notation should not be ambiguous due to the vectorized density matrix double ket notation.

Finally, the expression (1.37) for a time-independent Liouvillian leads to the straightforward solution

$$\boxed{|\rho(t)\rangle\rangle = e^{\mathcal{L}t}|\rho(0)\rangle\rangle,} \tag{1.38}$$

where $|\rho(0)\rangle\rangle$ is the initial state of the (vectorized) density matrix at time $t = 0$.

1.5 Spectral Theory of Liouvillians

The vectorized formalism allowing for a matrix representation of the Liouvillian $\mathcal{L}$ sets a straightforward framework for the analysis of the spectrum of the Liouvillian needed to determine the dynamics of the system. First, note that the Liouvillian, in contrast with the Hamiltonian, is non-Hermitian (and in general non-normal[9]). In this master thesis, we will only consider cases where the Liouvillian is diagonalizable meaning that it admits right and left eigenvectors, $|r_i\rangle\rangle$

Liouvillian are mapped to density operators.

[8]The Kronecker product is used as a concrete way to compute the tensor product between 2 operators using their matrix representation. Let A and B be two arbitrary matrices of sizes $m \times n$ and $p \times q$, respectively. Their Kronecker product is defined as [21]

$$A \otimes B = \begin{pmatrix} A_{11}B_{11} & \dots & A_{11}B_{1q} & \dots & A_{1n}B_{11} & \dots & A_{1n}B_{1q} \\ \vdots & \ddots & \vdots & & \vdots & \ddots & \vdots \\ A_{11}B_{p1} & \dots & A_{11}B_{pq} & \dots & A_{1n}B_{p1} & \dots & A_{1n}B_{pq} \\ \vdots & & \vdots & & \vdots & & \vdots \\ A_{m1}B_{11} & \dots & A_{m1}B_{1q} & \dots & A_{mn}B_{11} & \dots & A_{mn}B_{1q} \\ \vdots & \ddots & \vdots & & \vdots & \ddots & \vdots \\ A_{m1}B_{p1} & \dots & A_{m1}B_{pq} & \dots & A_{mn}B_{p1} & \dots & A_{mn}B_{pq} \end{pmatrix},$$

where A_{ij} and B_{ij} denotes the matrix coefficients of A and B, respectively. In a condensed form, we have

$$A \otimes B = \begin{pmatrix} A_{11}B & \dots & A_{1n}B \\ \vdots & & \vdots \\ A_{m1}B & \dots & A_{mn}B \end{pmatrix}.$$

[9]Let A be an arbitrary operator, A is normal if $AA^\dagger = A^\dagger A$, i.e., a normal operator is one that commutes with its Hermitian conjugate. If $A{=}A^\dagger$, A is called Hermitian [22].

and $|l_i\rangle\!\rangle$, defined by

$$\boxed{\begin{aligned}\mathcal{L}|r_i\rangle\!\rangle &= \lambda_i|r_i\rangle\!\rangle \\ \langle\!\langle l_i|\mathcal{L} &= \lambda_i\langle\!\langle l_i|,\end{aligned}} \tag{1.39}$$

where λ_i denotes the associated complex eigenvalue. These right and left eigenvectors form a biorthonormal basis, i.e. $\langle\!\langle l_i|r_i\rangle\!\rangle = \delta_{ij}$, and satisfy the completeness relation $\sum_i |r_i\rangle\!\rangle\langle\!\langle l_i| = \mathbb{1}$ [7].

Theoretical Concept 1.2. Left and right eigenvectors [23]

Let A be a square matrix in $\mathbb{C}^{n\times n}$, a non-zero vector $r_i \in \mathbb{C}^n$ is a right eigenvector associated with an eigenvalue λ_i of A if

$$Ar_i = \lambda_i r_i. \tag{1.40}$$

On the other hand, a non-zero vector $l_i \in \mathbb{C}^n$ is a left eigenvector associated with an eigenvalue λ_i of A if

$$l_i^\dagger A = \lambda_i l_i^\dagger. \tag{1.41}$$

Note that the symbol $\dagger$ denotes the conjugate transpose meaning that while r_i and l_i are column vectors, $l_i^\dagger$ is a row vector.
In Dirac notation, (1.40) takes the form

$$A\,|r_i\rangle = \lambda_i\,|r_i\rangle\,,$$

while (1.41) is written as

$$\langle l_i|\,A = \lambda_i\,\langle l_i|\,.$$

The following properties can be shown.
A left eigenvector $|l_i\rangle$ relative to the eigenvalue λ_i of A is a right eigenvector of its hermitian conjugate $A^\dagger$ relative to the complex conjugate eigenvalue λ_i^*, i.e., $A^\dagger\,|l_i\rangle = \lambda_i^*\,|l_i\rangle$.

Moreover, $|l_i^*\rangle$ is a right eigenvector of the transpose A^T relative to λ_i, i.e., $A^T\,|l_i^*\rangle = \lambda_i\,|l_i^*\rangle$.

Having introduced the eigenvectors and eigenvalues of $\mathcal{L}$, the solution of the Lindblad ME (1.38) can be expressed as

$$|\rho\rangle\!\rangle = \sum_i e^{\lambda_i t}\,\langle\!\langle l_i|\rho(0)\rangle\!\rangle\,|r_i\rangle\!\rangle. \tag{1.42}$$

Moreover, it can be proved that $\mathrm{Re}(\lambda_i) \leq 0\ \forall i$ and that time-independent Liouvillians always admit a zero eigenvalue [24]. The eigenstate associated with this zero eigenvalue thus corresponds to

$$\mathcal{L}|\rho_{ss}\rangle\!\rangle = 0 \tag{1.43}$$

and is called a *steady state* of the system which is time-independent given that $0 = \mathcal{L}|\rho_{ss}\rangle\!\rangle = |\dot{\rho}_{ss}\rangle\!\rangle$[10].

Over time, the state of the system relaxes to the steady state up to possible persistent oscillatory contributions associated with purely imaginary Liouvillian eigenvalues. Indeed, since $\mathrm{Re}(\lambda_i) \leq 0$, when $t \to \infty$, the majority of the terms in Eq. (1.42) tends to zero and the only remaining terms are ones for which $\mathrm{Re}(\lambda_i) = 0$. These surviving terms correspond to the zero eigenvalue $\lambda_0 = 0$ associated with the steady state of the system and the terms relative to purely

[10]Note that the Liouvillian might present multiple steady states if the zero eigenvalue is degenerated.

imaginary eigenvalues λ_i responsible for oscillations by the rotating phase $e^{i\lambda_i t}$ [11].

Finally, it is useful to define the *Liouvillian gap*:

$$\Delta = \min_{i \neq 0} |\mathrm{Re}(\lambda_i)|, \tag{1.44}$$

which corresponds to the slowest relaxation rate. Indeed, since all nonzero eigenvalues have negative real parts, the larger $|\mathrm{Re}(\lambda_i)|$ is, the faster the corresponding dynamics. Conversely, as $|\mathrm{Re}(\lambda_i)|$ decreases, the decay rate becomes smaller. In Figure 1.2 this can be understood as follows: the closer an eigenvalue lies to the imaginary axis, the slower the corresponding decay dynamics becomes, except for purely oscillating modes, which must be treated separately.

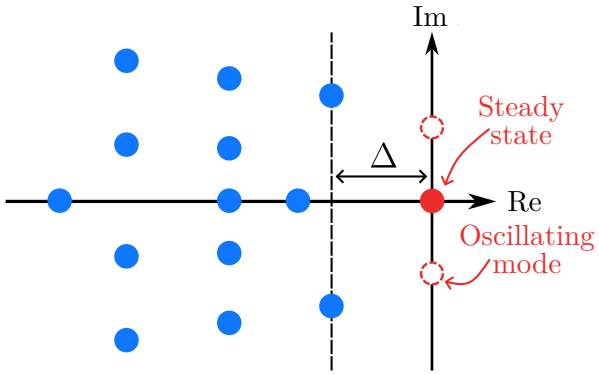

Figure 1.2: Illustration of the spectrum of a Liouvillian reproduced from [25] where the blue eigenvalues are associated with decaying modes, the solid red eigenvalue corresponds to the steady state(s) of the system and the red dashed circles are related to oscillating modes. The Liouvillian gap Δ is also represented. One may note the general property that the eigenvalues of a Liouvillian are either real or occur in complex-conjugate pairs.

1.6 Adjoint Master Equation

This section presents the Heisenberg-picture[12] analog of the Lindblad master equation (1.25), called the *Adjoint Master Equation* (AME). In this picture, the density matrix describing the state of a system does not depend on time anymore. However, the operators evolve over time according to the AME, thus providing information on the dynamics. Indeed, consider the evolution of the density matrix governed by the master equation:

$$\dot{\rho}(t) = \mathcal{L}\rho(t), \tag{1.45}$$

in the Schrödinger picture. It can be proven that, for a time-independent Liouvillian in the Heisenberg picture, the time evolution of an arbitrary operator O is governed by the following

[11] A clear way to see this is to separate Eq. (1.42) into two terms, one corresponding to the steady state ρ_{ss} associated to the eigenvalue $\lambda_0 = 0$ and the second containing all the remaining terms for which $\lambda_i \neq 0 \; \forall i \neq 0$:

$$|\rho\rangle\!\rangle = e^{0t} \langle\!\langle l_0|\rho(0)\rangle\!\rangle \; |r_0\rangle\!\rangle + \sum_{i \neq 0} e^{\lambda_i t} \langle\!\langle l_i|\rho(0)\rangle\!\rangle \; |r_i\rangle\!\rangle$$

with $|r_0\rangle\!\rangle \equiv \rho_{ss}$ by definition. The sum over $i \neq 0$ contains terms with purely imaginary eigenvalues which will not decay over time but be responsible for phase oscillations. However, the terms for which $\mathrm{Re}(\lambda_i) \neq 0$ decay since the Liouvillian properties imply $\mathrm{Re}(\lambda_i) \leq 0$.

[12] See Theoretical Concept 1.1 for a reminder about Heisenberg picture.

master equation:

$$\boxed{\dot{O}_H(t) = \mathcal{L}^\dagger O_H(t),} \tag{1.46}$$

where $\mathcal{L}^\dagger$ is the *adjoint Liouvillian* defined by the identity

$$\mathrm{Tr}\left[A\mathcal{L}B\right] = \mathrm{Tr}\left[\mathcal{L}^\dagger(A)B\right], \tag{1.47}$$

for arbitrary operators A and B [26].

Proof. Let us begin from the fact that the expectation values in both pictures are equal such that

$$\langle O\rangle = \mathrm{Tr}\left[O_H(t)\rho_H\right] = \mathrm{Tr}\left[O_S\rho_S(t)\right], \tag{1.48}$$

where the operators in the Schrödinger picture and in the Heisenberg picture have been denoted by O_S and $O_H(t)$ respectively, highlighting the fact that O_S is time-independent while $O_H(t)$ evolves over time. Similarly, the Schrödinger picture density matrix $\rho_S(t)$ depends on time while ρ_H does not and $\rho_H = \rho_S(0)$, by construction of the Heisenberg picture. As introduced at the end of Section 1.4, if the Liouvillian is time-independent, Eq. (1.45) yields

$$\rho_S(t) = e^{\mathcal{L}t}\rho_S(0) = e^{\mathcal{L}t}\rho_H. \tag{1.49}$$

Substituting the later in Eq. (1.48) gives [26]

$$\langle O\rangle = \mathrm{Tr}\left[O_H(t)\rho_H\right] = \mathrm{Tr}\left[O_S e^{\mathcal{L}t}\rho_H\right]. \tag{1.50}$$

Making use of the previously defined adjoint Liouvillian (1.47), Eq. (1.50) can be written as

$$\langle O\rangle = \mathrm{Tr}\left[O_H(t)\rho_H\right] = \mathrm{Tr}\left[e^{\mathcal{L}^\dagger t}O_S\rho_H\right], \tag{1.51}$$

which means that the time evolution of the Heisenberg operator $O_H(t)$ reads

$$O_H(t) = e^{\mathcal{L}^\dagger t}O_S = e^{\mathcal{L}^\dagger t}O_H(0). \tag{1.52}$$

Hence, in the Heisenberg picture, the operators obey the following master equation

$$\dot{O}_H(t) = \mathcal{L}^\dagger O_H(t). \tag{1.53}$$

□

Recalling the general Lindblad form (1.25) introduced in Section 1.3, the definition (1.47) allows one to obtain an explicit expression of the adjoint Liouvillian $\mathcal{L}^\dagger$ such that

$$\mathcal{L}^\dagger[\cdot] = i\left[H,\cdot\right] + \sum_k \gamma_k\left(L_k^\dagger\cdot L_k - \frac{1}{2}\left\{L_k^\dagger L_k,\cdot\right\}\right). \tag{1.54}$$

Proof. The definition (1.47) of the adjoint Liouvillian enables to write [26]

$$\mathrm{Tr}\left[\mathcal{L}^\dagger(O)\rho\right] = \mathrm{Tr}\left[O\mathcal{L}\rho\right]. \tag{1.55}$$

Inserting the explicit Lindblad form of the Liouvillian given by (1.25) into Eq. (1.55) provides

$$\mathrm{Tr}\left[O\mathcal{L}\rho\right] = -i\mathrm{Tr}\left[O\left[H,\rho\right]\right] + \sum_k \mathrm{Tr}\Big[O\,\gamma_k\left(L_k\rho L_k^\dagger - \frac{1}{2}\left\{L_k^\dagger L_k,\rho\right\}\right)\Big] \tag{1.56}$$

$$= i\mathrm{Tr}\left[\rho\left[H,O\right]\right] + \sum_k \mathrm{Tr}\Big[\rho\,\gamma_k\left(L_k^\dagger O L_k - \frac{1}{2}\left\{L_k^\dagger L_k,O\right\}\right)\Big], \tag{1.57}$$

where the second equality is a direct consequence of the cyclic property of the trace [26]. Finally, since the last equation holds for an arbitrary density matrix ρ, comparison with Eq. (1.55) yields Eq. (1.54). □

Summary 1. Open quantum systems

In Chapter 1, we introduced the theoretical framework used to describe the dynamics of open quantum systems, i.e., quantum systems interacting with an external environment. Since the state of such systems is not necessarily pure, the appropriate tool for describing their dynamics is the density operator

$$\rho = \sum_i p_i |\psi_i\rangle\langle\psi_i|.$$

For a bipartite system composed of a system S and a bath B, the reduced density matrix $\rho_S = \mathrm{Tr}_B[\rho_{\mathrm{tot}}]$ describes the state of the system after eliminating the environmental degrees of freedom.

If we consider a system which interacts weakly with a bath, the reduced dynamics can be described within the Markovian master equation in the interaction picture:

$$\dot{\rho}_S(t) = -\int_0^\infty \mathrm{Tr}_B\left[V(t), [V(t-\tau), \rho_S(t)\otimes\rho_B]\right] d\tau,$$

in which memory effects are neglected. With a slight abuse of terminology, it is also referred to as Redfield equation.

After a further secular approximation, the dynamics of a Markovian open quantum system can be written in Lindblad form as

$$\dot{\rho}_S = -i[H_S + H_{LS}, \rho_S] + \sum_k \gamma_k \left(L_k \rho_S L_k^\dagger - \frac{1}{2}\left\{L_k^\dagger L_k, \rho_S\right\}\right) \equiv \mathcal{L}[\rho_S],$$

which separates the unitary evolution generated by the Hamiltonian from the dissipative evolution generated by the dissipator.

The vectorization formalism was then introduced in order to represent the Liouvillian superoperator as a matrix. Under this mapping, an operator ρ is written as a vector $|\rho\rangle\!\rangle$, and the master equation becomes

$$|\dot{\rho}\rangle\!\rangle = \mathcal{L}|\rho\rangle\!\rangle,$$

with

$$\mathcal{L} = -i\left(H\otimes\mathbb{1} - \mathbb{1}\otimes H^T\right) + \sum_k \gamma_k \left(L_k\otimes L_k^* - \frac{1}{2}L_k^\dagger L_k\otimes\mathbb{1} - \frac{1}{2}\mathbb{1}\otimes L_k^T L_k^*\right).$$

Next, we discussed the spectrum of the Liouvillian which admits left and right eigenvectors since it is generally non-Hermitian. Moreover, the real parts of its eigenvalues determine the relaxation rates of the system, while purely imaginary eigenvalues correspond to persistent oscillations. In particular, the Liouvillian always admits at least one zero eigenvalue which is associated with the steady state(s) of the system.

Finally, the adjoint master equation was introduced as the Heisenberg-picture formulation of the Lindblad master equation. In this picture, the density matrix is time-independent and the operators evolve according to

$$\dot{O}_H(t) = i[H, O_H(t)] + \sum_k \gamma_k \left(L_k^\dagger O_H(t) L_k - \frac{1}{2}\left\{L_k^\dagger L_k, O_H(t)\right\}\right) \equiv \mathcal{L}^\dagger[O_H(t)].$$

Chapter 2

Readout of a Superconducting Qubit

Having established the theoretical framework for describing open quantum systems in Chapter 1, we now turn to the physical system at the heart of this thesis. A superconducting qubit is a macroscopic circuit that functions as an anharmonic oscillator, utilizing its quantum degrees of freedom to store information [4].
In this chapter, we start by introducing the Hamiltonian describing this type of qubit in Section 2.1. We then discuss the fundamental concept underlying their readout in Section 2.2. After that, we introduce the notion of dispersive regime and its consequences for the readout in Section 2.3, through the presentation of the so-called *Schrieffer-Wolff transformation*. Finally, we motivate the research carried out in this master's thesis in Section 2.4, by highlighting the limitations of the dispersive regime.

Theoretical Concept 2.1. Superconductivity

Superconductivity is a quantum phenomenon occurring in certain materials below a critical temperature. Electrons then form bound pairs, called Cooper pairs, which condense into a single collective quantum state. This quantum state is described by a wave function $\Psi(r) = |\Psi(r)|e^{i\phi(t)}$, whose phase ϕ is the macroscopic superconducting phase. As a result, a superconductor can carry an electrical current without resistance and behaves as a perfect diamagnet, expelling magnetic fields through the Meissner effect [27]. In superconducting circuits, the collective phase and charge of the condensate can be treated as quantum variables, providing the basis for the quantization of circuit variables such as flux and charge [28].

Theoretical Concept 2.2. Qubit

A *qubit* is a quantum two-level system and forms the basic unit of information in quantum computing. Its name is a contraction of quantum bit and is referring to its classical analog, the classical bit [8].

2.1 Transmon Hamiltonian

Before introducing the *transmon* superconducting qubit, let us begin with a linear LC circuit (see Figure 2.1a). In this circuit, energy oscillates between electrical energy stored in the capacitor and magnetic energy stored in the inductor. The Hamiltonian of such system takes the form

$$H = \frac{Q^2}{2C} + \frac{\Phi^2}{2L}, \tag{2.1}$$

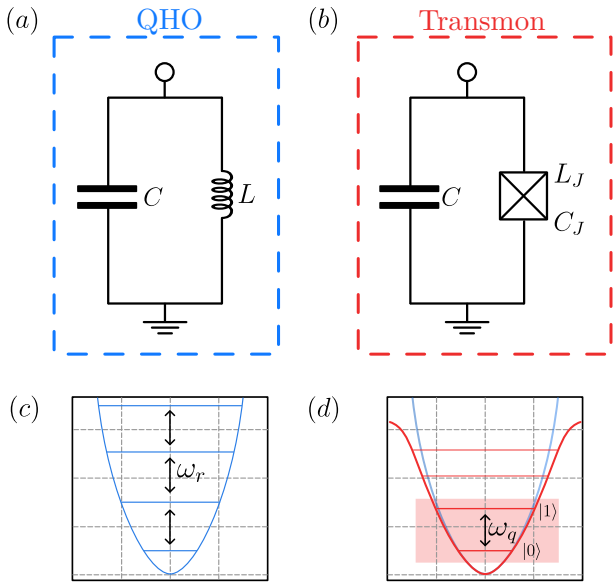

Figure 2.1: (a) Circuit for a parallel LC-oscillator (equivalent to a quantum harmonic oscillator, QHO), with inductance L and capacitance C. (b) Transmon qubit circuit, where the nonlinear inductance L_J (Josephson junction) is connected in parallel with a capacitance C. (c) Quadratic energy landscape for the QHO where energy levels are separated by a constant spacing $\hbar\omega_r$. (d) The non linear inductance reshapes the QHO quadratic energy potential (blue) into a sinusoid (red), which leads to a non-uniform spectrum. This allows for the isolation of the two lowest energy levels $|0\rangle$ and $|1\rangle$, creating a computational subspace[4].

where Q is the charge and C is the capacitance of the capacitor, while Φ and L denote the magnetic flux and the inductance of the inductor, respectively [4]. This Hamiltonian shares a direct mathematical structure with the classical mechanical harmonic oscillator. Indeed, identifying C as the mass m and the oscillator frequency as $\omega_r = \sqrt{1/LC}$, Eq. (2.1) is perfectly equivalent to

$$H = \frac{p^2}{2m} + \frac{1}{2}m\omega_r^2 x^2, \tag{2.2}$$

when identifying Q and Φ as the general position and momentum coordinates x and p. Hence, the electrical energy can be mapped to the kinetic energy and the magnetic energy to the potential energy of the mechanical oscillator.
This last Hamiltonian is of course classical. In order to get its quantum description, the physical quantities x an p must be replaced by the observable $\hat{x}$ and $\hat{p}$ satisfying

$$[\hat{x}, \hat{p}] = i\hbar. \tag{2.3}$$

Then, the second quantization yields a more straightforward manner to write the quantum harmonic oscillator (QHO) Hamiltonian, i.e.,

$$H = \hbar\omega_r \left(\hat{a}^\dagger \hat{a} + \frac{1}{2}\right), \tag{2.4}$$

where the well-known annihilation and creation operators of one single excitation of the system have been defined as [29]:

$$\hat{a} = \frac{1}{\sqrt{2}} \left(\sqrt{\frac{m\omega_r}{\hbar}} \hat{x} + i \sqrt{\frac{1}{m\omega_r \hbar}} \hat{p} \right) \tag{2.5}$$

$$\hat{a}^\dagger = \frac{1}{\sqrt{2}} \left(\sqrt{\frac{m\omega_r}{\hbar}} \hat{x} - i \sqrt{\frac{1}{m\omega_r \hbar}} \hat{p} \right). \tag{2.6}$$

Similarly, the charge and flux coordinates Q and Φ of the LC circuit Hamiltonian (2.1) must become observables in order to get a quantum description of the system. We denote them $\hat{Q}$ and $\hat{\Phi}$. The mathematical mapping between the LC circuit Hamiltonian and quantum harmonic oscillator still holds, hence $\hat{Q}$ and $\hat{\Phi}$ satisfy the commutation relation

$$\left[\hat{\Phi}, \hat{Q} \right] = i\hbar. \tag{2.7}$$

Moreover, annihilation and creation operators $\hat{a}$ and $\hat{a}^\dagger$ can be defined similar to (2.5) and (2.6) as

$$\hat{a} = \frac{1}{\sqrt{2}} \left(\sqrt{\frac{1}{Z\hbar}} \hat{\Phi} + i \sqrt{\frac{Z}{\hbar}} \hat{Q} \right) \tag{2.8}$$

$$\hat{a}^\dagger = \frac{1}{\sqrt{2}} \left(\sqrt{\frac{Z}{\hbar}} \hat{\Phi} - i \sqrt{\frac{Z}{\hbar}} \hat{Q} \right), \tag{2.9}$$

where $Z = \sqrt{L/C}$ is the impedance of the linear LC circuit, in order to recover expression (2.4).

Those relations can, of course, be inverted to obtain

$$\hat{\Phi} = \sqrt{\frac{\hbar Z}{2}} \left(\hat{a} + \hat{a}^\dagger \right) \tag{2.10}$$

$$\hat{Q} = i \sqrt{\frac{\hbar}{2Z}} \left(\hat{a} - \hat{a}^\dagger \right). \tag{2.11}$$

It is common to define the reduced flux $\phi = 2\pi\Phi/\Phi_0$ (with $\Phi_0 = h/(2e)$, the superconducting magnetic flux quantum) and the reduced charge $n = Q/(2e)$, as well as the associated observables $\hat{\phi} = 2\pi\hat{\Phi}/\Phi_0$ and $\hat{n} = \hat{Q}/(2e)$. Given these, the quantum Hamiltonian of the LC circuit reads

$$\boxed{H = 4E_C \hat{n}^2 + \frac{1}{2} E_L \hat{\phi}^2,} \tag{2.12}$$

where $E_C = e^2/(2C)$ represents the charging energy of single electrons and $E_L = \left(\Phi_0/(2\pi)\right)^2 / L$ denotes the inductive energy.
Having established the quantization framework, the hats notation on operators will be omitted for brevity.

The last Hamiltonian is thus perfectly equivalent to the quantum harmonic oscillator (2.4). Therefore, its eigenvalues are equidistantly spaced by $\hbar\omega_r = \hbar/\sqrt{LC}$ (see Figure 2.1c). However, the objective is to create a qubit, i.e., a two level quantum system. Therefore, anharmonicity can be added to enable the driving of a selected transition without exciting other energy levels of the system. One mean to achieve this is to replace the linear inductance of the quantum harmonic oscillator by a Josephson junction, i.e., a nonlinear inductor (see Figure 2.1b) [4]. The

thereby newly constructed circuit is widely referred to as *transmon*. This change in the circuit modifies the Hamiltonian (2.12) into

$$\boxed{H = 4E_C n^2 - E_J \cos(\phi),} \tag{2.13}$$

with $E_C = e^2/(2C_{\text{tot}})$ with $C_{\text{tot}} = C + C_J$ being the total capacitance containing the capacitor's capacitance C as well as the self-capacitance C_J of the Josephson junction, and $E_J = I_c\Phi_0/(2\pi)$ is the Josephson energy with I_c, the critical current of the junction (see Theoretical Concept 2.3).

Theoretical Concept 2.3. Josephson effect - junction

The *Josephson effect* describes the tunneling of Cooper pairs between two superconductors separated by a very thin tunnel barrier ($d < 30$ Å) at zero voltage [27].
The flowing current of Cooper pairs thereby generated is known as the *supercurrent* and is given by

$$I = I_c \sin(\delta), \tag{2.14}$$

where I_c is the *critical current*. This is known as the *dc Josephson effect* [30]. Moreover, δ represents the phase difference between the wavefunctions of the superconductors. Indeed, these wavefunctions are defined as $\Psi_{1,2} = \psi_{1,2}e^{i\varphi_{1,2}}$, where $|\Psi_i|^2$ can be identified as the density of Cooper pairs present in the respective superconductors.

If a DC voltage V is applied across the junction, the phase difference δ evolves over time according to

$$\dot{\delta} = -2eV/\hbar \equiv -\frac{2\pi}{\Phi_0}V, \tag{2.15}$$

implying $\delta(t) = \delta(0) - 2eVt/\hbar$. Hence, the supercurrent can be expressed as $I = I_c \sin[\delta(0) - (2eVt/\hbar)]$ and the currrent oscillates at a frequency $\omega = 2eV/\hbar$. This specific effect is called the *AC Josephson effect* [30].

Moreover, applying Faraday's law of induction to (2.15) yields

$$\dot{\delta} = \frac{2\pi}{\Phi_0}\dot{\Phi}, \tag{2.16}$$

and integrating this relation, directly leads to

$$\delta = \frac{2\pi}{\Phi_0}\Phi \equiv \phi. \tag{2.17}$$

We thus see that the previously defined reduced flux ϕ corresponds to the time dependent phase difference $\delta(t)$ between the two superconductors separated by the thin barrier.

Finally, experimental implementations of those junctions are called Josephson junctions and create nonlinear inductors.

This new Hamiltonian no longer features a quadratic form for its "potential" energy but rather a cosinusoïdal expression which creates anharmonicity in the Hamiltonian spectrum and creates a separately accessible two-level quantum system (see Figure 2.1d), as detailed in the remainder of this section.

When replacing the linear inductance by a Josephson junction, the system's dynamics is governed by the leading term in (2.13), characterized by the ratio E_J/E_C. Experimentalists find that an effective regime for qubit configurations is $E_J \gg E_C$, it is thus the regime which will be

addressed here [28]. In this case, the reduced flux $\phi = \Phi/\Phi_0$ can be considered small compared to E_J since $E_J \propto \Phi_0$. In this sense, the cosine function in (2.13) can be expanded into its power series yielding the following expression for the "potential energy"

$$E_J \cos(\phi) = \frac{1}{2} E_J \phi^2 - \frac{1}{24} E_J \phi^4 + \mathcal{O}(\phi^6). \tag{2.18}$$

The leading term of the series expansion renders back the linear LC circuit of (2.12), i.e., the quantum harmonic oscillator, while the second term modifies the eigenspectrum of the Hamiltonian and introduces anharmonicity. Injecting Eq. (2.18) into (2.13) and expressing the Hamiltonian in terms of the previously introduced creation and annihilation operators a and $a^\dagger$ yields

$$H = \hbar\omega_q \left(a^\dagger a + \frac{1}{2}\right) - E_J \phi_{ZPF}^4 \frac{\left(a^\dagger + a\right)^4}{24}, \tag{2.19}$$

where $\phi_{FPZ} = \frac{1}{\Phi_0}\sqrt{\hbar Z/2}$ is the zero-point phase fluctuation and ω_q is the qubit frequency. Restricting H to excitation-preserving terms[1], it takes the form

$$\boxed{H = \hbar(\omega_q - \alpha) a^\dagger a - \frac{\hbar\alpha}{2} a^\dagger a^\dagger a a,} \tag{2.20}$$

where $\alpha = E_J \phi_{ZPF}^4/2 = -E_C$ [4].
Furthermore, since the terms proportional to α takes their origin within the higher order of the series expansion (2.18), we have $|\hbar\alpha| \ll \hbar\omega_q$ meaning that the transmon qubit is eventually a weakly anharmonic oscillator. Hence, provided that $|\alpha|$ is sufficiently large to prevent non computational states to be excited, this weakly anharmonic oscillator can be treated as a two-level system and the Hamiltonian can be simplified to

$$H = \frac{\omega_q}{2}\sigma_z, \tag{2.21}$$

where σ_z is the Pauli-z operator and we adopted the convention $\hbar = 1$ which we will keep throughout this thesis [4] .

Theoretical Concept 2.4. Pauli operator σ_z

In a two-level system with a basis $\{|g\rangle, |e\rangle\}$, σ_z is defined as $\sigma_z = |e\rangle\langle e| - |g\rangle\langle g|$ [9].
Hence, σ_z applied on the excited state $|e\rangle$ gives $+|e\rangle$, while it leads to $-|g\rangle$ if applied on the ground state $|g\rangle$.
Introducing the ladder operators restricted to the two-level subspace: $\sigma_+ = |e\rangle\langle g|$ and $\sigma_- = |g\rangle\langle e|$, which play the role of $a^\dagger$ ad a within the truncated Hilbert space, we have $\sigma_+\sigma_- = (\sigma_z + \mathbb{1})/2$.
Since, the Hamiltonian is defined up to an irrelevant constant, we have $H = \omega_q\sigma_+\sigma_-$ is equivalent to $H = \omega_q\sigma_z/2$.

2.2 Readout

In order to access the information encoded in the transmon, the idea is to couple the qubit to an external electromagnetic field in the microwave regime. However, to avoid destroying the state during the measurement process, the transmon is not measured directly. Instead, it is coupled

[1] "excitation-preserving terms" are terms where a and $a^\dagger$ appear in equal quantities. Hence, $\left(a + a^\dagger\right)^4 \simeq 6a^\dagger a^\dagger a a + 12 a^\dagger a$.

to a resonator, which in turn interacts with the applied electromagnetic field, as illustrated in Figure 2.2. This architecture enables a quantum non-demolition measurement by probing the microwave cavity mode of the resonator, thereby allowing information about the qubit state to be extracted while preserving it [31].

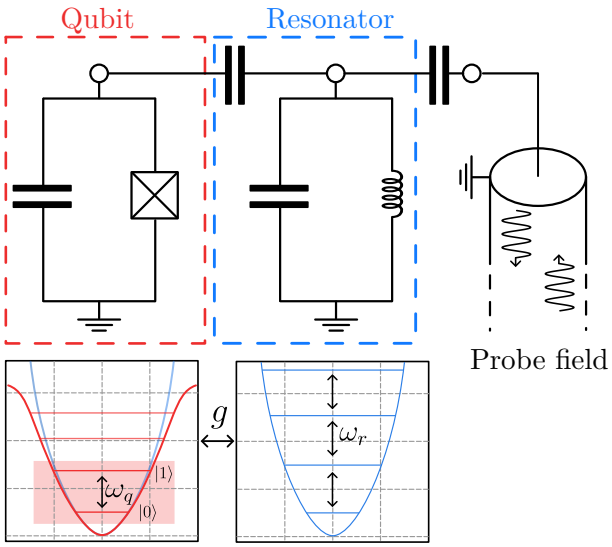

Figure 2.2: Fundamental architecture for the measurement of a superconducting qubit. The transmon superconducting qubit (in red) is coupled to a resonator (in blue) which is probed by a microwave electromagnetic field.

The system "qubit + resonator", where the qubit and the resonator are coupled through a capacitor, can be described by the Jaynes-Cummings (JC) Hamiltonian [4]:

$$\boxed{H_{JC} = \frac{1}{2}\omega_q \sigma_z + \omega_r a^\dagger a + g(\sigma_+ a + \sigma_- a^\dagger),} \tag{2.22}$$

where ω_q is the transition frequency of the qubit, ω_r is the transition frequency of the resonator, g is the coupling rate describing the interaction and a ($a^\dagger$) and σ_+ (σ_-) are the raising (lowering) operators of the resonator and the qubit, respectively. The Jaynes-Cummings Hamiltonian is commonly used in the field of quantum optics to model the interaction between a two-level atom and a cavity described by a single quantized mode [32]. In this sense, the term "cavity" will be used interchangeably with "resonator".
Furthermore, the driving of the resonator by the electromagnetic field can be treated semi-classically and added with the following Hamiltonian:

$$H_d = \epsilon a e^{i\omega_d t} + \epsilon^* a^\dagger e^{-i\omega_d t}, \tag{2.23}$$

where ϵ sets the drive strength/amplitude and ω_d corresponds to the drive frequency [5].
Finally, the total Hamiltonian describing the non-demolition readout of a superconducting qubit is given by

$$H = \frac{1}{2}\omega_q \sigma_z + \omega_r a^\dagger a + g(\sigma_+ a + \sigma_- a^\dagger) + \epsilon a e^{i\omega_d t} + \epsilon^* a^\dagger e^{-i\omega_d t}. \tag{2.24}$$

Now that the Hamiltonian describing the readout of a superconducting qubit has been derived, let us move on to the dissipative dynamics of the system. Indeed, the resonator must be considered "leaky" since we need to monitor the output field of the cavity to obtain indirect information about the state of the qubit. In this sense, the Lindblad master equation describing the system

is

$$\boxed{\dot{\rho} = -i\,[H, \rho] + \gamma\left(a\rho a^\dagger - \frac{1}{2}\{a^\dagger a, \rho\}\right),} \tag{2.25}$$

where ρ is the density operator corresponding to the state of the system "qubit + resonator" and γ represents the loss rate of excitations in the resonator [33]. As introduced in Section 1.3, the first term of (2.25) accounts for the unitary evolution of the system while the second term is called the dissipator and describes the dissipative dynamics.

2.3 Dispersive Limit and Schrieffer-Wolff Transformation

Let us consider the system "qubit + resonator" and rewrite the JC Hamiltonian describing it :

$$H_{JC} = \underbrace{\frac{1}{2}\omega_q\sigma_z + \omega_r a^\dagger a}_{\equiv H_0} + \underbrace{g(\sigma_+ a + \sigma_- a^\dagger)}_{\equiv V}. \tag{2.26}$$

The dispersive limit stands for the case when the detuning between the qubit and the resonator is large compared with the coupling rate, i.e., $|\omega_q - \omega_r| \gg g$. In this case, the JC Hamiltonian can be expanded in terms of g/Δ (with $\Delta \equiv \omega_q - \omega_r$) and a second-order Hamiltonian, known as dispersive Hamiltonian, can be derived, within the limit of a few photons in the resonator ($n < \Delta^2/(4g^2)$) [4]. This approximation is called the "dispersive approximation" and gives

$$H_{\text{disp}} = \frac{1}{2}\left(\omega_q + \chi\right)\sigma_z + \left(\omega_r + \chi\sigma_z\right)\left(a^\dagger a + \frac{1}{2}\right), \tag{2.27}$$

where $\chi = g^2/\Delta$ is referred to as the *dispersive shift*.

The last Hamiltonian shows that, in the dispersive limit, the qubit and the resonator do not exchange energy anymore. However, the frequency of the resonator is shifted by an amount dependent of the qubit state through the appearance of the term $\chi\sigma_z a^\dagger a$. Hence, probing the resonator enables to infer information about the qubit state as illustrated in Figure 2.3. Additionally, the frequency of the qubit is displaced by a lamb shift χ due to vacuum fluctuations in the resonator.

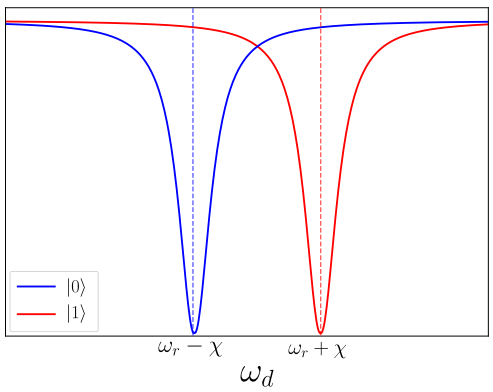

Figure 2.3: Illustration of the absorption spectrum of the resonator obtained by probing it with an external field (see Figure 2.2). The graph shows that the resonator spectrum differs depending on the qubit state ($|0\rangle \equiv$ground state or $|1\rangle \equiv$excited state), as expected from Eq. (2.27)[4].

The standard derivation of this second-order dispersive Hamiltonian (2.27) uses the so-called

Schrieffer-Wolff transformation [34]. It corresponds to the application of a unitary transformation on H_{JC}, i.e., $H' = e^S H_{JC} e^{-S}$ allowing for a direct expansion of the Hamiltonian using the *Baker-Campbell-Hausdorff formula*

$$\boxed{H' = e^S H e^{-S} = \sum_{n=0}^{\infty} \frac{[S,H]^{(n)}}{n!},} \tag{2.28}$$

where

$$[S,H]^{(n)} \equiv [S,[S,H]^{(n-1)}],$$

and

$$[S,H]^{(0)} = H,$$

or in a more explicit way $H^{(n)} \equiv [\overbrace{S,[\ldots,[S}^{n \text{ times}},H]\ldots]]$ [34, 35].

In the case of the JC Hamiltonian $H_{JC} = H_0 + V$, the formula, to first order in V yields

$$H' = H_0 + V + [S,H_0] + [S,V] + \frac{1}{2}[S,[S,H_0]] + \frac{1}{2}[S,[S,V]] + \mathcal{O}(V^2). \tag{2.29}$$

Furthermore, the operator S defining the unitary application is chosen to make the transformed Hamiltonian H' diagonal to first order in V. Hence, S is chosen so that

$$[S,H_0] = -V, \tag{2.30}$$

in order to remove the off-diagonal term to the lowest order [34], which implies

$$S = \frac{g}{\Delta}(\sigma_- a^\dagger - \sigma_+ a).$$

As a consequence, (2.29) becomes

$$H' \simeq H_0 + \frac{1}{2}[S,V] \equiv H_{disp}. \tag{2.31}$$

Computing the commutator using the commutation relation $[a,a^\dagger] = \mathbb{1}$ along with the identities $\sigma_-\sigma_+ = \frac{1}{2}(\mathbb{1}+\sigma_z)$ and $\sigma_+\sigma_- = \frac{1}{2}(\mathbb{1}-\sigma_z)$ renders the dispersive Hamiltonian (2.27).

The Schrieffer-Wolff transformation that was just presented can be applied to any Hamiltonian which can be decomposed into an unperturbed part H_0 and a perturbation V. The condition (2.30) involves that V is anti-Hermitian, i.e. $V^\dagger = -V$, which guaranties the unitarity of the similarity transformation (2.28) [34].

Theoretical Concept 2.5. Similarity transformation

A similarity transformation applied to an operator A takes the form $A \to A' = X^{-1}AX$ for an invertible operator X and preserves the spectrum of A. Hence a unitary transformation is a specific case of similarity transformation where X is unitary, i.e., $X^\dagger = X^{-1}$.

2.4 Accuracy of the Dispersive Approximation

In the final section of this chapter about the dispersive readout of superconducting qubits, we examine the validity of the dispersive approximation and its limitations. Indeed, although the dispersive approximation is widely used in the literature due to its excellent agreement with

experimental results, it restricts the set of usable parameters: typically g must remain small compared to the detuning Δ between the qubit and the cavity.

Figures 2.4 to 2.6 in the following pages present numerical simulations for a qubit of frequency ω_q coupled (through a coupling parameter g) to a resonator of frequency ω_r with damping rate γ. The graphs show the time evolutions of $\langle\sigma_z\rangle$ for the qubit and of $\langle a^\dagger a\rangle$ corresponding to the average number of excitations in the resonator. They illustrate the failure of the dispersive approximation in the case of a qubit initially prepared in its excited (or ground) state, i.e., $\langle\sigma_z\rangle = 1$ (or $\langle\sigma_z\rangle = -1$), and a resonator initially prepared in its ground state, i.e., the vacuum, $\langle a^\dagger a\rangle$=0. Indeed, it completely neglects any energy exchange between the qubit and the cavity, meaning that, if the qubit is prepared in its excited state, it remains in this state since the dispersive approximation prevents both decay into the resonator and excitation through it, and similarly if the qubit is prepared in its ground state. However, the resonator has its state modified as a result of the drive excitation.

For a small coupling strength g, compared to the detuning, the resonator dynamics obtained within the dispersive approximation is in excellent agreement with the exact result in the case of a driven cavity, even though the qubit dynamics does not reproduce the exact evolution, as illustrated in Figure 2.4 d) and Figure 2.5 d).
In contrast, when g becomes significant compared to the detuning, meaning that the coupling between the qubit and the cavity can no longer be neglected, the cavity dynamics under the dispersive approximation begins to deviate from the exact dynamics, as shown in Figure 2.4 f) and Figure 2.6 d).

This observation is the starting point of the research conducted in this master's thesis. Indeed, the dispersive approximation is derived by applying the Schrieffer-Wolff transformation to the Hamiltonian describing the qubit coupled to the cavity. However, when the coupling between them becomes large, this model is no longer sufficient. A potential solution investigated in this master's thesis relies on applying the Schrieffer-Wolff transformation, not to the Hamiltonian, but rather to the Liouvillian in order to obtain a better reduced description of the qubit dynamics. The general method will be presented in Chapter 3, followed by an application to the system of a qubit coupled to a damped resonator in Chapter 4.

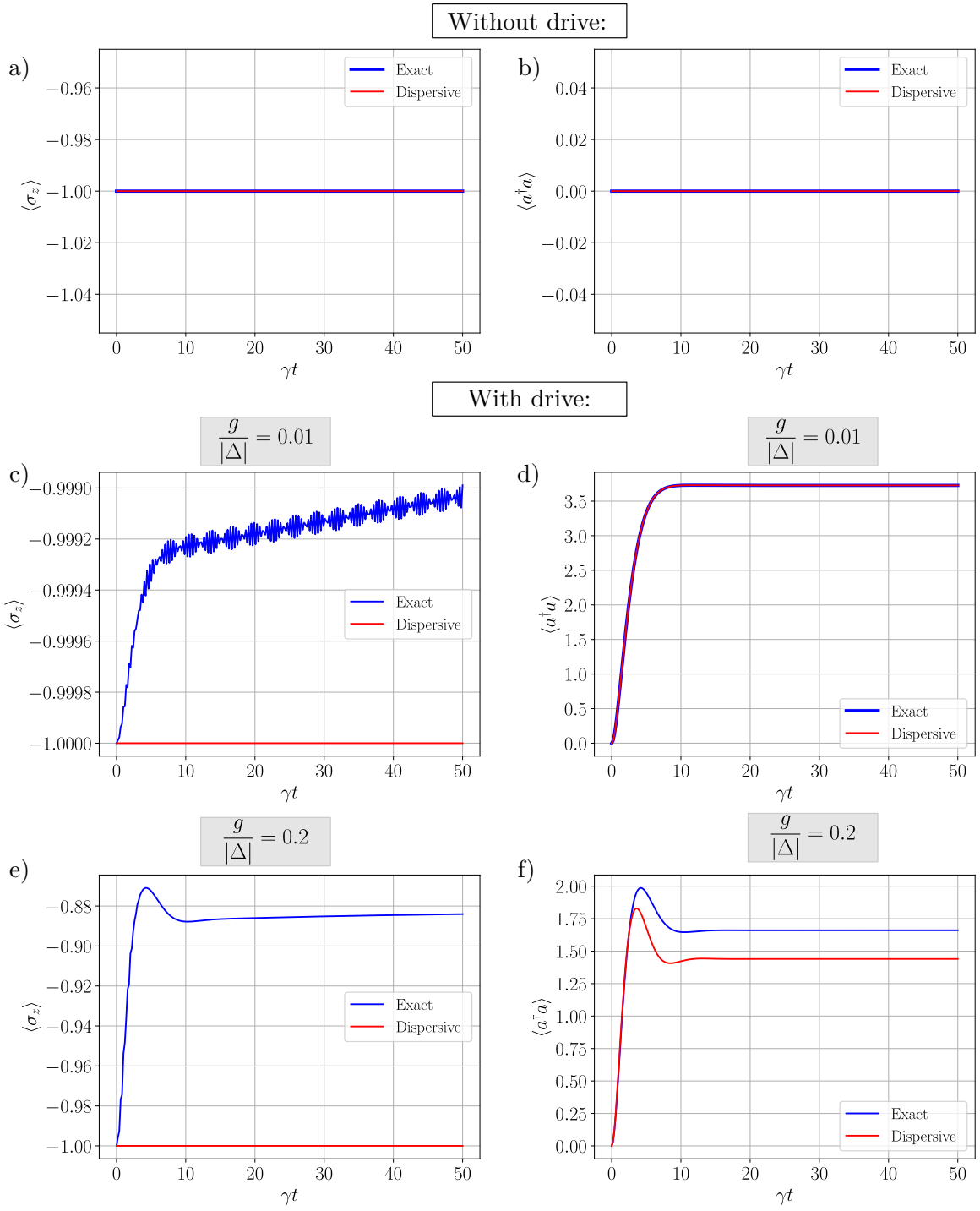

Figure 2.4: Time-dependent dynamics of $\langle\sigma_z\rangle$ (first column) and $\langle a^\dagger a\rangle$ (second column) for the qubit initially prepared in its ground state and the resonator in the vacuum state, for different values of g to highlight the regime of validity of the dispersive approximation. a, b) The resonator is damped but not driven. No dynamics takes place because the initial state of the system is the ground state, for any g and Δ. c, d, e, f) The resonator is damped and driven with a drive intensity ϵ and a frequency ω_d for $g/|\Delta| = 0.01$ (panels c and d) and for $g/|\Delta| = 0.2$ (panels e and f). c, d) $g/|\Delta|$ is sufficiently small for the dispersive Hamiltonian to reproduce accurately the exact dynamics of the driven cavity (see panel d) even though the qubit dynamics is not accounted for (see panel c). e, f) $g/|\Delta|$ is not small enough such that the dynamics of the driven cavity in the dispersive approximation deviates from the exact dynamics (see panel f). Moreover, comparing c) with e), we see a stronger deviation from the exact dynamics in e) where $g/|\Delta|$ is larger.
Numerical parameters: c, d) $g = 0.1$ GHz. e, f) $g = 2$ GHz. c, d, e, f) $\omega_q = 1$ GHz, $\omega_r = \omega_d = 11$ GHz, $\gamma = 0.6$ GHz , $\epsilon = 0.6$ GHz

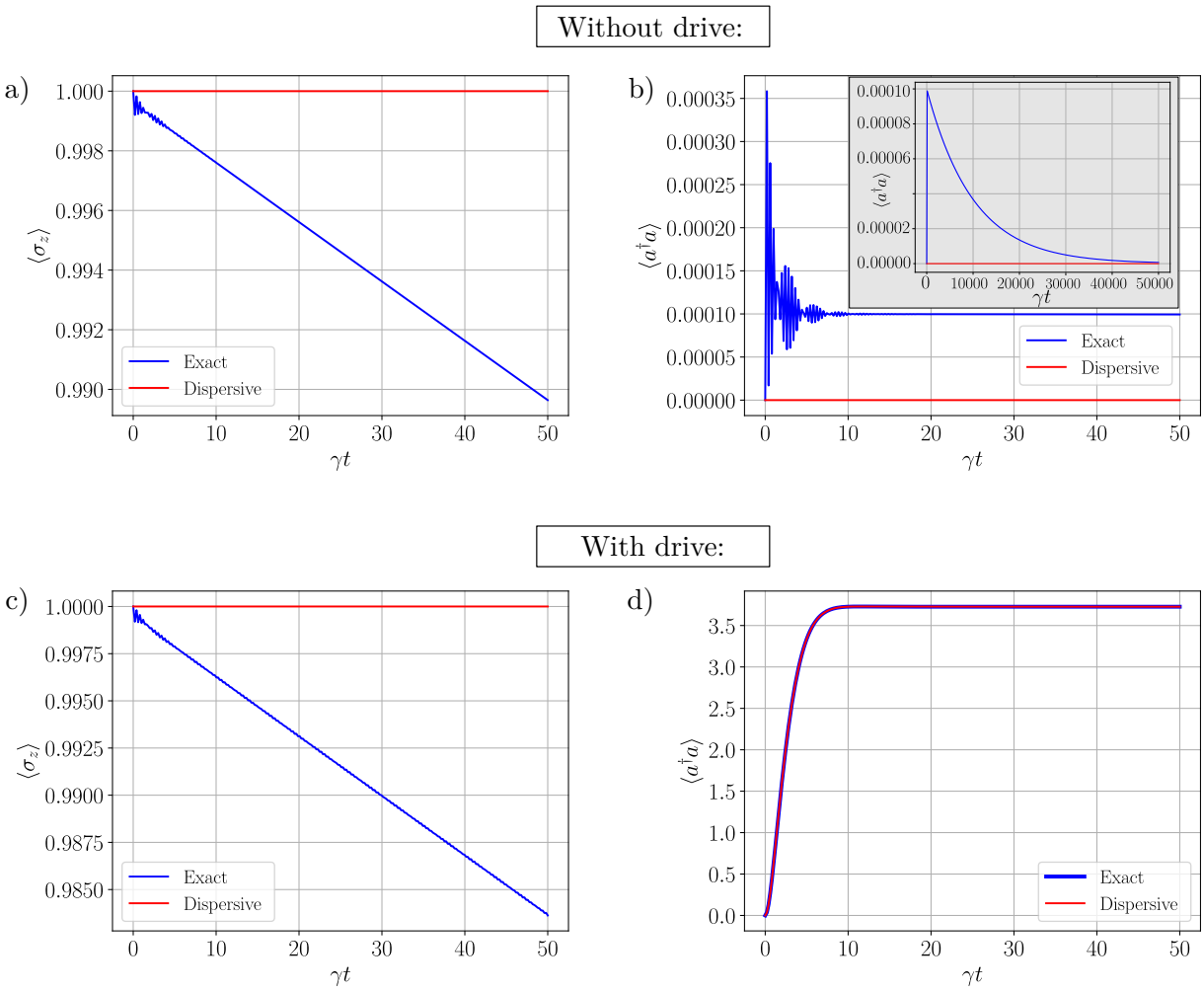

Figure 2.5: Time-dependent dynamics of $\langle\sigma_z\rangle$ (first column) and $\langle a^\dagger a\rangle$ (second column) for the qubit initially prepared in its excited state and the resonator in the vacuum state. a, b) The resonator is damped but not driven. The exact dynamics shows the qubit slow decay into the cavity, which is not reproduced by the dispersive approximation. The exact dynamics of the cavity represented by $\langle a^\dagger a\rangle$ shows exchanges between the qubit and the cavity which leads to damped oscillations due to the cavity damping rate. The cavity decays to $\langle a^\dagger a\rangle = 0$, at first sight it may appear differently in b) but it is in fact a transient dynamics that takes place and the analysis of a substantially longer timescale shows the decay to zero as presented in the included graph with gray background. c, d) The resonator is damped and driven with a drive intensity ϵ and a frequency ω_d. Here, $g/|\Delta| = 0.01$ is sufficiently small, thus the dispersive Hamiltonian reproduces accurately the exact dynamics of the driven cavity (see d)) even though the qubit decay is not accounted for (see c)).
Numerical parameters: $g = 0.1$ GHz, $\omega_q = 1$ GHz, $\omega_r = \omega_d = 11$ GHz, $\gamma = 0.6$ GHz , $\epsilon = 0.6$ GHz

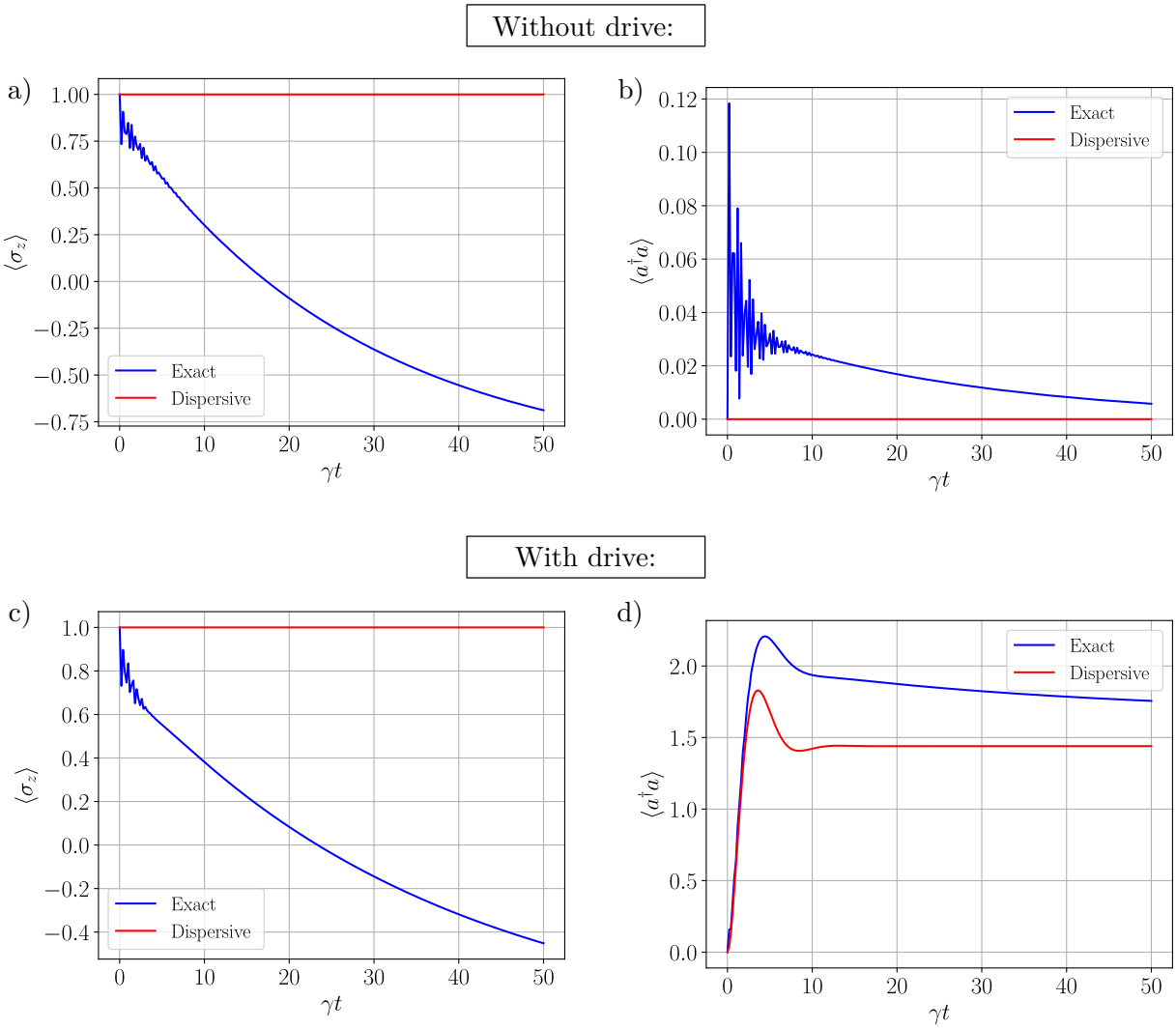

Figure 2.6: Time-dependent dynamics of $\langle\sigma_z\rangle$ (first column) and $\langle a^\dagger a\rangle$ (second column) for the qubit initially prepared in its excited state and the resonator in the vacuum state. Here, $g/|\Delta| = 0.2$. It corresponds to a regime where the dispersive approximation is inaccurate. a, b) The resonator is damped but not driven. As in Figure 2.5 a), the exact dynamics shows the qubit decay into the cavity, which is not reproduced by the dispersive approximation, moreover the decay is significantly stronger compared to Figure 2.5 a) due to the larger ratio $g/|\Delta|$. The exact dynamics of the cavity again shows exchanges between the qubit and the cavity which lead to damped oscillations to zero. c, d) The resonator is damped and driven with a drive intensity ϵ and a frequency ω_d. Since $g/|\Delta|$ is not small enough, the dynamics of the driven cavity in the dispersive approximation deviates from the exact dynamics (see d)). Moreover, comparing c) with Figure 2.5 c), we see a stronger deviation from the exact dynamics in the present case where $g/|\Delta|$ is larger.
Numerical parameters: $g = 2$ GHz, $\omega_q = 1$ GHz, $\omega_r = \omega_d = 11$ GHz, $\gamma = 0.6$ GHz , $\epsilon = 0.6$ GHz

Summary 2. Dispersive readout of a transmon

First, Chapter 2 introduced the physical system underlying the readout of a superconducting qubit. Starting from the quantization of an LC circuit behaving as a quantum harmonic oscillator, we established that replacing the linear inductance by a Josephson junction introduces anharmonicity in the energy spectrum. Working in a specific regime enables to isolate the two lowest energy levels and describe the transmon as an effective two-level quantum system, i.e., a qubit described by the Hamiltonian

$$H = \frac{\omega_q}{2}\sigma_z. \tag{2.21}$$

Moreover, the readout of a qubit is performed by coupling it to a microwave resonator which is probed by an external magnetic field, leading to the total Hamiltonian:

$$H = \frac{1}{2}\omega_q\sigma_z + \omega_r a^\dagger a + g(\sigma_+ a + \sigma_- a^\dagger) + \epsilon\left(ae^{i\omega_d t} + a^\dagger e^{-i\omega_d t}\right). \tag{2.24}$$

In the dispersive regime $|\Delta| = |\omega_q - \omega_r| \gg g$, a Schrieffer-Wolff transformation removes the direct qubit-resonator exchange to second order and yields the dispersive Hamiltonian for the system "qubit+resonator":

$$H_{\text{disp}} = \frac{1}{2}\left(\omega_q + \chi\right)\sigma_z + \left(\omega_r + \chi\sigma_z\right)\left(a^\dagger a + \frac{1}{2}\right), \tag{2.27}$$

which results in the resonator frequency being dependent of the state of the qubit allowing for a nondestructive readout of the qubit.

Finally, numerical examples show that this approximation works well for small $g/|\Delta|$, but fails when the coupling increases. This motivates the application of the Schrieffer-Wolff method directly to the Liouvillian in the following chapters.

Chapter 3

Generalized Schrieffer-Wolff Method

As seen in the previous chapter, the standard Schrieffer-Wolff method is a type of perturbation theory which consists in the application onto the exact Hamiltonian of a unitary transformation enabling the derivation of a diagonal Hamiltonian describing the system's low-energy dynamics. This section presents the generalization of this formalism to Liouvillians, as introduced by Kessler in "Generalized Schrieffer-Wolff Formalism for Dissipative Systems" [7]. To this end, Section 3.1 formulates the general framework underlying the subsequent derivation and Section 3.2 establishes the main result upon which the rest of this thesis relies.

3.1 General Framework

In analogy with the Hamiltonian Schrieffer-Wolff transformation, the goal is to find a similarity transformation such that the Liouvillian becomes block-diagonal (instead of diagonal in the Hamiltonian case).

We consider the case of an open quantum system described by a Lindblad ME where the Liouvillian is time-independent, diagonalizable and can be written as the addition of an unperturbed term $\mathcal{L}_0$ and a perturbation $\epsilon\mathcal{V}$ as follows

$$\dot{\rho}(t) = \mathcal{L}\rho(t) = (\mathcal{L}_0 + \epsilon\mathcal{V})\,\rho(t), \tag{3.1}$$

where ϵ is a dimensionless perturbation parameter and ρ is the density operator of the system. First, let us recall the vectorized formalism, introduced in Section 1.4, implying that the superoperators $\mathcal{L}$, $\mathcal{L}_0$ and $\mathcal{V}$ can be represented by matrices while the density matrix ρ can be mapped to a vector. Within this framework, the left and right eigenvectors $|l_i\rangle\!\rangle$ and $|r_i\rangle\!\rangle$ of the non-Hermitian superoperator $\mathcal{L}_0$ can be computed as follows:

$$\mathcal{L}_0|r_i\rangle\!\rangle = \lambda_i|r_i\rangle\!\rangle, \tag{3.2}$$

$$\langle\!\langle l_i|\mathcal{L}_0 = \lambda_i\langle\!\langle l_i|. \tag{3.3}$$

Let us recall that the eigenvalues λ_i are in general complex since $\mathcal{L}_0$ is non-Hermitian. Furthermore, we define two subsets within the spectrum of $\mathcal{L}_0$:

$$\mathcal{P} = \{\lambda_\alpha|\lambda_\alpha = 0\} \neq \{\}\,, \tag{3.4}$$

corresponding to the zero eigenvalues of $\mathcal{L}_0$, and

$$\mathcal{Q} = \{\lambda_i|\lambda_i \neq 0\} \tag{3.5}$$

denoting the non-zero eigenvalues of $\mathcal{L}_0$. Henceforth, the Greek and Arabic indices will correspond to the sets $\mathcal{P}$ and $\mathcal{Q}$, respectively. Subsequently, (generally non-orthogonal) projectors[1] onto the corresponding subspaces are introduced as

$$P = \sum_{\alpha:\lambda_\alpha \in \mathcal{P}} |r_\alpha\rangle\rangle\langle\langle l_\alpha|, \tag{3.6}$$

$$Q = \mathbb{1} - P = \sum_{i:\lambda_i \in \mathcal{Q}} |r_i\rangle\rangle\langle\langle l_i|, \tag{3.7}$$

and define the so-called *slow* and *fast spaces*, respectively [7].
These subspaces allow for the definition of a useful block configuration for an arbitrary linear superoperator A in the $\mathcal{L}_0$-eigenbasis as

$$A = \begin{pmatrix} \overline{A^P} & \overline{A^-} \\ \overline{A^+} & \overline{A^Q} \end{pmatrix} = \begin{pmatrix} \overline{PAP} & \overline{PAQ} \\ \overline{QAP} & \overline{QAQ} \end{pmatrix}, \tag{3.8}$$

where we introduced $A^P = PAP$, $A^Q = QAQ$, $A^+ = QAP$ and $A^- = PAQ$, along with the overline notation, which denotes their reduced representation. Indeed, the expressions (3.6)-(3.7) define the projectors P and Q as square matrices of dimension $d^2 \times d^2$ with d being the dimension of the density matrix. Additionally, A being (in the vectorized formalism) a matrix of dimension $d^2 \times d^2$, the product PAP is ultimately a $d^2 \times d^2$ matrix. Consequently, PAP is the full size matrix where the only non-zero element is the upper-left block, i.e.,

$$A^{\mathrm{P}} \equiv PAP = \begin{pmatrix} \overline{A^P} & \mathbb{0} \\ \mathbb{0} & \mathbb{0} \end{pmatrix}. \tag{3.9}$$

Naturally, the notations A^+, A^- and A^Q and their reduced representation $\overline{A^+}$, $\overline{A^-}$ and $\overline{A^Q}$ can be understood accordingly.

The following notations are also introduced for the block diagonal and block off-diagonal parts of the operator A

$$A^{\mathrm{D}} = \begin{pmatrix} \overline{A^P} & \mathbb{0} \\ \mathbb{0} & \overline{A^Q} \end{pmatrix}, \tag{3.10}$$

$$A^{\mathrm{O}} = \begin{pmatrix} \mathbb{0} & \overline{A^-} \\ \overline{A^+} & \mathbb{0} \end{pmatrix}, \tag{3.11}$$

respectively [7].

From this representation, it is for instance immediate to see that $\mathcal{L}_0^P = P\mathcal{L}_0 P = 0$ by definition of P which projects onto the slow subspace relative to its zero eigenvalues. Similarly, $\mathcal{L}_0^+ = 0$ and $\mathcal{L}_0^- = 0$, since $\mathcal{L}_0$ is diagonal in its own basis. We can thus write $\mathcal{L}_0 = \mathcal{L}_0^{\mathrm{D}} = \mathcal{L}_0^Q$.
On the other hand, the perturbation in general includes both diagonal and off-diagonal elements, i.e., $\mathcal{V} = \mathcal{V}^{\mathrm{D}} + \mathcal{V}^{\mathrm{O}}$.

After establishing the theoretical background and clarifying the notations, we can now focus on the generalized Schrieffer-Wolff transformation.
As presented earlier, the aim is to find a similarity transformation

$$\mathcal{L} \to L = U^{-1}\mathcal{L}U, \tag{3.12}$$

[1] A square matrix P is a projector if $P^2 = P$. P is orthogonal if $PP^T = P^TP \Rightarrow P^T = P^{-1}$.

choosing U to make the transformed Liouvillian L block-diagonal, i.e.,

$$\boxed{L^{\mathrm{O}} = 0,} \tag{3.13}$$

leading to the decoupling of the slow and fast spaces and L conserving the same spectrum as $\mathcal{L}$.

Since $\mathcal{V}$ is a bounded operator[2], the perturbation induces a displacement of the eigenvalues in the complex plane of at most $\epsilon\|\mathcal{V}\|$. Thus, in the perturbative regime where the Liouvillian gap Δ is larger than $2\epsilon\|\mathcal{V}\|$, the separation between the eigenvalues in $\mathcal{P}$ and $\mathcal{Q}$ is preserved. This means that the perturbation may change the actual positions of the eigenvalues, but they nevertheless remain within their respective subspaces (see Figure 3.1) [7].

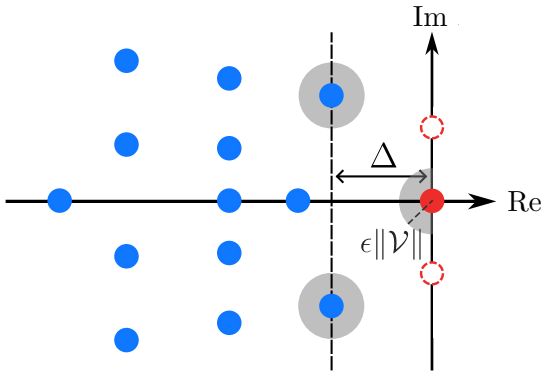

Figure 3.1: Schematic representation of the spectrum of $\mathcal{L}_0$ wiht Δ the associated Liouvillian gap as introduced in Section 1.5. The subspace $\mathcal{P}$ of zero eigenvalues of $\mathcal{L}_0$ corresponds to the solid red dot, which is associated with the steady state(s) of the system. Additionally, the subspace $\mathcal{Q}$, corresponding to the non-zero eigenvalues of $\mathcal{L}_0$, contains the blue dots and red dashed circles, related to dissipative and oscillating modes, respectively, as explained in Section 1.5. When a bounded perturbation $\epsilon\mathcal{V}$ is added to $\mathcal{L}_0$, the eigenvalues are displaced within the gray disks of radius $\epsilon\|\mathcal{V}\|$ surrounding them. In the perturbative regime, this displacement nonetheless preserves a spectral separation between the subspaces $\mathcal{P}$ and $\mathcal{Q}$.

Therefore, the following *effective Liouvillian*

$$L_{\mathrm{eff}} = PLP \tag{3.14}$$

coincides with the exact low-excitation spectrum of $\mathcal{L}$ and the dynamics of the system near the steady state is accurately described by the following master equation:

$$\dot{\mu} = L_{\mathrm{eff}}\mu, \tag{3.15}$$

where we introduced the reduced density matrix μ on the slow subspace [7].

3.2 Derivation of the Expansion

As in the Hamiltonian case, the main asset of the method resides in the fact that the transformation (3.12) enables a direct expansion of L via the Baker-Campbell-Hausdorff formula (2.28). Indeed, in [7], Kessler considers the so-called "canonical" choice $U = e^S$ imposing S to be block off-diagonal, i.e., $S^{\mathrm{D}} = 0$[3]. Hence, the Baker-Campbell-Hausdorff formula (2.28) introduced in

[2] If $\mathcal{V}$ is not bounded, it can always be truncated through physical justifications.

[3] Other choices are possible with $S^{\mathrm{D}} \neq 0$ leading to different perturbation theories but these lie outside the scope of this thesis.

the previous chapter yields

$$L = e^{-S}\mathcal{L}e^{S} = \sum_{n=0}^{\infty} \frac{[S,\mathcal{L}]^{(n)}}{n!}. \tag{3.16}$$

Furthermore, introducing the notation $\hat{A}$, expressing the commutator with an operator A as

$$\hat{A}B = [A, B] \tag{3.17}$$

when applied to an arbitrary operator B, yields

$$\boxed{L \equiv \sum_{n=0}^{\infty} \frac{\hat{S}^n}{n!}\mathcal{L} = e^{\hat{S}}\mathcal{L}.} \tag{3.18}$$

Theoretical Concept 3.1. Behavior of $\hat{S}\cdot = [S, \cdot]$

Recalling that S is block off-diagonal, it can be shown that the superoperator $\hat{S} = [S, \cdot]$ flips the diagonal/off-diagonal characteristic of the matrix on which it acts.
Indeed, if O is a purely block off-diagonal matrix and D is a purely diagonal matrix, $\hat{S}O$ is block diagonal while $\hat{S}D$ is block off-diagonal, i.e.,

$$\left(\hat{S}O\right)^{\mathrm{O}} = 0,$$
$$\left(\hat{S}D\right)^{\mathrm{D}} = 0.$$

Hence, if an even power of $\hat{S}$ is applied on O (D), the result will stay block off-diagonal (diagonal). However, if an odd power of $\hat{S}$ is applied, the block structure will change.

As a consequence, since the superoperator $\mathbf{cosh}(\hat{\mathbf{S}})$ only contains even powers of $\hat{S}$, it **keeps the diagonal/off-diagonal character unchanged**. **In opposition,** $\mathbf{sinh}(\hat{\mathbf{S}})$ contains only odd powers of $\hat{S}$, thus it **flips the matrix from block diagonal to block off-diagonal, or conversely**.

At this point, in order to get the expressions of the different terms in the series expansion, we must derive a general expression for S.
In the light of this, the condition (3.13) is rewritten as [7]

$$L^{\mathrm{O}} = 0 \Leftrightarrow \left(e^{\hat{S}}\mathcal{L}\right)^{\mathrm{O}} = 0 \tag{3.19}$$

and yields

$$\boxed{\hat{S}\mathcal{L}_0 = -\hat{S}\epsilon\mathcal{V}^{\mathrm{D}} - \epsilon\hat{S}\coth(\hat{S})\mathcal{V}^{\mathrm{O}}.} \tag{3.20}$$

Proof. In order to prove the relation (3.20), let us decompose $\mathcal{L}$ in its diagonal and off-diagonal blocks

$$\begin{aligned} L^{\mathrm{O}} = 0 &\Leftrightarrow \left(e^{\hat{S}}\mathcal{L}\right)^{\mathrm{O}} = 0 \\ &\Leftrightarrow \left(e^{\hat{S}}\left(\mathcal{L}^{\mathrm{D}} + \mathcal{L}^{\mathrm{O}}\right)\right)^{\mathrm{O}} = 0. \end{aligned} \tag{3.21}$$

Then, let us decompose $e^{\hat{S}}$ into its even and odd terms [7]

$$e^{\hat{S}} = \cosh(\hat{S}) + \sinh(\hat{S}). \tag{3.22}$$

Due to the properties mentioned in Theoretical Concept 3.1, $\cosh(\hat{S})$ keeps the block-diagonal structure of L while $\sinh(\hat{S})$ flips it and the condition (3.21) becomes

$$\sinh(\hat{S})\mathcal{L}^{\mathrm{D}} + \cosh(\hat{S})\mathcal{L}^{\mathrm{O}} = 0. \tag{3.23}$$

Multiplying by the inverse of $\sinh(\hat{S})$ and then by $\hat{S}$ yields[4]

$$\hat{S}\mathcal{L}^{\mathrm{D}} + \hat{S}\coth(\hat{S})\mathcal{L}^{\mathrm{O}} = 0.$$

Finally, making use of $\mathcal{L}^{\mathrm{D}} = \mathcal{L}_0 + \epsilon\mathcal{V}^{\mathrm{D}}$ and $\mathcal{L}^{\mathrm{O}} = \epsilon\mathcal{V}^{\mathrm{O}}$ renders Eq. (3.20). □

Furthermore, solving (3.20) yields an implicit expression for the matrix S generating the Schrieffer-Wolff transformation that renders the Liouvillian operator block diagonal:

$$S = \epsilon\mathcal{R}_0\left(\hat{S}\mathcal{V}^{\mathrm{D}}\right) + \epsilon\mathcal{R}_0\left(\hat{S}\coth(\hat{S})\mathcal{V}^{\mathrm{O}}\right), \tag{3.24}$$

where we introduced the resolvent operator

$$\mathcal{R}_0(\cdot) = Q\mathcal{L}_0^{-1}\cdot P - P\cdot\mathcal{L}_0^{-1}Q, \tag{3.25}$$

giving particularly $\mathcal{R}_0(\hat{X}\mathcal{L}_0) = -X$ with X being a purely block off-diagonal operator[7].
The hyperbolic functions of the superoperator $\hat{S}$ are understood as formal Taylor series. Hence, the manipulations involving $\cosh(\hat{S})$, $\sinh(\hat{S})$ and $\hat{S}\coth(\hat{S})$ are well-defined for infinitesimal $\hat{S}$, which is ensured by a sufficiently small perturbation parameter ϵ [36].

Theoretical Concept 3.2. Resolvent Operator

A resolvent of an operator works as a generalized inverse for this operator. In this precise case, solving (3.20) would require to invert $\mathcal{L}_0$. However, $\mathcal{L}_0$ is not invertible on the full space because it contains zero eigenvalues (corresponding to the slow space $\mathcal{P}$). Hence, a restricted inverse $\mathcal{L}_0^{-1} \equiv (Q\mathcal{L}_0Q)^{-1}$ on the fast subspace is introduced and the resolvent operator $\mathcal{R}_0$ is defined in order to inverse the map $X \to [\mathcal{L}_0, X]$ where X is a block off-diagonal operator.

Having derived the implicit expression (3.24) for S depending on Q, P, $\mathcal{L}_0$ and $\mathcal{V}$, we return to (3.18) and recall that L is constructed by the similarity transformation to be block-diagonal such that

$$L = L^{\mathrm{D}} = \left(e^{\hat{S}}\mathcal{L}\right)^{\mathrm{D}}, \tag{3.26}$$

which leads to

$$\boxed{L = \mathcal{L}_0 + \epsilon\left(\mathcal{V}^{\mathrm{D}} + \tanh(\hat{S}/2)\mathcal{V}^{\mathrm{O}}\right).} \tag{3.27}$$

[4] More precisely, one rewrites $\sinh(\hat{S}) = \frac{\sinh(\hat{S})}{\hat{S}}\hat{S}$ and multiplies by the inverse of $\sinh(\hat{S})/\hat{S}$ since $\sinh(\hat{S})$ is in fact not invertible but $\frac{\sinh(\hat{S})}{\hat{S}}$ is. Similarly, strictly speaking, $\hat{S}\coth(\hat{S})$ is not obtained by inverting $\sinh(\hat{S})$ directly. It denotes the regular Taylor series of the analytic function $x\coth x$ evaluated at $\hat{S}$.

Furthermore, defining

$$\boxed{\mathcal{W} = \epsilon \left(\mathcal{V}^{\mathrm{D}} + \tanh(\hat{S}/2)\mathcal{V}^{\mathrm{O}} \right),} \tag{3.28}$$

and substituting it into Eq. (3.27) yields

$$L = \mathcal{L}_0 + \mathcal{W}. \tag{3.29}$$

Hence, the effective Liouvillian in the slow space is given by

$$\boxed{L_{\mathrm{eff}} = PLP = P\mathcal{W}P,} \tag{3.30}$$

since by construction $P\mathcal{L}_0 P = 0$.

Proof. As in the proof for (3.20), let us separate $e^{\hat{S}}$ into its odd and even powers and $\mathcal{L}$ into its diagonal and off diagonal elements, in (3.26). Recalling the properties of $\cosh(\hat{S})$ and $\sinh(\hat{S})$ yields

$$L = L^{\mathrm{D}} = \cosh(\hat{S})\mathcal{L}^{\mathrm{D}} + \sinh(\hat{S})\mathcal{L}^{\mathrm{O}}. \tag{3.31}$$

Referring back to the fact that L is block diagonal, i.e., $L^{\mathrm{O}} = 0$ and rewriting the resulting criterion (3.23) as

$$\begin{aligned} L^{\mathrm{O}} &= \mathcal{L}^{\mathrm{O}} + \tanh(\hat{S})\mathcal{L}^{\mathrm{D}} = 0 \\ &\Leftrightarrow \mathcal{L}^{\mathrm{D}} = -\frac{1}{\tanh(\hat{S})}\mathcal{L}^{\mathrm{O}}. \end{aligned} \tag{3.32}$$

First, let us substitute this relation into (3.31), then add and subtract $\mathcal{L}^{\mathrm{D}}$ in order to rearrange the expression by applying (3.32) once more. Finally, using the hyperbolic identity $\sinh(x) - (\cosh(x) - 1)/\tanh(x) = \tanh(x/2)$, one obtains

$$\begin{aligned} L &= -\frac{\cosh(\hat{S})}{\tanh(\hat{S})}\mathcal{L}^{\mathrm{O}} + \sinh(\hat{S})\mathcal{L}^{\mathrm{O}} + \mathcal{L}^{\mathrm{D}} - \mathcal{L}^{\mathrm{D}} \\ &= -\frac{\cosh(\hat{S})}{\tanh(\hat{S})}\mathcal{L}^{\mathrm{O}} + \sinh(\hat{S})\mathcal{L}^{\mathrm{O}} + \mathcal{L}^{\mathrm{D}} + \frac{1}{\tanh(\hat{S})}\mathcal{L}^{\mathrm{O}} \\ &= \mathcal{L}^{\mathrm{D}} + \tanh(\hat{S}/2)\mathcal{L}^{\mathrm{O}}. \end{aligned}$$

In order to complete the derivation, we recall $\mathcal{L}^{\mathrm{D}} = \mathcal{L}_0 + \epsilon\mathcal{V}^{\mathrm{D}}$ and $\mathcal{L}^{\mathrm{O}} = \epsilon\mathcal{V}^{\mathrm{O}}$ to get Eq. (3.27). □

However, in general, the exact form of the matrix S that decouples the fast and slow space is difficult to find and the interest of the SW transformation resides in the ability to expand S in the perturbation parameter ϵ [7]:

$$S = \sum_{n=0}^{\infty} \epsilon^n S_n. \tag{3.33}$$

In fact, expanding both sides of Eq. (3.24) yields

$$\begin{aligned} S &= S_0 + \epsilon S_1 + \epsilon^2 S_2 + \epsilon^3 S_3 + \epsilon^4 S_4 + \epsilon^5 S_5 + \mathcal{O}(\epsilon^6) \\ &= \epsilon \mathcal{R}_0 \left(\left(\hat{S}_0 + \epsilon \hat{S}_1 + \epsilon^2 \hat{S}_2 + \epsilon^3 \hat{S}_3 + \epsilon^4 \hat{S}_4 + \mathcal{O}(\epsilon^5) \right) \mathcal{V}^{\mathrm{D}} \right) \\ &\quad + \epsilon \mathcal{R}_0 \left(\left(\mathbb{1} + \frac{\hat{S}^2}{3} - \frac{\hat{S}^4}{45} + \mathcal{O}(\hat{S}^6) \right) \mathcal{V}^{\mathrm{O}} \right), \end{aligned} \tag{3.34}$$

where we used the following expansion

$$\hat{S} \coth \hat{S} = \mathbb{1} + \frac{\hat{S}^2}{3} - \frac{\hat{S}^4}{45} + \mathcal{O}(\hat{S}^6). \tag{3.35}$$

Subsequently expanding $\hat{S}$ appearing in the $\hat{S}\coth(\hat{S})$ series[5] and identifying the coefficients of equal powers of ϵ on both sides of Eq. (3.34), we obtain

$$S_0 = 0 \tag{3.36a}$$
$$S_1 = \mathcal{R}_0 \left(\hat{S}_0 \mathcal{V}^{\mathrm{D}} \right) + \mathcal{R}_0 \mathcal{V}^{\mathrm{O}} = \mathcal{R}_0 \mathcal{V}^{\mathrm{O}} \tag{3.36b}$$
$$S_2 = \mathcal{R}_0 \left(\hat{S}_1 \left(\mathcal{V}^{\mathrm{D}} \right) \right) \tag{3.36c}$$
$$S_3 = \mathcal{R}_0 \left(\hat{S}_2 \left(\mathcal{V}^{\mathrm{D}} \right) \right) + \frac{1}{3} \mathcal{R}_0 \left(\hat{S}_1^2 \left(\mathcal{V}^{\mathrm{O}} \right) \right) \tag{3.36d}$$
$$S_4 = \mathcal{R}_0 \left(\hat{S}_3 \left(\mathcal{V}^{\mathrm{D}} \right) \right) + \frac{1}{3} \mathcal{R}_0 \left[\left(\hat{S}_2 \hat{S}_1 + \hat{S}_1 \hat{S}_2 \right) \left(\mathcal{V}^{\mathrm{O}} \right) \right] \tag{3.36e}$$
$$S_5 = \mathcal{R}_0 \left(\hat{S}_4 \left(\mathcal{V}^{\mathrm{D}} \right) \right) + \frac{1}{3} \mathcal{R}_0 \left[\left(\hat{S}_1 \hat{S}_3 + \hat{S}_3 \hat{S}_1 + \hat{S}_2^2 \right) \left(\mathcal{V}^{\mathrm{O}} \right) \right] - \frac{1}{45} \mathcal{R}_0 \left(\hat{S}_1^4 \left(\mathcal{V}^{\mathrm{O}} \right) \right) \tag{3.36f}$$
...

We thus get a series expansion where each term can be expressed as a function of the preceding ones. However, ultimately, each terms only depends on $\mathcal{R}_0 = Q\mathcal{L}_0^{-1} \cdot P - P \cdot \mathcal{L}_0^{-1} Q$ and elements of $\mathcal{V}$. For instance, we can write

$$S_2 = \mathcal{R}_0 \left(\hat{S}_1 \left(\mathcal{V}^{\mathrm{D}} \right) \right) = -\mathcal{R}_0 \left(\hat{\mathcal{V}}^{\mathrm{D}} S_1 \right) = -\mathcal{R}_0 \left(\hat{\mathcal{V}}^{\mathrm{D}} \left(\mathcal{R}_0 \mathcal{V}^{\mathrm{O}} \right) \right) \tag{3.37}$$
$$S_3 = \mathcal{R}_0 \left(\hat{\mathcal{V}}^{D} \left(\mathcal{R}_0 \hat{\mathcal{V}}^{D} \left(\mathcal{R}_0 \mathcal{V}^{\mathrm{O}} \right) \right) \right) + \frac{1}{3} \mathcal{R}_0 \left(\left(\mathcal{R}_0 \mathcal{V}^{\mathrm{O}} \right)^2 \mathcal{V}^{\mathrm{O}} \right). \tag{3.38}$$

We are now equipped to derive the power series for the perturbative correction $\mathcal{W} = \epsilon(\mathcal{V}^{\mathrm{D}} + \tanh(\hat{S}/2)\mathcal{V}^{\mathrm{O}})$. Indeed, as previously, we write

$$\mathcal{W} = \sum_{n=0}^{\infty} \epsilon^n \mathcal{W}_n. \tag{3.39}$$

Moreover, we follow the same procedure as for finding S_n meaning that we expand the term in

[5] In the Taylor series of $\hat{S}\coth\hat{S}$ given by Eq. (3.35), we substitute

$$\begin{aligned} \hat{S}^2 &= \left(\hat{S}_0 + \epsilon \hat{S}_1 + \epsilon^2 \hat{S}_2 + \epsilon^3 \hat{S}_3 + \mathcal{O}(\epsilon^4) \right)^2 \\ &\simeq \hat{S}_1^2 \epsilon^2 + \left(\hat{S}_2 \hat{S}_1 + \hat{S}_1 \hat{S}_2 \right) \epsilon^3 + \left(\hat{S}_1 \hat{S}_3 + \hat{S}_3 \hat{S}_1 + \hat{S}_2 \right) \epsilon^4 \end{aligned}$$

keeping in this case only terms up to fourth order in ϵ. Proceeding similarly for $\hat{S}^4$ and keeping only terms in ϵ^4 yields $\hat{S}^4 = \hat{S}_1^4 \epsilon^4$.
The reader might notice the absence of $\hat{S}_0$. This is explained by the fact that $S_0 = 0 \Rightarrow \hat{S} = 0$ (see Eq. (3.36)).

$\hat{S}$ in (3.28) using the Taylor expansion

$$\tanh(\hat{S}/2) = \frac{\hat{S}}{2} - \frac{\hat{S}^3}{24} + \frac{\hat{S}^5}{240} + \mathcal{O}(\hat{S}^7). \tag{3.40}$$

This leads to

$$\begin{aligned}\mathcal{W} &= \mathcal{W}_0 + \mathcal{W}_1\epsilon + \mathcal{W}_2\epsilon^2 + \mathcal{W}_3\epsilon^3 + \mathcal{W}_4\epsilon^4 + \mathcal{W}_5\epsilon^5 + \mathcal{W}_6\epsilon^6 + \mathcal{O}(\epsilon^7) \\ &= \epsilon\mathcal{V}^{\mathrm{D}} + \epsilon\left(\frac{\hat{S}}{2} - \frac{\hat{S}^3}{24} + \frac{\hat{S}^5}{240} + \mathcal{O}(\hat{S}^7)\right).\end{aligned} \tag{3.41}$$

Once more, expanding $\hat{S}$ in its power series[6] and comparing the corresponding coefficients yields

$$\mathcal{W}_0 = 0 \tag{3.42a}$$
$$\mathcal{W}_1 = \mathcal{V}^{\mathrm{D}} \tag{3.42b}$$
$$\mathcal{W}_2 = \frac{1}{2}\hat{S}_1\left(\mathcal{V}^{\mathrm{O}}\right) = -\frac{1}{2}\hat{\mathcal{V}}^{\mathrm{O}}S_1 = -\frac{1}{2}\hat{\mathcal{V}}^{\mathrm{O}}\left(\mathcal{R}_0\mathcal{V}^{\mathrm{O}}\right) \tag{3.42c}$$
$$\mathcal{W}_3 = \frac{1}{2}\hat{S}_2\left(\mathcal{V}^{\mathrm{O}}\right) = -\frac{1}{2}\hat{\mathcal{V}}^{\mathrm{O}}S_2 = \frac{1}{2}\hat{\mathcal{V}}^{\mathrm{O}}\mathcal{R}_0\hat{\mathcal{V}}^{\mathrm{D}}\mathcal{R}_0\mathcal{V}^{\mathrm{O}} \tag{3.42d}$$
$$\mathcal{W}_4 = \frac{1}{2}\hat{S}_3\left(\mathcal{V}^{\mathrm{O}}\right) - \frac{1}{24}\hat{S}_1^3\left(\mathcal{V}^{\mathrm{O}}\right) \tag{3.42e}$$
$$\mathcal{W}_5 = \frac{1}{2}\hat{S}_4\left(\mathcal{V}^{\mathrm{O}}\right) - \frac{1}{24}\left(\hat{S}_2\hat{S}_1^2 + \hat{S}_1\hat{S}_2\hat{S}_1 + \hat{S}_1^2\hat{S}_2\right)\left(\mathcal{V}^{\mathrm{O}}\right) \tag{3.42f}$$
$$\begin{aligned}\mathcal{W}_6 = &\frac{1}{2}\hat{S}_5\left(\mathcal{V}^{\mathrm{O}}\right) \\ &- \frac{1}{24}\left(\hat{S}_1^2\hat{S}_3 + \hat{S}_3\hat{S}_1^2 + \hat{S}_1\hat{S}_3\hat{S}_1 + \hat{S}_1\hat{S}_2^2 + \hat{S}_2^2\hat{S}_1 + \hat{S}_2\hat{S}_1\hat{S}_2\right)\left(\mathcal{V}^{\mathrm{O}}\right) + \frac{1}{240}\hat{S}_1^5\end{aligned} \tag{3.42g}$$
$$\ldots$$

Again, we obtain a series expansion in which each contribution can be written in terms of the previous ones, while eventually depending solely on $\mathcal{R}_0$ and $\mathcal{V}$.

Finally, projecting the Taylor matrices (3.42) onto the slow space gives the expansion of the effective Liouvillian which can thus be written as follows:

$$L_{\mathrm{eff}} = PLP = P\mathcal{W}P = \sum_{n=0}^{\infty}\epsilon^n P\mathcal{W}_n P. \tag{3.43}$$

Defining

$$\boxed{L_n^{\mathrm{eff}} = P\mathcal{W}_n P,} \tag{3.44}$$

[6]Following the same procedure as in Footnote 5 : In the Taylor series of $\tanh(\hat{S}/2)$ given by Eq. (3.40), we substitute

$$\hat{S} = \hat{S}_0 + \epsilon\hat{S}_1 + \epsilon^2\hat{S}_2 + \epsilon^3\hat{S}_3 + \epsilon^4\hat{S}_4 + \epsilon^5\hat{S}_5 + \mathcal{O}(\epsilon^6)$$

and

$$\begin{aligned}\hat{S}^3 &= \left(\hat{S}_0 + \epsilon\hat{S}_1 + \epsilon^2\hat{S}_2 + \epsilon^3\hat{S}_3 + \mathcal{O}(\epsilon^4)\right)^3 \\ &\simeq \hat{S}_1^3\epsilon^3 + \left(\hat{S}_2\hat{S}_1^2 + \hat{S}_1\hat{S}_2\hat{S}_1 + \hat{S}_1^2\hat{S}_2\right)\epsilon^4 \\ &\quad + \left(\hat{S}_1^2\hat{S}_3 + \hat{S}_1\hat{S}_3\hat{S}_1 + \hat{S}_3\hat{S}_1^2 + \hat{S}_1\hat{S}_2^2 + \hat{S}_2\hat{S}_1\hat{S}_2 + \hat{S}_2^2\hat{S}_1\right)\epsilon^5\end{aligned}$$

keeping in this case only terms up to fifth order in ϵ. Proceeding similarly for $\hat{S}^5$ and keeping only terms in ϵ^5 yields $\hat{S}^5 = \hat{S}_1^5\epsilon^5$.

leads to

$$L_{\text{eff}} = \sum_{n=0}^{\infty} \epsilon^n L_n^{\text{eff}}, \tag{3.45}$$

which in particular yields

$$L_0^{\text{eff}} = 0 \tag{3.46a}$$
$$L_1^{\text{eff}} = P\mathcal{V}^{\text{D}}P = \mathcal{V}^P \tag{3.46b}$$
$$L_2^{\text{eff}} = -\mathcal{V}^-\mathcal{L}_0^{-1}\mathcal{V}^+ \tag{3.46c}$$
$$L_3^{\text{eff}} = \mathcal{V}^-\mathcal{L}_0^{-1}\mathcal{V}^Q\mathcal{L}_0^{-1}\mathcal{V}^+ - \frac{1}{2}\left\{\mathcal{V}^P, \mathcal{V}^-\mathcal{L}_0^{-2}\mathcal{V}^+\right\} \tag{3.46d}$$
$$\ldots$$

Readers not concerned with the proofs of Eqs. (3.46c) and (3.46d) may proceed directly to page 41.

Proof. **2nd order term of the effective Liouvillian series: L_2^{eff}**
In order to establish the final explicit expression for L_2^{eff} Eq. (3.46c), let us write its expression explicitly as

$$L_2^{\text{eff}} = P\mathcal{W}_2P = P\left(\frac{1}{2}\hat{\mathcal{V}}^{\text{O}}\left(\mathcal{R}_0\mathcal{V}^{\text{O}}\right)\right)P \tag{3.47}$$

expanding the hidden commutator in $\hat{\mathcal{V}}$

$$L_2^{\text{eff}} = \frac{1}{2}P\left(\mathcal{V}^{\text{O}}\mathcal{R}_0\mathcal{V}^{\text{O}} - \mathcal{R}_0\mathcal{V}^{\text{O}}\mathcal{V}^{\text{O}}\right)P \tag{3.48}$$

We recall the resolvent operator expression (3.25) reproduced here for convenience

$$\mathcal{R}_0(\cdot) = Q\mathcal{L}_0^{-1}\cdot P - P\cdot\mathcal{L}_0^{-1}Q.$$

In consequence, we have

$$\mathcal{R}_0(\mathcal{V}^{\text{O}}) = Q\mathcal{L}_0^{-1}\mathcal{V}^{\text{O}}P - P\mathcal{V}^{\text{O}}\mathcal{L}_0^{-1}Q, \tag{3.49}$$

which we substitute into (3.48), yielding

$$L_2^{\text{eff}} = \frac{1}{2}P\left(\mathcal{V}^{\text{O}}Q\mathcal{L}_0^{-1}\mathcal{V}^{\text{O}}P - \mathcal{V}^{\text{O}}P\mathcal{V}^{\text{O}}\mathcal{L}_0^{-1}Q - Q\mathcal{L}_0^{-1}\mathcal{V}^{\text{O}}P\mathcal{V}^{\text{O}} + P\mathcal{V}^{\text{O}}\mathcal{L}_0^{-1}Q\mathcal{V}^{\text{O}}\right)P. \tag{3.50}$$

The property of the projector P

$$P^2 = P \tag{3.51}$$

as well as

$$PQ = P(\mathbb{1} - P) = P - P^2 = P - P = 0 = QP, \tag{3.52}$$

imply that the second and third term of Eq. (3.50) vanish, leading to

$$L_{\text{eff}} = \frac{1}{2}\left(P\mathcal{V}^{\text{O}}Q\mathcal{L}_0^{-1}\mathcal{V}^{\text{O}}P + P\mathcal{V}^{\text{O}}\mathcal{L}_0^{-1}Q\mathcal{V}^{\text{O}}P\right). \tag{3.53}$$

Additionally, we recall the definitions of Eq. (3.8):

$$P\mathcal{V}^{\mathrm{O}}Q = P\mathcal{V}Q = \mathcal{V}^{-} \tag{3.54}$$

$$Q\mathcal{V}^{\mathrm{O}}P = Q\mathcal{V}P = \mathcal{V}^{+} \tag{3.55}$$

Also for an arbitrary operator A we have $A^{\mathrm{O}} = A^{-} + A^{+}$. Hence, we get

$$\mathcal{V}^{\mathrm{O}}P = (\mathcal{V}^{-} + \mathcal{V}^{+})P = (P\mathcal{V}Q + Q\mathcal{V}P)P = Q\mathcal{V}P = \mathcal{V}^{+} \tag{3.56}$$

and similarly

$$P\mathcal{V}^{\mathrm{O}} = P\mathcal{V}Q = \mathcal{V}^{-}. \tag{3.57}$$

In light of these identities, Eq. (3.53) becomes

$$L_2^{\mathrm{eff}} = \frac{1}{2}\left(\mathcal{V}^{-}\mathcal{L}_0^{-1}\mathcal{V}^{+} + \mathcal{V}^{-}\mathcal{L}_0^{-1}\mathcal{V}^{+}\right) = \mathcal{V}^{-}\mathcal{L}_0^{-1}\mathcal{V}^{+} \tag{3.58}$$

□

Proof. **3rd order term of the effective Liouvillian series : L_3^{eff}**

We have

$$L_3^{\mathrm{eff}} = P\mathcal{W}_3P = \frac{1}{2}P\left[\hat{\mathcal{V}}^{\mathrm{O}}\left(\mathcal{R}_0\left(\hat{\mathcal{V}}^{\mathrm{D}}\left(\mathcal{R}_0\mathcal{V}^{\mathrm{O}}\right)\right)\right)\right]P \tag{3.59}$$

Developing the commutator hidden in $\hat{\mathcal{V}}^{\mathrm{O}}$, we get

$$L_3^{\mathrm{eff}} = \frac{1}{2}P\left[\mathcal{V}^{\mathrm{O}}\left(\mathcal{R}_0\left(\hat{\mathcal{V}}^{\mathrm{D}}\left(\mathcal{R}_0\mathcal{V}^{\mathrm{O}}\right)\right)\right)\right]P - \frac{1}{2}P\left[\left(\mathcal{R}_0\left(\hat{\mathcal{V}}^{\mathrm{D}}\left(\mathcal{R}_0\mathcal{V}^{\mathrm{O}}\right)\right)\right)\mathcal{V}^{\mathrm{O}}\right]P \tag{3.60}$$

$$\equiv \frac{1}{2}P\mathcal{V}^{\mathrm{O}}\left(\mathcal{R}_0\xi\right)P - \frac{1}{2}P\left(\mathcal{R}_0\xi\right)\mathcal{V}^{\mathrm{O}}P \tag{3.61}$$

$$= \frac{1}{2}\mathcal{V}^{-}\left(\mathcal{R}_0\xi\right)P - \frac{1}{2}P\left(\mathcal{R}_0\xi\right)\mathcal{V}^{+} \tag{3.62}$$

where we defined $\xi = \hat{\mathcal{V}}^{\mathrm{D}}\left(\mathcal{R}_0\mathcal{V}^{\mathrm{O}}\right) = \mathcal{V}^{\mathrm{D}}\left(\mathcal{R}_0\mathcal{V}^{\mathrm{O}}\right) - \left(\mathcal{R}_0\mathcal{V}^{\mathrm{O}}\right)\mathcal{V}^{\mathrm{D}}$.
Let us now compute ξ by recalling the expression (3.49) of $\mathcal{R}_0\mathcal{V}^{\mathrm{O}}$, we obtain

$$\xi = \underbrace{\mathcal{V}^{\mathrm{D}}Q\mathcal{L}_0^{-1}\mathcal{V}^{\mathrm{O}}P}_{\xi_I}\underbrace{-\mathcal{V}^{\mathrm{D}}P\mathcal{V}^{\mathrm{O}}\mathcal{L}_0^{-1}Q}_{\xi_{II}}\underbrace{-Q\mathcal{L}_0^{-1}\mathcal{V}^{\mathrm{O}}P\mathcal{V}^{\mathrm{D}}}_{\xi_{III}}\underbrace{+P\mathcal{V}^{\mathrm{O}}\mathcal{L}_0^{-1}Q\mathcal{V}^{\mathrm{D}}}_{\xi_{IV}}. \tag{3.63}$$

Next, we evaluate $\mathcal{R}_0\xi$. By linearity, we have $\mathcal{R}_0\xi = \mathcal{R}_0\xi_I + \mathcal{R}_0\xi_{II} + \mathcal{R}_0\xi_{III} + \mathcal{R}_0\xi_{IV}$. Developing the action of $\mathcal{R}_0$ on ξ_i, we get

$$\mathcal{R}_0\xi_I = Q\mathcal{L}_0^{-1}\left(\mathcal{V}^{\mathrm{D}}Q\mathcal{L}_0^{-1}\mathcal{V}^{\mathrm{O}}P\right)P - P\left(\mathcal{V}^{\mathrm{D}}Q\mathcal{L}_0^{-1}\mathcal{V}^{\mathrm{O}}P\right)\mathcal{L}_0^{-1}Q$$

Since $P\mathcal{V}^{\mathrm{D}}Q = 0$ by definition, the second term vanishes leading to

$$\mathcal{R}_0\xi_I = Q\mathcal{L}_0^{-1}\mathcal{V}^{\mathrm{D}}Q\mathcal{L}_0^{-1}\mathcal{V}^{\mathrm{O}}P \tag{3.64}$$

where we used $P^2 = P$. Moreover,

$$\begin{aligned}\mathcal{R}_0\xi_{II} &= -Q\mathcal{L}_0^{-1}\left(\mathcal{V}^{\mathrm{D}}P\mathcal{V}^{\mathrm{O}}\mathcal{L}_0^{-1}Q\right)P + P\left(\mathcal{V}^{D}P\mathcal{V}^{\mathrm{O}}\mathcal{L}_0^{-1}Q\right)\mathcal{L}_0^{-1}Q \\ &= \mathcal{V}^{P}\mathcal{V}^{\mathrm{O}}\mathcal{L}_0^{-1}Q\mathcal{L}_0^{-1}Q.\end{aligned} \tag{3.65}$$

where $QP = PQ = 0$ justifies the vanishing first term. Using similar arguments, we get

$$\mathcal{R}_0\xi_{III} = -Q\mathcal{L}_0^{-1}\left(Q\mathcal{L}_0^{-1}\mathcal{V}^{\mathrm{O}}P\mathcal{V}^{\mathrm{D}}\right)P + P\left(Q\mathcal{L}_0^{-1}\mathcal{V}^{\mathrm{O}}P\mathcal{V}^{\mathrm{D}}\right)\mathcal{L}_0^{-1}Q \tag{3.66}$$

$$= -Q\mathcal{L}_0^{-1}Q\mathcal{L}_0^{-1}\mathcal{V}^{\mathrm{O}}\mathcal{V}^{\mathrm{P}} \tag{3.67}$$

using $P\mathcal{V}^{\mathrm{D}}P = \mathcal{V}^P$. Lastly,

$$\mathcal{R}_0\xi_{IV} = Q\mathcal{L}_0^{-1}\left(P\mathcal{V}^{\mathrm{O}}\mathcal{L}_0^{-1}Q\mathcal{V}^{\mathrm{D}}\right)P - P\left(P\mathcal{V}^{\mathrm{O}}\mathcal{L}_0^{-1}Q\mathcal{V}^{\mathrm{D}}\right)\mathcal{L}_0^{-1}Q$$

$$= -P\mathcal{V}^{\mathrm{O}}\mathcal{L}_0^{-1}Q\mathcal{V}^{\mathrm{D}}\mathcal{L}_0^{-1}Q \tag{3.68}$$

remembering $Q\mathcal{V}^{\mathrm{D}}P = 0$ by definition.
These expressions of $\mathcal{R}_0\xi_i$ can be simplified. For instance, we have

$$\mathcal{V}^{\mathrm{D}}Q = (P\mathcal{V}P + Q\mathcal{V}Q)Q = Q\mathcal{V}Q = Q\mathcal{V}^Q Q \quad \text{since } \mathcal{Q}^2 = Q \text{ and } PQ = 0 \tag{3.69}$$

$$Q\mathcal{L}_0^{-1}Q = \mathcal{L}_0^{-1} \quad \text{since } \mathcal{L}_0^{-1} = \mathcal{L}_0^Q = Q\mathcal{L}_0^{-1}Q \text{ and } Q^2 = Q \tag{3.70}$$

as well as the identity $\mathcal{V}^{\mathrm{O}}P = \mathcal{V}^+$ deduced in the previous proof, which enables to rewrite Eq. (3.64) as

$$\mathcal{R}_0\xi_I = \mathcal{L}_0^{-1}\mathcal{V}^Q\mathcal{L}_0^{-1}\mathcal{V}^+. \tag{3.71}$$

Likewise, we write

$$\mathcal{R}_0\xi_{II} = \mathcal{V}^P\mathcal{V}^-\mathcal{L}_0^{-2}, \tag{3.72}$$

$$\mathcal{R}_0\xi_{III} = -\mathcal{L}_0^{-2}\mathcal{V}^+\mathcal{V}^P, \tag{3.73}$$

$$\mathcal{R}_0\xi_{IV} = -\mathcal{V}^-\mathcal{L}_0^{-1}\mathcal{V}^Q\mathcal{L}_0^{-1}. \tag{3.74}$$

Substituting the resulting expression of $\mathcal{R}_0\xi$ back into Eq. (3.61), remembering $PQ = QP = 0$, we obtain

$$L_3^{\mathrm{eff}} = \frac{1}{2}\mathcal{V}^-\left(\mathcal{R}_0\xi_I + \mathcal{R}_0\xi_{III}\right)P - \frac{1}{2}P\left(\mathcal{R}_0\xi_{II} + \mathcal{R}_0\xi_{IV}\right)\mathcal{V}^+, \tag{3.75}$$

which, using Eqs. (3.71) to (3.74), is expressed as

$$L_3^{\mathrm{eff}} = \frac{1}{2}\mathcal{V}^-\mathcal{L}_0^{-1}\mathcal{V}^Q\mathcal{L}_0^{-1}\mathcal{V}^+ - \frac{1}{2}\mathcal{V}^-\mathcal{L}_0^{-2}\mathcal{V}^+\mathcal{V}^P - \frac{1}{2}\mathcal{V}^P\mathcal{V}^-\mathcal{L}_0^{-2}\mathcal{V}^+ + \frac{1}{2}\mathcal{V}^-\mathcal{L}_0^{-1}\mathcal{V}^Q\mathcal{L}_0^{-1}\mathcal{V}^+. \tag{3.76}$$

Finally leading to

$$L_3^{\mathrm{eff}} = \mathcal{V}^-\mathcal{L}_0^{-1}\mathcal{V}^Q\mathcal{L}_0^{-1}\mathcal{V}^+ - \frac{1}{2}\left\{\mathcal{V}^P, \mathcal{V}^-\mathcal{L}_0^{-2}\mathcal{V}^+\right\}. \tag{3.77}$$

□

The reader might ask why simplified expressions for further orders are not derived here. They will find an answer by looking at the corresponding proof for the third order term provided above and get a sense of the complexity of a further order derivation. It is interesting for this thesis to see the dependence of L_n^{eff} on $\mathcal{L}_0^{-1}$ and $\mathcal{V}$. However, the compact expressions (3.46) are not necessary for further calculations, since it is an iterative series where each term depends on the previous ones. Hence, computing further orders is done using Eq. (3.44). Additionally, in the context of numerical simulations, using Eq. (3.44) is considerably more straightforward than deriving multiple pages of analytical calculations.

As introduced in Section 3.1, the effective Liouvillian describes the low energy dynamics of the system in the vicinity of the steady state and its expansion into the terms given by Eq. (3.46) yields the following reduced effective master equation

$$\dot{\mu} = \left(\epsilon L_1^{\text{eff}} + \epsilon^2 L_2^{\text{eff}} + \epsilon^3 L_3^{\text{eff}} + ...\right) \mu. \tag{3.78}$$

Having established the wanted series expansion of the effective Liouvillian, the main observation is that L_n^{eff} ultimately depends solely on the restricted inverse $\mathcal{L}_0^{-1}$ of $\mathcal{L}_0$ and on the contribution $\mathcal{V}$ of the Liouvillian. We can note that L_n^{eff} shows a $\mathcal{V}^n \mathcal{L}_0^{-n+1}$ dependence for $n > 0$, where we introduced the notation $\left(\mathcal{L}_0^{-1}\right)^n = \mathcal{L}_0^{-n}$. Moreover, $\mathcal{V}$ being treated as a perturbation, the separation of the general Liouvillian $\mathcal{L}$ into its contributions $\mathcal{L}_0$ and $\epsilon\mathcal{V}$ must be done carefully in order to keep the spectral separation between the eigenvalues related to the slow space and the ones in the fast space, recalling Figure 3.1.

Finally, restricting the series expansion to second order, such that

$$\dot{\mu} \simeq \left(\epsilon L_1^{\text{eff}} + \epsilon^2 L_2^{\text{eff}}\right) \mu, \tag{3.79}$$

reproduces the result of *adiabatic elimination*. This method consists in deriving a reduced model by elimination of rapidly decaying degrees of freedom, yielding an effective model for the slow dynamics of the system [7, 37].

Summary 3. Generalized Schrieffer-Wolff transformation

Chapter 3 presented the generalized Schrieffer-Wolff method applied to the Liouvillian governing the dynamics of an open quantum system

$$\mathcal{L} = \mathcal{L}_0 + \epsilon\mathcal{V},$$

instead of the Hamiltonian. The spectrum of $\mathcal{L}_0$ is separated into a slow subspace $\mathcal{P}$, associated with its zero eigenvalues corresponding to the steady states, and a fast subspace $\mathcal{Q}$, associated with the non zero eigenvalues. The method relies on the application of a similarity transformation that block-diagonalizes the Liouvillian, hence decoupling the two subspaces:

$$\mathcal{L} \to L = U^{-1}\mathcal{L}U$$

with L block-diagonal.

This transformation allows for the expansion of the new Liouvillian L through the Baker-Campbell-Hausdorff formula leading to

$$L = \mathcal{L}_0 + \mathcal{W}.$$

Then projecting L onto the slow subspace gives the effective Liouvillian

$$L_{\text{eff}} = PLP = P\mathcal{W}P = \sum_{n=0}^{\infty} \epsilon^n L_n^{\text{eff}}.$$

where the second order reproduces the result of adiabatic elimination.
Finally, the slow dynamics near the steady state are governed by an effective reduced master equation

$$\dot{\mu} = L_{\text{eff}}\mu.$$

The key result is that dissipative degrees of freedom can be eliminated perturbatively while keeping their effect on the reduced dynamics.

Chapter 4

Application to a Qubit Coupled to a Damped Resonator

The present chapter constitutes the main original contribution of this thesis. It presents the implementation of the generalized Schrieffer-Wolff formalism, developed in Chapter 3, to a system composed of a qubit coupled to a damped resonator, which constitutes the core model of dispersive readout of superconducting qubits.
First, Section 4.1 introduces the Lindblad master equation governing the total dynamics of this system as illustrated in Figure 4.1. Section 4.2 then derives an effective master equation for the reduced density matrix of the qubit through adiabatic elimination of the resonator degrees of freedom. Finally, Section 4.3 presents the application of the generalized Schrieffer-Wolff formalism to the "qubit + resonator" system. After discussing the restriction to the single-excitation subspace and the appropriate separation $\mathcal{L}_0 + \mathcal{V}$, we show that the second-order expansion reproduces the result of adiabatic elimination obtained in Section 4.2. Higher-order corrections are then assessed through fidelity comparisons with the exact solution of the enlarged master equation, before concluding with an analysis of the validity conditions of the expansion.

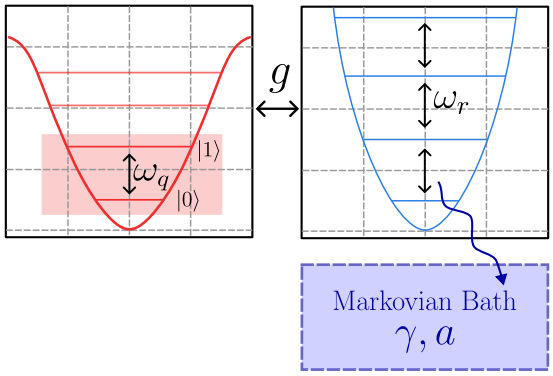

Figure 4.1: Illustration of a qubit coupled to a resonator, which is damped through its coupling to a Markovian bath. In this scenario, the dynamics of the total system made of the qubit and the resonator is well described by a Lindblad master equation.

4.1 Master Equation

As introduced in Section 2.2, the Lindblad Master Equation describing the "qubit + resonator" system is given by

$$\dot{\rho} = -i\left[H, \rho\right] + \gamma\left(a\rho a^\dagger - \frac{1}{2}\left\{a^\dagger a, \rho\right\}\right) \equiv \mathcal{L}\left[\rho\right]. \tag{4.1}$$

Since the system of interest is a qubit coupled to an undriven damped resonator, the Hamiltonian is the Jaynes-Cummings Hamiltonian introduced in Section 2.2:

$$H = \frac{1}{2}\omega_q \sigma_z + \omega_r a^\dagger a + g\left(\sigma_- a^\dagger + \sigma_+ a\right) \equiv H_0 + V. \tag{4.2}$$

4.2 Adiabatic Elimination

In this section, an effective Redfield master equation describing the evolution of the reduced density matrix of the qubit is derived, hence eliminating the resonator degrees of freedom. This reduction is an instance of adiabatic elimination.
In Section 1.2, we presented the general formalism underlying the Redfield master equation, which describes the dynamics of a quantum system coupled to a bath. This led to a general equation for the system given by Eq. (1.24). In the context of dispersive readout, the Hamiltonian $H = \frac{1}{2}\omega_q\sigma_z + \omega_r a^\dagger a + g(\sigma_+ a + \sigma_- a^\dagger)$ can be written as $H = H_S + H_B + V$, where $H_S = \frac{1}{2}\omega_q\sigma_z$ describes the qubit, that is, the system of interest, $H_B = \omega_r a^\dagger a$ characterizes the resonator treated as an effective bath for the qubit, and $V = g(\sigma_+ a + \sigma_- a^\dagger)$ describes the interaction between the system (qubit) and its bath (resonator). Hence, Eq. (1.24), introduced in Section 1.3, reads

$$\dot{\rho}_{q,I}(t) = -\int_0^{t\to\infty} \mathrm{Tr}_B\Big(\Big[V_I(t), [V_I(t-\tau), \rho_{q,I}(t)\otimes\rho_{B,I}]\Big]\Big)d\tau, \tag{4.3}$$

where $\rho_{q,I}(t)$ is the reduced density matrix of the qubit in the interaction picture. Given the explicit form of the interaction V, this equation can be further simplified. Readers wishing to omit the detailed derivation may proceed directly to Eq. (4.29).

Interaction picture

First, the Hamiltonian (4.2) must be transformed from the Schrödinger picture to the interaction picture, i.e., the relevant frame to perform the perturbative treatment of the interaction needed to derive the master equation. As recalled in Theoretical Concept 1.1, we have

$$\begin{aligned} H_I(t) = V_I(t) = e^{iH_0 t} V e^{-iH_0 t} &= g\left(e^{iH_0 t}\sigma_- a^\dagger e^{-iH_0 t} + e^{iH_0 t}\sigma_+ a e^{-iH_0 t}\right) \\ &= g\left(\sigma_{-,I}(t) a_I^\dagger(t) + \sigma_{+,I}(t) a_I(t)\right), \end{aligned} \tag{4.4}$$

where the last equality follows from inserting $e^{iH_0 t}e^{-iH_0 t}$ between the qubit and cavity operators, thereby making the interaction picture expressions of the operators explicit. In the remainder of this proof the subscripts I will be omitted for readability. However, the explicit time dependence of operators will indicate that they are expressed in the interaction picture.

Expanding the commutators and using the linearity properties of the trace in Eq. (4.3) yields

$$\begin{aligned} \dot{\rho}_q(t) = &\underbrace{-\int_0^{t\to\infty} \mathrm{Tr}_B\Big(V(t)V(t-\tau)\rho_q(t)\otimes\rho_B\Big)d\tau}_{\text{I}} \ \underbrace{+\int_0^{t\to\infty} \mathrm{Tr}_B\Big(V(t)\rho_q(t)\otimes\rho_B V(t-\tau)\Big)d\tau}_{\text{II}} \\ &\underbrace{+\int_0^{t\to\infty} \mathrm{Tr}_B\Big(V(t-\tau)\rho_q(t)\otimes\rho_B V(t)\Big)d\tau}_{\text{III}} \ \underbrace{-\int_0^{t\to\infty} \mathrm{Tr}_B\Big(\rho_q(t)\otimes\rho_B V(t-\tau)V(t)\Big)d\tau}_{\text{IV}}, \end{aligned} \tag{4.5}$$

with

$$V(t) = g\left(\sigma_-(t)a^\dagger(t) + \sigma_+(t)a(t)\right). \tag{4.6}$$

The time dependence of the qubit and resonator operators appearing in V may be obtained via two distinct methods. On the one hand, $\sigma_+(t)$ and $\sigma_-(t)$ are calculated using the Baker-Campbell-Hausdorff formula, introduced earlier in Eq. (2.28), and recalled here for convenience:

$$H' = e^S H e^{-S} = \sum_{n=0}^{\infty} \frac{[S,H]^{(n)}}{n!}, \tag{4.7}$$

with $[S,H]^{(n)} \equiv [S,[S,H]^{(n-1)}]$, and $[S,H]^{(0)} = H$. On the other hand, $a(t)$ and $a^\dagger(t)$ are obtained from the corresponding Heisenberg equations (4.13) describing the isolated cavity subject to damping at rate γ. Indeed, computing for instance $a = e^{iH_0 t} a e^{-iH_0 t}$ would lead to $a(t) = e^{-i\omega_r t} a$ using BCH formula (4.7), as shown below for $\sigma_\pm$, and would therefore omit the dissipative dynamics.
Having clarified this point, we derive the expression for $\sigma_-(t)$. We have

$$\sigma_-(t) = e^{iH_0 t} \sigma_- e^{-iH_0 t} = \sum_n \frac{[iH_0 t, \sigma_-]^{(n)}}{n!}, \tag{4.8}$$

where computing the commutator by induction gives

$$\boxed{\sigma_-(t) = \sum_n \frac{(-i\omega_q t)^n}{n!} \sigma_- = e^{-i\omega_q t} \sigma_-.} \tag{4.9}$$

Proof. We have

$$[iH_0 t, \sigma_-] = \frac{i\omega_q t}{2} [\sigma_z, \sigma_-] = -(i\omega_q t)\sigma_-, \tag{4.10}$$

since $[\sigma_z, \sigma_-] = -2\sigma_-$. Assume that $[iH_0 t, \sigma_-]^{(n)} = (-i\omega_q t)^n \sigma_-$ holds, and let us prove that $[iH_0 t, \sigma_-]^{(n+1)} = (-i\omega_q t)^{n+1} \sigma_-$. We have

$$\begin{aligned} [iH_0 t, \sigma_-]^{(n+1)} &= \left[iH_0 t, [iH_0 t, \sigma_-]^{(n)}\right] = [iH_0 t, (-i\omega_q t)^n \sigma_-] = (-i\omega_q t)^n [iH_0 t, \sigma_-] \\ &= (-i\omega_q t)^{n+1} \sigma_-, \end{aligned}$$

where we used the definition of the nested commutators introduced in the BCH formula, applied the induction hypothesis and factored out $(-i\omega_q t)^n$ to finally use (4.10) and obtain the desired result. As a result, we proved that $[iH_0 t, \sigma_-]^{(n)} = (-i\omega_q t)^n \sigma_-$, which, when inserted into Eq. (4.8), yields Eq. (4.9). □

By simple Hermitian conjugation, we obtain

$$\boxed{\sigma_+(t) = e^{i\omega_q t} \sigma_+.} \tag{4.11}$$

Bath correlation functions

As explained earlier, restraining the time evolution of the cavity operators $a(t)$ and $a^\dagger(t)$ to their interaction picture expressions would omit the dissipative dynamics. Instead, their time evolution are governed by the corresponding adjoint master equations, introduced in Section 1.6. Hence, for the isolated damped cavity, the AME reads

$$\dot{\mathcal{O}}(t) = i [H_B, \mathcal{O}(t)] + \gamma \left(a^\dagger \mathcal{O}(t) a - \frac{1}{2} \left\{ a^\dagger a, \mathcal{O} \right\} \right) \equiv \mathcal{L}^\dagger [\mathcal{O}(t)], \tag{4.12}$$

where $H_B = \omega_r a^\dagger a$. Evaluating Eq. (4.12) for the cavity operators yields the following *Heisenberg equations*:

$$\boxed{\begin{aligned}\dot{a}(t) &= -i\omega_r a(t) - \frac{\gamma}{2}a(t) \\ \dot{a}^\dagger(t) &= i\omega_r a^\dagger(t) - \frac{\gamma}{2}a^\dagger(t),\end{aligned}} \tag{4.13a}$$

(4.13b)

whose solutions are

$$\boxed{\begin{aligned}a(t) &= e^{(-i\omega_r - \frac{\gamma}{2})t}a \\ a^\dagger(t) &= e^{(i\omega_r - \frac{\gamma}{2})t}a.\end{aligned}} \tag{4.14}$$

(4.15)

Proof. To simplify the notation, the explicit time dependence will be omitted in the following. When evaluated for a, Eq. (4.12) gives

$$\dot{a} = i\left[\omega_r a^\dagger a, a\right] + \gamma\left(a^\dagger a a - \frac{1}{2}\left\{a^\dagger a, a\right\}\right), \tag{4.16}$$

which yields

$$\dot{a} = -i\omega_r a - \frac{\gamma}{2}a, \tag{4.17}$$

since $\left[a^\dagger a, a\right] = -a$. The time evolution of $a^\dagger(t)$ is given by the hermitian conjugate of Eq. (4.17). □

Note that the steady state of the cavity, defined by $\dot{a}(t) = \dot{a}^\dagger(t) = 0$, i.e., the cavity state is stationary, corresponds to $a(t) = a^\dagger(t) = 0$. As a consequence, the steady state of the cavity is the vacuum state, since $\langle a^\dagger a\rangle = 0$. Moreover, throughout this chapter, the resonator is assumed to be initially prepared in this state [38],

$$\boxed{\rho_B = |0\rangle\langle 0|,} \tag{4.18}$$

where $|0\rangle$ denotes the ground state of the cavity, i.e., the Fock state with zero excitation. This is a valid approximation if one consider the resonator in thermal equilibrium at low temperature compared to the resonator frequency.

Let us compute the first term I of Eq. (4.5). Its integrand is

$$\begin{aligned}g^2\Big(&\mathrm{Tr}_B\left(a(t)a^\dagger(t-\tau)\rho_B\right)\sigma_+(t)\sigma_-(t-\tau)\rho_q(t) + \mathrm{Tr}_B\left(a^\dagger(t)a(t-\tau)\rho_B\right)\sigma_-(t)\sigma_+(t-\tau)\rho_q(t) \\ &+ \mathrm{Tr}_B\left(a^\dagger(t)a^\dagger(t-\tau)\rho_B\right)\sigma_-(t)\sigma_-(t-\tau)\rho_q(t) + \mathrm{Tr}_B\left(a(t)a(t-\tau)\rho_B\right)\sigma_+(t)\sigma_+(t-\tau)\rho_q(t)\Big).\end{aligned}$$

Only the first term survives, because it contains the only nonzero *bath correlation function*.

Theoretical Concept 4.1. Bath correlation function (BCF)

Consider the general framework of open quantum system with Hamiltonian $H = H_S + H_B + V$, as introduced in Section 1.2. Let us decompose the interaction Hamiltonian V as

$$V = \sum_\alpha S_\alpha \otimes B_\alpha, \tag{4.19}$$

where S_α acts on the system Hilbert space $\mathcal{H}_S$, while B_α acts on the bath Hilbert space $\mathcal{H}_B$. A *bath correlation function* is defined as

$$\alpha(t) = \mathrm{Tr}_B\left(B_\alpha^\dagger(t)B_\alpha(t-\tau)\rho_B\right) = \langle B_\alpha^\dagger(t)B_\alpha(t-\tau)\rangle, \tag{4.20}$$

where the second equality follows from the definition (1.4) of the expectation value of an operator given in Section 1.1 [11]. The characteristic decay time of the BCF is the bath correlation time τ_B, introduced in Section 1.2 as the time over which the bath loses memory of information received from the system. If ρ_B is a stationary state, then the following property holds:

$$\mathrm{Tr}_B\left(B_\alpha(t)B_\alpha^\dagger(t-\tau)\rho_B\right) = \mathrm{Tr}_B\left(B_\alpha(\tau)B_\alpha^\dagger(0)\rho_B\right). \tag{4.21}$$

Using property (4.21) of the bath correlation function and inserting the explicit time evolution of the resonator operator $a(\tau)$ given by Eq. (4.14), gives, for example,

$$\mathrm{Tr}_B\left(a(t)a^\dagger(t-\tau)\rho_B\right) = \mathrm{Tr}_B\left(a(\tau)a^\dagger(0)\rho_B\right) = \mathrm{Tr}_B\left(e^{\left(-i\omega_r-\frac{\gamma}{2}\right)\tau}aa^\dagger\rho_B\right). \tag{4.22}$$

Using $\rho_B = |0\rangle\langle 0|$, the definition of the trace and $aa^\dagger|0\rangle = |0\rangle$, one finds

$$\mathrm{Tr}_B\left(aa^\dagger\rho_B\right) = \sum_n \langle n|\, aa^\dagger\, |0\rangle\langle 0|n\rangle = \sum_n \langle n|0\rangle\langle 0|n\rangle = 1,$$

since the only non zero term is obtained for $n = 0$, with $\langle 0|0\rangle = 1$. Substituting this result back into Eq. (4.22) yields

$$\boxed{\langle a(t)a^\dagger(t-\tau)\rangle = \langle a(\tau)a^\dagger(0)\rangle = \mathrm{Tr}_B\left(a(\tau)a^\dagger(0)\rho_B\right) = e^{\left(-i\omega_r-\frac{\gamma}{2}\right)\tau}.} \tag{4.23}$$

By the same reasoning, the BCFs of the three remaining terms vanish. Hence, the integrand of term I in Eq. (4.5) becomes

$$g^2 e^{\left(-i\omega_r-\frac{\gamma}{2}\right)\tau}\sigma_+(t)\sigma_-(t-\tau)\rho_q(t) = g^2 e^{\left(-i\omega_r+i\omega_q-\frac{\gamma}{2}\right)\tau}\sigma_+\sigma_-\rho_q(t),$$

where (4.9) and (4.11) have been used to make the time evolutions of the qubit operators explicit.

Effective equation

Having determined the bath correlations functions and the resulting integrand, the integral I in Eq. (4.5) can be evaluated as

$$\int_0^{t\to\infty} \mathrm{Tr}_B\Big(V(t)V(t-\tau)\rho_q(t)\otimes\rho_B\Big)d\tau = -g^2\int_0^{t\to\infty}\langle a(t)a^\dagger(t-\tau)\rangle\sigma_+(t)\sigma_-(t-\tau)\rho_q(t)\,d\tau \tag{4.24}$$

$$= -g^2\int_0^{t\to\infty} e^{\left(-i\omega_r+i\omega_q-\frac{\gamma}{2}\right)\tau}\,d\tau\;\sigma_+\sigma_-\rho_q(t) \tag{4.25}$$

$$= \frac{g^2}{i(\omega_q-\omega_r)-\frac{\gamma}{2}}\sigma_+\sigma_-\rho_q(t). \tag{4.26}$$

Term II in Eq. (4.5) is obtained analogously[1] while terms III and IV are the hermitian conjugate of terms II and I, respectively. Ultimately, the Redfield equation reads

$$\dot{\rho}_q(t) = \underbrace{\frac{g^2}{i(\omega_q-\omega_r)-\frac{\gamma}{2}}\sigma_+\sigma_-\rho_q(t)}_{\text{I}} \underbrace{-\frac{g^2}{-i(\omega_q-\omega_r)-\frac{\gamma}{2}}\sigma_-\rho_q(t)\sigma_+}_{\text{II}} \underbrace{-\frac{g^2}{i(\omega_q-\omega_r)-\frac{\gamma}{2}}\sigma_-\rho_q(t)\sigma_+}_{\text{III}} + \underbrace{\frac{g^2}{-i(\omega_q-\omega_r)-\frac{\gamma}{2}}\rho_q(t)\sigma_+\sigma_-}_{\text{IV}}. \tag{4.27}$$

This expression can be simplified further by writing the fractions with a common denominator and introducing the detuning $\Delta = \omega_q - \omega_r$, which yields

$$\begin{aligned}\dot{\rho}_q(t) =& \frac{g^2\left(-\frac{\gamma}{2}-i\Delta\right)}{\left(\frac{\gamma}{2}\right)^2+\Delta^2}\sigma_+\sigma_-\rho_q(t) - \frac{g^2\left(-\frac{\gamma}{2}+i\Delta\right)}{\left(\frac{\gamma}{2}\right)^2+\Delta^2}\sigma_-\rho_q(t)\sigma_+ \\ & - \frac{g^2\left(-\frac{\gamma}{2}-i\Delta\right)}{\left(\frac{\gamma}{2}\right)^2+\Delta^2}\sigma_-\rho_q(t)\sigma_+ + \frac{g^2\left(-\frac{\gamma}{2}+i\Delta\right)}{\left(\frac{\gamma}{2}\right)^2+\Delta^2}\rho_q(t)\sigma_+\sigma_-.\end{aligned} \tag{4.28}$$

The remaining terms can then be grouped into an Hamiltonian and a dissipative component, such that the effective Redfield equation for the qubit in the interaction picture finally reads

$$\dot{\rho}_{q,I}(t) = -i\,\omega_{\text{eff}}\left[\sigma_+\sigma_-, \rho_{q,I}(t)\right] + \gamma_{\text{eff}}\left(\sigma_-\rho_{q,I}(t)\sigma_+ - \frac{1}{2}\left\{\sigma_+\sigma_-, \rho_{q,I}(t)\right\}\right), \tag{4.29}$$

with ω_{eff} and γ_{eff} given respectively by

$$\boxed{\omega_{\text{eff}} = \frac{g^2\Delta}{(\frac{\gamma}{2})^2+\Delta^2},} \tag{4.30}$$

and

$$\boxed{\gamma_{\text{eff}} = \frac{g^2\gamma}{(\frac{\gamma}{2})^2+\Delta^2},} \tag{4.31}$$

with the detuning $\Delta = \omega_q - \omega_r$.

Back to Schrödinger picture

For consistency, one may express Eq. (4.29) in the Schrödinger picture by using

$$\rho_{q,I}(t) = e^{iH_0t}\rho_{q,S}(t)e^{-iH_0t}. \tag{4.32}$$

Defining

$$H_{\text{eff}} = \omega_{\text{eff}}\sigma_+\sigma_-, \tag{4.33}$$

dropping the Schrödinger subscript S and combining the commutators into a single term by linearity, the effective Redfield equation describing the time evolution of the reduced density matrix of the qubit reads

[1] The cyclic property of the trace proves useful when evaluating the bath correlation function.

Key Result 4.1. Redfield equation in Schrödinger picture

$$\dot{\rho}_q(t) = -i\left[H_0 + H_{\text{eff}}, \rho_q(t)\right] + \gamma_{\text{eff}}\left(\sigma_-\rho_q(t)\sigma_+ - \frac{1}{2}\left\{\sigma_+\sigma_-, \rho_q(t)\right\}\right). \tag{4.34}$$

Proof. Let us derive Eq. (4.34) from Eq. (4.29). For readability, the explicit time dependence of the density matrices and the subscript q are omitted throughout. Using Eq. (4.32), one obtains

$$\dot{\rho}_I = (iH_0)e^{iH_0t}\rho_S e^{-iH_0t} + e^{iH_0t}\dot{\rho}_S e^{-iH_0t} + e^{iH_0t}\rho_S e^{-iH_0t}(-iH_0). \tag{4.35}$$

where care must be taken since H_0 and ρ_S do not necessarily commute. Multiplying (4.35) on the left by e^{-iH_0t} and on the right by e^{iH_0t} yields

$$e^{-iH_0t}\dot{\rho}_I e^{iH_0t} = iH_0\rho_S + \dot{\rho}_S - \rho_S iH_0 = \dot{\rho}_S + i\left[H_0, \rho_S\right], \tag{4.36}$$

which corresponds to the left-hand side of Eq. (4.29) transformed accordingly.
Acting in the same way on the right-hand side and expanding the commutator, the unitary contribution becomes

$$e^{-iH_0t}\left(-i\,\omega_{\text{eff}}\left[\sigma_+\sigma_-, \rho_I\right]\right)e^{iH_0t} = -i\,\omega_{\text{eff}}\,e^{-iH_0t}\left(\sigma_+\sigma_-\rho_I - \rho_I\sigma_+\sigma_-\right)e^{iH_0t}.$$

Substituting Eq. (4.32) into the above expression gives

$$-i\omega_{\text{eff}}\left(e^{-iH_0t}\sigma_+\sigma_-e^{iH_0t}\rho_S - \rho_S e^{-iH_0t}\sigma_+\sigma_-e^{iH_0t}\right). \tag{4.37}$$

To simplify this expression, we compute[2] $e^{-iH_0t}\sigma_+\sigma_-e^{iH_0t}$. Inserting $e^{iH_0t}e^{-iH_0t}$ between σ_+ and σ_- and applying the BCH formula (2.28) yields

$$e^{-iH_0t}\sigma_+e^{iH_0t} = e^{-i\omega_1 t}\sigma_+ \tag{4.38}$$

$$e^{-iH_0t}\sigma_-e^{iH_0t} = e^{+i\omega_1 t}\sigma_-. \tag{4.39}$$

As a consequence, $e^{-iH_0t}\sigma_+\sigma_-e^{iH_0t} = \sigma_+\sigma_-$ and Eq. (4.37) reduces to

$$-i\omega_{\text{eff}}\left[\sigma_+\sigma_-, \rho_S\right]. \tag{4.40}$$

Through similar considerations, the dissipative contribution transforms as:

$$e^{-iH_0t}\gamma_{\text{eff}}\left(\sigma_-\rho_I\sigma_+ - \frac{1}{2}\left\{\sigma_+\sigma_-, \rho_I\right\}\right)e^{iH_0t} = \gamma_{\text{eff}}\left(\sigma_-\rho_S\sigma_+ - \frac{1}{2}\left\{\sigma_+\sigma_-, \rho_S\right\}\right). \tag{4.41}$$

Finally, combining (4.36), (4.40) and (4.41) allows one to rewrite the Redfield master equation (4.29) in the Schrödinger picture as

$$\dot{\rho}_S(t) = -i\left[H_0 + H_{\text{eff}}, \rho_S(t)\right] + \gamma_{\text{eff}}\left(\sigma_-\rho_S(t)\sigma_+ - \frac{1}{2}\left\{\sigma_+\sigma_-, \rho_S(t)\right\}\right), \tag{4.42}$$

with

$$H_{\text{eff}} \equiv \omega_{\text{eff}}\sigma_+\sigma_-. \tag{4.43}$$

Dropping the Schrödinger subscript S and combining the commutators by linearity, we finally obtain Eq. (4.34).

[2]The reader might note that $\sigma_\pm$ are already expressed in the Schrödinger picture. Hence, the similarity transformation performed here does not correspond to a change between the interaction and Schrödinger pictures.

□

Eq. (4.34) is an effective master equation for the qubit, obtained by eliminating the degrees of freedom of the resonator, which was treated as an effective bath for the qubit[3].
In particular, Eq. (4.34) takes a Lindblad form even though we did not perform the secular approximation as explained in Section 1.3. Indeed, the Jaynes-Cummings Hamiltonian is itself an approximate Hamiltonian, obtained from a more general qubit-resonator interaction by neglecting rapidly oscillating terms, following the same averaging principle that underlies the secular approximation [32].
Physically, Eq. (4.34) describes a qubit whose transition frequency is shifted by ω_{eff} and whose relaxation is governed by the effective decay rate γ_{eff}. Furthermore, H_{eff} constitutes the Lamb-Shift Hamiltonian H_{LS} introduced in Eq. (1.25) in Section 1.3, which represents the unitary contribution to the dynamics of the qubit due to its interaction with the resonator.

4.3 Generalized SW Transformation

In the previous section, we derived a second-order Redfield master equation for the qubit density matrix via an adiabatic elimination of the damped resonator. Here, by exploiting the generalized SW method introduced in Chapter 3, we can derive reduced theories for the qubit dynamics at different orders in a systematic way. At second order, we will recover the Redfield master equation (4.34). At higher orders, we will obtain corrections to the qubit dynamics, highlighting the capabilities of the method.

Single-excitation subspace

Throughout this section, we restrict our attention to processes involving the emission of at most one excitation, so that the cavity state belongs to the subspace spanned by $\{|0\rangle, |1\rangle\}$. Within this truncated subspace, the operators a and $a^\dagger$ can therefore be identified with σ_- and σ_+, respectively. Hence, the cavity can be treated as a two-level system, i.e., a qubit. Indeed, since the Jaynes-Cummings Hamiltonian conserves the total excitation number and the dissipator can only remove excitations from the bath, an initial state containing at most one excitation will never evolve into a state with more than one excitation. Throughout this chapter, we consider the cavity to be initially prepared in the vacuum state, while any potential excitation is provided by the qubit state.
In the single-excitation subspace, the Jaynes-Cummings Hamiltonian can thus formally be written as

$$H = \frac{\omega_q}{2}\sigma_z^{(q)} + \frac{\omega_r}{2}\sigma_z^{(r)} + g\left(\sigma_+^{(q)}\sigma_-^{(r)} + \sigma_-^{(q)}\sigma_+^{(r)}\right), \tag{4.44}$$

where the indices (q) and (r) refer to the qubit and the resonator, respectively. Moreover, the master equation (4.1) governing the system becomes

$$\dot{\rho} = -i\left[H, \rho\right] + \gamma\left(\sigma_-^{(r)}\rho\sigma_-^{(r)} - \frac{1}{2}\left\{\sigma_+^{(r)}\sigma_-^{(r)}, \rho\right\}\right) \equiv \mathcal{L}\left[\rho\right]. \tag{4.45}$$

In this expression, the cavity operators appearing in the dissipator are thus $\sigma_\pm^{(r)}$, instead of the original operators a and $a^\dagger$.

[3] A remark can be made regarding Eq. (4.34): $H_0 = \frac{\omega_q}{2}\sigma_z + \omega_r a^\dagger a$ acts on $\mathcal{H}_S \otimes \mathcal{H}_B$, but $[\omega_r a^\dagger a, \rho_q] = 0$ since the two operators act on distinct subspaces. Hence, Eq. (4.34) ultimately contains only operators acting on the qubit subspace associated with the Hilbert space $\mathcal{H}_S$.

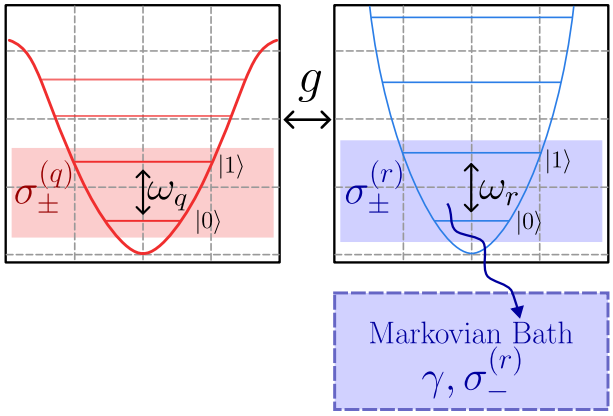

Figure 4.2: Illustration of the system "qubit + resonator", restricted to the single excitation subspace, where the resonator is damped through its coupling to a Markovian bath.

$\mathcal{L}_0 + \mathcal{V}$ separation

Before applying the generalized Schrieffer-Wolff transformation, the master equation (4.1) describing our system must be expressed as

$$\dot{\rho} = \mathcal{L}[\rho] \equiv (\mathcal{L}_0 + \mathcal{V})[\rho]. \tag{4.46}$$

Choosing correctly the separation of the Liouvillian into $\mathcal{L}_0$ and $\mathcal{V}$ is essential for the successful implementation of the method.
The aim is to obtain an effective equation for the reduced density operator of the qubit. Moreover, the Hilbert space of a qubit is two-dimensional, hence the density operator is represented by a 2×2 matrix, and once vectorized, by a 4-dimensional column vector. As seen when introducing the generalized Schrieffer-Wolff formalism in Chapter 3, the exact low-excitation spectrum of the Liouvillian is reproduced by an effective Liouvillian L_{eff} such that

$$\dot{\mu} = L_{\text{eff}}\mu, \tag{4.47}$$

where μ is the reduced density matrix on the slow subspace associated with the zero eigenvalues of $\mathcal{L}_0$, and L_{eff} is equal to the projection of a transformed block-diagonal Liouvillian $L = U^{-1}\mathcal{L}U$ onto the same subspace, i.e., $L_{\text{eff}} = PLP$. In order to get an equation which is compatible with the density operator represented by a $4D$ vector, L_{eff} needs to be represented by a 4×4 matrix. Hence, the Liouvillian $\mathcal{L}_0$ must admit exactly 4 zero eigenvalues.

Furthermore, the Liouvillian contribution $\mathcal{V}$ must be treated as a perturbation. In the case of dispersive readout, as seen in Section 2.3, the coupling parameter g must be considered small compared to the detuning Δ between the qubit and the resonator. In this sense, it seems natural to separate the total Liouvillian as follows

$$\mathcal{L}_0[\cdot] = \gamma\left(\sigma_{-}^{(r)}\cdot\sigma_{+}^{(r)} - \frac{1}{2}\left\{\sigma_{+}^{(r)}\sigma_{-}^{(r)},\cdot\right\}\right) - i\left[\frac{\omega_q}{2}\sigma_z^{(q)} + \frac{\omega_r}{2}\sigma_z^{(r)},\cdot\right] \tag{4.48}$$

$$\mathcal{V}[\cdot] = -ig\left[\sigma_{-}^{(q)}\sigma_{+}^{(r)} + \sigma_{+}^{(q)}\sigma_{-}^{(r)},\cdot\right]. \tag{4.49}$$

In this case $\mathcal{L}_0$ is expressed not only in terms of the qubit's operators, but also of the resonator's. Hence, it acts on a density matrix of dimension 4×4 which, when vectorized, corresponds to a $16D$ vector. Analyzing the spectrum of $\mathcal{L}_0$, we find that only two of its eigenvalues vanish, meaning that the reduced density matrix on the corresponding subspace would be a $2D$ column vector which cannot describe a qubit. A qualitative sketch of the spectrum of $\mathcal{L}_0$ is given in

Figure 4.3 a).

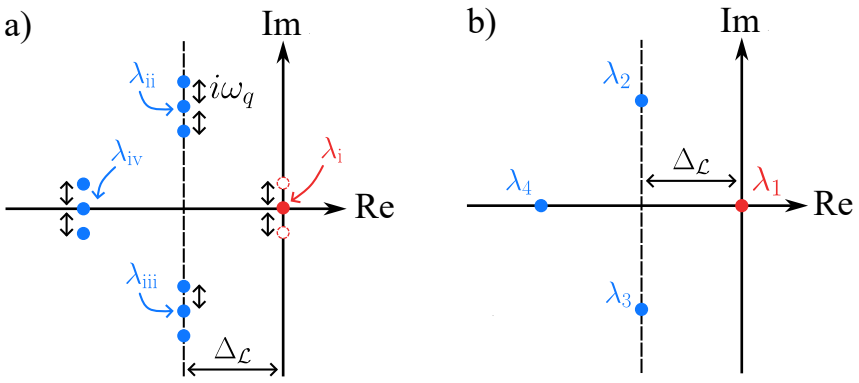

Figure 4.3: a) Sketch of the spectrum of a wrong choice (4.48) for $\mathcal{L}_0$ where the eigenvalues denoted λ_i are twofold-degenerated while the remaining eigenvalues are not. The blue eigenvalues are associated with decaying mode, the solid red eigenvalue (twofold-degenerate) corresponds to the steady state of the system and the red dashed circles are related to oscillating modes. b) Sketch of the spectrum of $\mathcal{L}_0^{RF}$ in the rotating frame $R(t) = e^{-i\tilde{H}t}$ with $\tilde{H} = \frac{1}{2}\omega_q \left(\sigma_z^{(q)} + \sigma_z^{(r)}\right)$, where the subspace $\mathcal{P}$ corresponds to the red eigenvalue and the subspace $\mathcal{Q}$ contains the blue eigenvalues. In both figures, $\Delta_{\mathcal{L}}$ denotes the Liouvillian gap as defined by Eq. (1.44) in Section 1.5 where the subscript $\mathcal{L}$ is added to avoid confusion with the detuning $\Delta = \omega_q - \omega_r$.

A solution would be to define the slow subspace as referring to eigenvalues with a vanishing real part instead of zero-eigenvalues. However, in this case, the generalized Schrieffer-Wolff formalism developed in Chapter 3 no longer applies. Consequently, we must find another separation than given by Eqs. (4.48) and (4.49).

One might try to put the unitary Hamiltonian contribution of the free qubit $\omega_q \sigma_z^{(q)}/2$ into the $\mathcal{V}$ part. However, the method requires $\mathcal{V}$ to be treated as a perturbation. Consequently, treating both g and ω_q as perturbation parameters would be misleading.

Finally, the last and valid option, which will yield the results of adiabatic elimination to second order, as mentioned in the final part of Chapter 3, is to do the derivation within a rotating frame in which $\mathcal{L}_0$ admits a zero eigenvalue which is fourfold-degenerate. Additionally, $\mathcal{V}$ should only depend on the coupling parameter g. This rotating frame exists and is defined by

$$R(t) = e^{-i\tilde{H}t} \text{ with } \tilde{H} = \frac{1}{2}\omega_q \left(\sigma_z^{(q)} + \sigma_z^{(r)}\right). \tag{4.50}$$

A schematic representation of the spectrum of $\mathcal{L}_0^{\mathrm{RF}}$ in this rotating frame is shown in Figure 4.3 b). $R(t)$ transforms the Hamiltonian of the system, given by Eq. (4.44), into

$$H^{RF} = \frac{1}{2}\left(\omega_r - \omega_q\right)\sigma_z^{(r)} + g\left(\sigma_+^{(q)}\sigma_-^{(r)} + \sigma_-^{(q)}\sigma_+^{(r)}\right). \tag{4.51}$$

The frequency of the qubit is set to zero while the frequency of the resonator corresponds to the the detuning $\omega_r - \omega_q$ between the resonator and the quit. As in the previous chapter, we define $\Delta = \omega_q - \omega_r$. As for the interaction Hamiltonian, it remains unchanged because $\sigma_{\pm,RF}^{(r,q)} = e^{\pm i\omega_q t}\sigma_{\pm}^{(r,q)}$.
Hence, the appropriate starting point of the Schrieffer-Wolff formalism is

$$\dot{\rho}^{RF} = \mathcal{L}^{RF}[\rho^{RF}] \equiv \left(\mathcal{L}_0^{RF} + \mathcal{V}^{RF}\right)[\rho^{RF}]. \tag{4.52}$$

with

$$\mathcal{L}_0^{RF}[\cdot] = \gamma\left(\sigma_-^{(r)}\cdot\sigma_+^{(r)} - \frac{1}{2}\left\{\sigma_+^{(r)}\sigma_-^{(r)},\cdot\right\}\right) - i\left[-\frac{\Delta}{2}\sigma_z^{(r)},\cdot\right] \tag{4.53}$$

$$\mathcal{V}^{RF}[\cdot] = -ig\left[\sigma_-^{(q)}\sigma_+^{(r)} + \sigma_+^{(q)}\sigma_-^{(r)},\cdot\right]. \tag{4.54}$$

In the vectorized formalism, we write

$$|\dot{\rho}^{RF}\rangle\!\rangle = \mathcal{L}^{RF}|\rho^{RF}\rangle\!\rangle = \left(\mathcal{L}_0^{RF} + \mathcal{V}^{RF}\right)|\rho^{RF}\rangle\!\rangle \tag{4.55}$$

with

$$\boxed{\begin{aligned}\mathcal{L}_0^{RF} &= \gamma\left(\sigma_-^{(r)}\otimes\sigma_-^{(r)} - \frac{1}{2}\left(\sigma_+^{(r)}\sigma_-^{(r)}\otimes\mathbb{1}_2 + \mathbb{1}_2\otimes\sigma_+^{(r)}\sigma_-^{(r)}\right)\right)\\ &\quad + i\frac{\Delta}{2}\left(\sigma_z^{(r)}\otimes\mathbb{1}_2 - \mathbb{1}_2\otimes\sigma_z^{(r)}\right) \qquad (4.56)\\ \mathcal{V}^{RF} &= -ig\Big(\left(\sigma_+^{(r)}\sigma_-^{(q)} + \sigma_-^{(r)}\sigma_+^{(q)}\right)\otimes\mathbb{1}_4 - \mathbb{1}_4\otimes\left(\sigma_+^{(r)}\sigma_-^{(q)} + \sigma_-^{(r)}\sigma_+^{(q)}\right)\Big). \qquad (4.57)\end{aligned}}$$

The notation $\mathbb{1}_n$ denotes the identity operator in an n-dimensional space. Note that $\mathcal{L}_0^{RF}$ only depends on operators of the resonator. It is thus defined in the corresponding subspace and can be represented by a 4×4 matrix since in the single-excitation subspace, the qubit is treated as a two-level system (thus represented by a $4D$ vector). Though, when extended to the full Hilbert space of the coupled qubit-resonator system, the resonator operators $\sigma_\pm^{(r)}$ are promoted from 2×2 to 4×4 matrices. Hence, $\mathcal{L}_0^{RF}$ becomes the full size 16×16 matrix and the identity matrices $\mathbb{1}_2$ appearing in its definition (4.56) must be replaced by $\mathbb{1}_4$. On the other hand, $\mathcal{V}^{RF}$ depends on both qubit and resonator operators. Hence, its matrix representation is a full-size matrix of dimension 16×16.

Second-order model

In the following, we derive a second-order effective Hamiltonian governing the evolution of the reduced density matrix of the qubit and reproducing the result of adiabatic elimination obtained in the previous section through the Redfield formalism.
For the sake of brevity, the superscript RF will be omitted in the following. The matrix representation of the free Liouvillian $\mathcal{L}_0$ given by Eq. (4.56), in the standard basis $\{|ee\rangle\!\rangle, |eg\rangle\!\rangle, |ge\rangle\!\rangle, |gg\rangle\!\rangle\}$ reads

$$\mathcal{L}_0 = \begin{pmatrix} -\gamma & 0 & 0 & 0\\ 0 & -\frac{\gamma}{2}+i\Delta & 0 & 0\\ 0 & 0 & -\frac{\gamma}{2}-i\Delta & 0\\ \gamma & 0 & 0 & 0\end{pmatrix}. \tag{4.58}$$

Note that the double ket vectors of the basis corresponds to the vectorized basis matrices of the space of reduced density operators of the resonator. Hence, $|gg\rangle\!\rangle$ is the vectorized form of $|g\rangle\langle g|$ (as introduced in Section 1.4 of Chapter 1 by Eqs. (1.31) and (1.32)) corresponding to the vacuum state of the cavity. Similarly, $|eg\rangle\!\rangle$ is the vectorized state $|e\rangle\langle g|$. As presented in Chapter 3, the Schrieffer–Wolff formalism requires knowledge of the eigenvalues of $\mathcal{L}_0$, together with the associated left and right eigenvectors. They are presented in Table 4.1.

	λ_i	$\|r_i\rangle\rangle$	$\|l_i\rangle\rangle$
#1	$\lambda_1 = 0$	$\|r_1\rangle\rangle = \|gg\rangle\rangle$	$\|l_1\rangle\rangle = \|gg\rangle\rangle + \|ee\rangle\rangle$
#2	$\lambda_2 = -\gamma/2 - i\Delta$	$\|r_2\rangle\rangle = \|ge\rangle\rangle$	$\|l_2\rangle\rangle = \|ge\rangle\rangle$
#3	$\lambda_3 = -\gamma/2 + i\Delta$	$\|r_3\rangle\rangle = \|eg\rangle\rangle$	$\|l_3\rangle\rangle = \|eg\rangle\rangle$
#4	$\lambda_4 = -\gamma$	$\|r_4\rangle\rangle = \|ee\rangle\rangle - \|gg\rangle\rangle$	$\|l_4\rangle\rangle = \|ee\rangle\rangle$

Table 4.1: Eigenvalues λ_i, and left and right eigenvectors, $|l_i\rangle\rangle$ and $|r_i\rangle\rangle$ of $\mathcal{L}_0$ in the chosen rotating frame.

Hence, $\mathcal{L}_0$ and $\mathcal{V}$ are expressed in the eigenbasis of the reduced size $\mathcal{L}_0$ as

$$\mathcal{L}_0 = \left(\begin{array}{c|ccc} 0 & 0 & 0 & 0 \\ \hline 0 & -\frac{\gamma}{2} - i\Delta & 0 & 0 \\ 0 & 0 & -\frac{\gamma}{2} + i\Delta & 0 \\ 0 & 0 & 0 & -\gamma \end{array}\right) \tag{4.59}$$

and

$$\mathcal{V} = \left(\begin{array}{c|ccc} \mathbb{0} & C & -C^\dagger & \mathbb{0} \\ \hline A & \mathbb{0} & \mathbb{0} & D \\ B & \mathbb{0} & \mathbb{0} & -D^\dagger \\ \mathbb{0} & B & A & \mathbb{0} \end{array}\right), \tag{4.60}$$

with[4]

$$A \equiv ig\left(\mathbb{1}_2 \otimes \sigma_-^{(q)}\right) \tag{4.61a}$$

$$B \equiv -ig\left(\sigma_-^{(q)} \otimes \mathbb{1}_2\right) \tag{4.61b}$$

$$C \equiv -ig\left(\sigma_-^{(q)} \otimes \mathbb{1}_2 - \mathbb{1}_2 \otimes \sigma_+^{(q)}\right) \tag{4.61c}$$

$$D \equiv -ig\left(\sigma_+^{(q)} \otimes \mathbb{1}_2 + \mathbb{1}_2 \otimes \sigma_-^{(q)}\right). \tag{4.61d}$$

The upper left block of Eqs. (4.59) and (4.60) thus corresponds to the subspace $\mathcal{P}$ of the zero eigenvalues of $\mathcal{L}_0$. Furthermore, projecting in this subspace corresponds to projecting the bath in its ground state. This can intuitively be understood by the fact that the right eigenstate of $\mathcal{L}_0$ corresponding to the zero eigenvalue is $|gg\rangle\rangle$, which denotes the vacuum state of the resonator as explained in the previous paragraph[5]. This first statement gives a sense on how the adiabatic elimination takes place in the present method. Indeed, the projection onto the slow space eliminates the fast varying degrees of freedom of the resonator by projecting it into its ground state, i.e., the vacuum state.
The matrix representations allow one to calculate the effective Liouvillian expansion

$$L_{\text{eff}} = PLP = L_1^{\text{eff}} + L_2^{\text{eff}} + ...$$

introduced in Eqs. (3.44) and (3.45) of Chapter 3 where the compact expressions of L_1^{eff} and L_2^{eff} are given by

$$L_1^{\text{eff}} = P\mathcal{V}^{\text{D}}P = \mathcal{V}^P \tag{4.62}$$

$$L_2^{\text{eff}} = -\mathcal{V}^-\mathcal{L}_0^{-1}\mathcal{V}^+. \tag{4.63}$$

[4]The following property of the Kronecker product is recalled: $(X \otimes Y)^\dagger = X^\dagger \otimes Y^\dagger$.
[5]More rigorously, this observation follows directly by returning to the standard basis.

First, Eq. (4.60) directly yields

$$L_1^{\text{eff}} = 0, \tag{4.64}$$

since $\mathcal{V}^D = 0$ (recall that $\mathcal{V}^D$ corresponds to the block diagonal matrix constituted of the diagonal blocks of $\mathcal{V}$ as defined in Eq. (3.10) in Section 3.1).
Recalling the following notation introduced in Chapter 3:

$$A = \begin{pmatrix} \overline{A^P} & \overline{A^-} \\ \overline{A^+} & \overline{A^Q} \end{pmatrix} = \begin{pmatrix} \overline{PAP} & \overline{PAQ} \\ \overline{QAP} & \overline{QAQ} \end{pmatrix}, \tag{4.65}$$

the explicit matrix representation of Eq. (4.63) reads

$$\overline{L_2^{\text{eff}}} = -\overline{\mathcal{V}^-}\overline{\mathcal{L}_0^{-1}}\overline{\mathcal{V}^+} = -\begin{pmatrix} C & -C^\dagger & 0 \end{pmatrix} \begin{pmatrix} -\frac{\gamma}{2} - i\Delta & 0 & 0 \\ 0 & -\frac{\gamma}{2} + i\Delta & 0 \\ 0 & 0 & -\gamma \end{pmatrix}^{-1} \begin{pmatrix} A \\ B \\ \mathbb{0} \end{pmatrix} \tag{4.66}$$

$$= -\begin{pmatrix} C\left(-\frac{\gamma}{2} - i\Delta\right)^{-1} & -C^\dagger\left(-\frac{\gamma}{2} + i\Delta\right)^{-1} & \mathbb{0} \end{pmatrix} \begin{pmatrix} A \\ B \\ \mathbb{0} \end{pmatrix} \tag{4.67}$$

$$= \frac{1}{\frac{\gamma}{2} + i\Delta} CA - \frac{1}{\frac{\gamma}{2} - i\Delta} C^\dagger B, \tag{4.68}$$

where the reduced matrix representation was used to avoid displaying matrices filled with zeros, since

$$L_2^{\text{eff}} = \left(\begin{array}{c|ccc} \overline{L_2^{\text{eff}}} & 0 & 0 & 0 \\ \hline 0 & 0 & 0 & 0 \\ 0 & 0 & 0 & 0 \\ 0 & 0 & 0 & 0 \end{array}\right). \tag{4.69}$$

Substituting A, B and C by their expressions, given by Eqs. (4.61a) to (4.61c), into Eq. (4.68) and recalling that $(A \otimes \mathbb{1})(\mathbb{1} \otimes B) = A \otimes B$, one gets

$$\begin{aligned}
\overline{L_2^{\text{eff}}} &= \frac{1}{\frac{\gamma}{2} + i\Delta}\left(-ig\left(\sigma_-^{(q)} \otimes \mathbb{1}_2 - \mathbb{1}_2 \otimes \sigma_+^{(q)}\right)\right)\left(ig\mathbb{1}_2 \otimes \sigma_-^{(q)}\right) \\
&\qquad - \frac{1}{\frac{\gamma}{2} - i\Delta}\left(ig\left(\sigma_+^{(q)} \otimes \mathbb{1}_2 - \mathbb{1}_2 \otimes \sigma_-^{(q)}\right)\right)\left(-ig\sigma_-^{(q)} \otimes \mathbb{1}_2\right) \\
&= \frac{g^2}{\frac{\gamma}{2} + i\Delta}\left(\left(\sigma_-^{(q)} \otimes \mathbb{1}_2 - \mathbb{1}_2 \otimes \sigma_+^{(q)}\right)\right)\left(\mathbb{1}_2 \otimes \sigma_-^{(q)}\right) \\
&\qquad - \frac{g^2}{\frac{\gamma}{2} - i\Delta}\left(\left(\sigma_+^{(q)} \otimes \mathbb{1}_2 - \mathbb{1}_2 \otimes \sigma_-^{(q)}\right)\right)\left(\sigma_-^{(q)} \otimes \mathbb{1}_2\right) \\
&= \frac{g^2}{\frac{\gamma}{2} + i\Delta}\left(\left(\sigma_-^{(q)} \otimes \sigma_-^{(q)} - \mathbb{1}_2 \otimes \sigma_+^{(q)}\sigma_-^{(q)}\right)\right) \\
&\qquad - \frac{g^2}{\frac{\gamma}{2} - i\Delta}\left(\left(\sigma_+^{(q)}\sigma_-^{(q)} \otimes \mathbb{1}_2 - \sigma_-^{(q)} \otimes \sigma_-^{(q)}\right)\right).
\end{aligned}$$

Writing the fractions with a common denominator yields

$$\begin{aligned}\overline{L_2^{\text{eff}}} &= \frac{g^2\left(\frac{\gamma}{2}-i\Delta\right)}{(\frac{\gamma}{2})^2+\Delta^2}\left(\left(\sigma_-^{(q)}\otimes\sigma_-^{(q)}-\mathbb{1}_2\otimes\sigma_+^{(q)}\sigma_-^{(q)}\right)\right)\\ &\qquad-\frac{g^2\left(\frac{\gamma}{2}+i\Delta\right)}{(\frac{\gamma}{2})^2+\Delta^2}\left(\left(\sigma_+^{(q)}\sigma_-^{(q)}\otimes\mathbb{1}_2-\sigma_-^{(q)}\otimes\sigma_-^{(q)}\right)\right)\\ &= \frac{g^2\gamma/2}{(\frac{\gamma}{2})^2+\Delta^2}\left(\left(\sigma_-^{(q)}\otimes\sigma_-^{(q)}-\mathbb{1}_2\otimes\sigma_+^{(q)}\sigma_-^{(q)}\right)-\left(\sigma_+^{(q)}\sigma_-^{(q)}\otimes\mathbb{1}_2-\sigma_-^{(q)}\otimes\sigma_-^{(q)}\right)\right)\\ &\qquad-i\frac{g^2\Delta}{(\frac{\gamma}{2})^2+\Delta^2}\left(\left(\sigma_-^{(q)}\otimes\sigma_-^{(q)}-\mathbb{1}_2\otimes\sigma_+^{(q)}\sigma_-^{(q)}\right)+\left(\sigma_+^{(q)}\sigma_-^{(q)}\otimes\mathbb{1}_2-\sigma_-^{(q)}\otimes\sigma_-^{(q)}\right)\right).\end{aligned}$$

Moreover, as in the previous section,

$$\omega_{\text{eff}}=\frac{g^2\Delta}{(\frac{\gamma}{2})^2+\Delta^2}\quad\text{and}\quad\gamma_{\text{eff}}=\frac{g^2\gamma}{(\frac{\gamma}{2})^2+\Delta^2},\tag{4.70}$$

hence, the matrix representation of the second-order effective Liouvillian finally reads

$$\begin{aligned}\overline{L_2^{\text{eff}}} &= \gamma_{\text{eff}}\left(\sigma_-^{(q)}\otimes\sigma_-^{(q)}-\frac{1}{2}\left(\mathbb{1}_2\otimes\sigma_+^{(q)}\sigma_-^{(q)}+\sigma_+^{(q)}\sigma_-^{(q)}\otimes\mathbb{1}_2\right)\right)\\ &\qquad-i\omega_{\text{eff}}\left(+\sigma_+^{(q)}\sigma_-^{(q)}\otimes\mathbb{1}_2-\mathbb{1}_2\otimes\sigma_+^{(q)}\sigma_-^{(q)}\right).\end{aligned}\tag{4.71}$$

However it is convenient to go back to the superoperator formalism to express the final master equation describing the evolution of the density matrix of the qubit. Hence, the master equation describing the effective motion of the qubit in the rotating frame $R(t)=e^{\frac{1}{2}\omega_q\left(\sigma_z^{(q)}+\sigma_z^{(r)}\right)}$ reads

$$\dot{\rho}_q(t)=-i\,\omega_{\text{eff}}\left[\sigma_+^{(q)}\sigma_-^{(q)},\rho_q(t)\right]+\gamma_{\text{eff}}\left(\sigma_-^{(q)}\rho_q(t)\sigma_+^{(q)}-\frac{1}{2}\left\{\sigma_+^{(q)}\sigma_-^{(q)},\rho_q(t)\right\}\right).\tag{4.72}$$

The resulting effective master equation is identical to the one obtained using the Redfield method in Section 4.2, given by Eq. (4.34), which is expressed in the interaction picture. Although different rotating frames are chosen at the beginning of the two derivations, namely the interaction picture with respect to $H_0=\frac{\omega_q}{2}\sigma_z+\omega_r a^\dagger a$ in the Redfield approach and the rotating frame with respect to $\tilde{H}=\omega_q(\sigma_z^{(q)}+\sigma_z^{(r)})/2$ in the SW approach, the elimination of the cavity degrees of freedom leads to the same effective equation for the qubit. Since the resulting master equation no longer contains cavity operators, the two reference frames are equivalent from the point of view of the reduced qubit dynamics. As before, expressing Eq. (4.72) in the Schrödinger picture yields the previously obtained effective master equation for the qubit:

Key Result 4.2. Second order SW effective equation ≡ Redfield equation

$$\dot{\rho}_1(t)=-i\left[H_0+H_{\text{eff}},\rho_q(t)\right]+\gamma_{\text{eff}}\left(\sigma_-\rho_q(t)\sigma_+-\frac{1}{2}\left\{\sigma_+\sigma_-,\rho_q(t)\right\}\right).\tag{4.73}$$

This second-order result captures the dominant qubit decay dynamics and the associated Lamb-Shift renormalization as explained in Section 4.2. However, it treats the resonator as a "simple" Markovian bath. Hence, effects such as the resonator back-action are not accounted for. This limitation motivates the systematic higher-order corrections provided by the generalized Schrieffer-Wolff transformation.

Numerical results

Having established that the second-order Schrieffer-Wolff expansion reproduces the result of adiabatic elimination when performed in a specific rotating frame equivalent to the interaction picture from the point of view of the qubit, we now turn to the computation of higher-order effective Liouvillians. To this end, substituting the definitions of $\mathcal{L}_0$ and $\mathcal{V}$ given by Eqs. (4.59) and (4.60) in the iterative expressions (3.36) and (3.42) derived in Chapter 3 allows for the systematic computation of L_n^{eff} via Eq. (3.44).

As a first step, recall the compact expression for L_3^{eff} derived in Chapter 3 as

$$L_3^{\text{eff}} = \mathcal{V}^- \mathcal{L}_0^{-1} \mathcal{V}^Q \mathcal{L}_0^{-1} \mathcal{V}^+ - \frac{1}{2} \left\{ \mathcal{V}^P, \mathcal{V}^- \mathcal{L}_0^{-2} \mathcal{V}^+ \right\}. \tag{4.74}$$

Proceeding as for the second-order by making the matrix products explicit, one finds

$$L_3^{\text{eff}} = 0. \tag{4.75}$$

More generally, all odd-order terms of the Schrieffer-Wolff expansion vanish in this particular case, meaning that only even-order contributions survive[6].

To assess the accuracy of the higher-order effective Liouvillians and their associated master equations, we compare the reduced density matrix of the qubit obtained through the Schrieffer-Wolff method with the exact result. The latter is obtained by solving the enlarged master equation (4.45) for the full "qubit + resonator" system and tracing out the resonator degrees of freedom. The agreement between the two is quantified using the *fidelity* of the corresponding density matrices.

Theoretical Concept 4.2. Fidelity

The *fidelity* is a measure of distance between quantum states [8]. Let ρ and χ be two density operators, the fidelity between them is defined as

$$F(\rho, \chi) = \text{Tr}\sqrt{\rho^{1/2} \chi \rho^{1/2}}. \tag{4.76}$$

We first consider the case of a qubit initially prepared in its excited state. Figure 4.4 displays the infidelity $1 - F$ between the qubit's reduced density matrix, governed by the 2^{nd}, 4^{th} and 6^{th} order effective master equations derived from the Schrieffer-Wolff expansion, and the exact result obtained from the enlarged master equation, as a function of time and of the coupling parameter g, which serves as the perturbation parameter of the expansion. The results show that higher-order corrections improve the accuracy of the effective description. Moreover, as expected from the perturbative nature of the expansion, the infidelity increases with g, reflecting the deviation of the effective master equation from the exact dynamics as the coupling strength grows. Finally, for all orders, the infidelity decreases at long times, which is consistent with the fact that the qubit ultimately relaxes toward its ground state regardless of the order of the expansion, so that all descriptions converge to the same steady state.

[6] This can be understood from symmetry arguments of the Liouvillian, though a detailed discussion lies outside the scope of the present thesis.

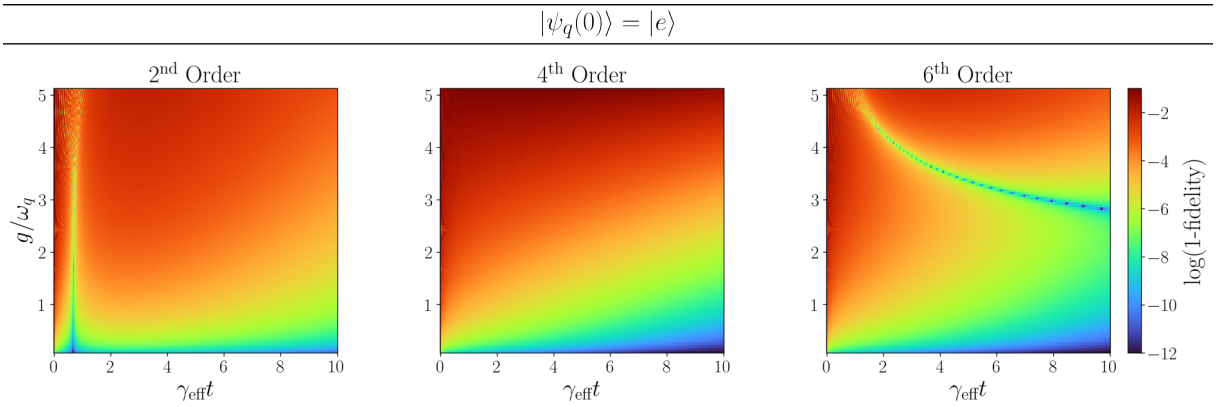

Figure 4.4: Infidelity between the reduced density matrix of the qubit governed by the n^{th}-order effective Liouvillian derived from the Schrieffer-Wolff expansion and the exact reduced density matrix obtained by tracing out the resonator from the solution of the enlarged master equation, for the qubit initially prepared in its excited state and the resonator prepared in its vacuum state.

We then consider, in Figure 4.5, the case of a qubit initially prepared in the superposition $|\psi_q(0)\rangle = (|e\rangle + |g\rangle)/\sqrt{2}$. The results are consistent with the previous case: higher-order effective master equations derived from the Schrieffer-Wolff expansion improve the fidelity of the reduced density matrix of the qubit. Conversely, increasing the coupling parameter g degrades the fidelity.

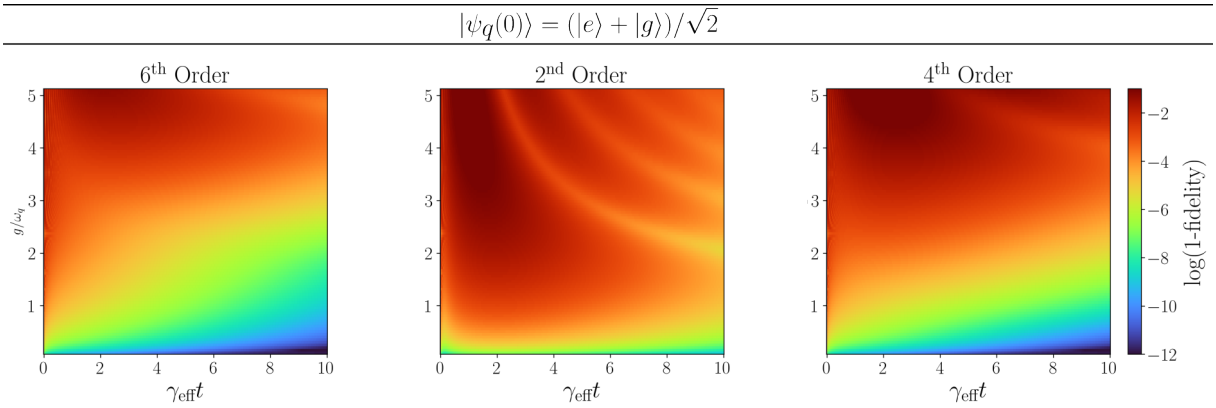

Figure 4.5: Infidelity between the reduced density matrix of the qubit governed by the n^{th}-order effective Liouvillian derived from the Schrieffer-Wolff expansion and the exact reduced density matrix obtained by tracing out the resonator from the solution of the enlarged master equation, for the qubit initially prepared in the superposition state $|\psi_q(0)\rangle = (|e\rangle + |g\rangle)/\sqrt{2}$ and the resonator prepared in its vacuum state.

Finally, Figure 4.6 presents the mean infidelity averaged over 100 random initial qubit states. The results are quantitavely highly similar to those obtained for the superposition state $|\psi_q(0)\rangle = (|e\rangle + |g\rangle)/\sqrt{2}$. Higher-order corrections systematically enhance the fidelity, while increasing g degrades it, as expected. This close agreement suggests that the superposition state is representative of the typical qubit dynamics for arbitrary initial states. Furthermore, the second row illustrates the behavior on a longer timescale, showing that, independently of the order of the expansion, the qubit eventually relaxes to its ground state, validating our previous statement regarding this matter. Consequently, all results converge to a vanishing infidelity. In addition, observing the dynamics over a longer timescale highlights that higher-order descriptions provide a more accurate characterization of the transient regimes, particularly for values of $g/\omega_q < 3$.

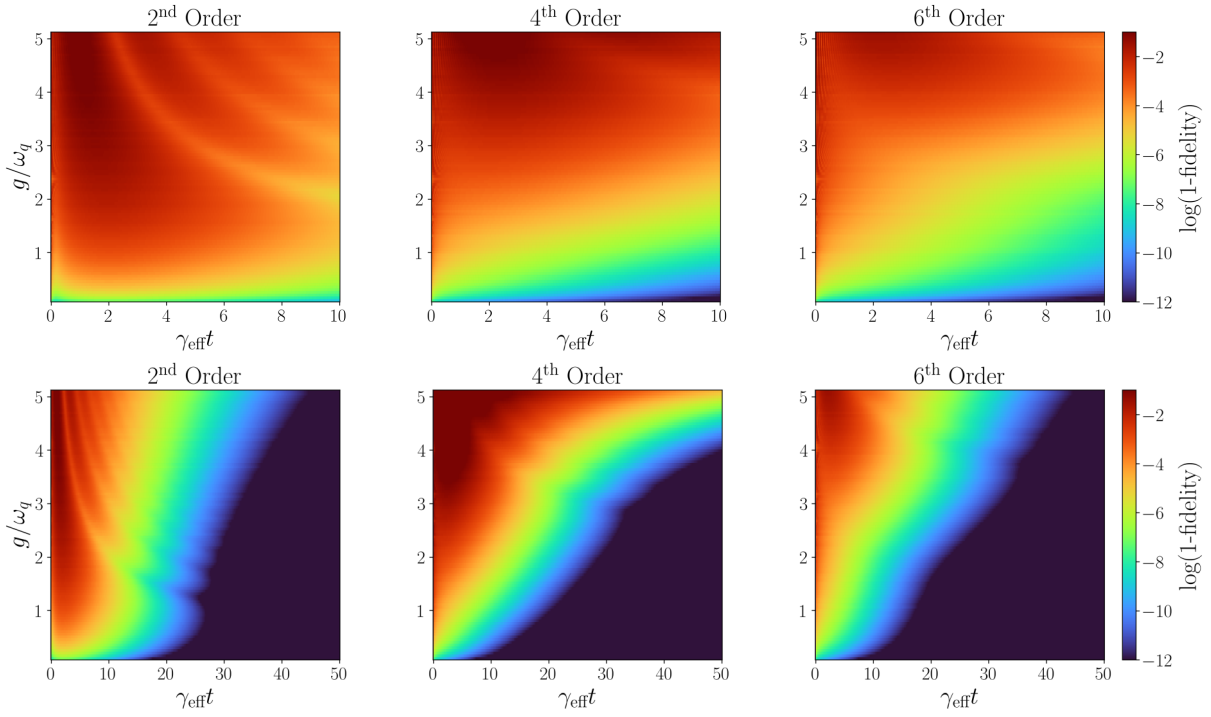

Figure 4.6: Mean infidelity between the reduced density matrix of the qubit governed by the n^{th}-order effective Liouvillian derived from the Schrieffer-Wolff expansion and the exact reduced density matrix obtained by tracing out the resonator from the solution of the enlarged master equation, averaged over 100 random initial qubit states, with the resonator prepared in its vacuum state. The first row corresponds to an observation over a time equivalent to Figures 4.4 and 4.5 while the second row makes explicit the relaxation of the qubit towards the steady state regardless of the order of the expansion.

Validity of the SW expansion

We conclude this chapter by revising the validity conditions of the Schrieffer-Wolff expansion as originally formulated by E. M. Kessler [7], and discussing how they compare to the parameter regime considered in this thesis, which turns out to differ from the strict validity domain of the original formulation.

In Chapter 3, the general condition ensuring the validity of the generalized Schrieffer-Wolff formalism was introduced as

$$2\epsilon\|\mathcal{V}\| < \Delta_{\mathcal{L}}. \tag{4.77}$$

Indeed, Kessler [7] introduces it as the condition under which the slow and fast subspaces of $\mathcal{L}_0$ maintain separate under the application of the perturbation $\epsilon\mathcal{V}$, see Figure 3.1. For the system of a qubit coupled to a damped resonator, analyzed in this chapter, $\|\mathcal{V}\| = 2|g|$ [7]. Given the eigenvalues of $\mathcal{L}_0$ listed in Table 4.1, the Liouvillian gap defined in Eq. (1.44) is

$$\Delta_{\mathcal{L}} = \min_{i\neq 0} |\text{Re}(\lambda_i)| = \text{Re}(\lambda_2) = \text{Re}(\lambda_3) = \frac{\gamma}{2}, \tag{4.79}$$

[7]The norm of the bounded operator $\mathcal{V}$, given by Eq. (4.57), is

$$\|\mathcal{V}\| = \sqrt{\lambda_{\max}(\mathcal{V}^\dagger\mathcal{V})} = 2g, \tag{4.78}$$

where the notation $\lambda_{\max}(\mathcal{V}^\dagger\mathcal{V})$ means the largest eigenvalue of $\mathcal{V}^\dagger\mathcal{V}$ [23].

and the condition (4.77) reads

$$2 \times 2g < \frac{\gamma}{2} \Leftrightarrow \boxed{8g < \gamma,} \tag{4.80}$$

taking $g > 0$, without loss of generality. However, this condition is too strong for the considered system. Indeed, the closest distance between the zero eigenvalue, associated to the steady state, and a non-zero eigenvalue is not given by the Liouvillian gap but by

$$d = \sqrt{\left(\frac{\gamma}{2}\right)^2 + \Delta^2}, \tag{4.81}$$

as illustrated in Figure 4.7. The relevant condition, instead of (4.80), is therefore

$$\boxed{4g < d.} \tag{4.82}$$

Indeed, we see in Figure 4.7 that if $\|\mathcal{V}\| = 2g$ exceeds $d/2$ the eigenvalues might be displaced in such a way that $\mathcal{P}$ and $\mathcal{Q}$ are no longer well separated.

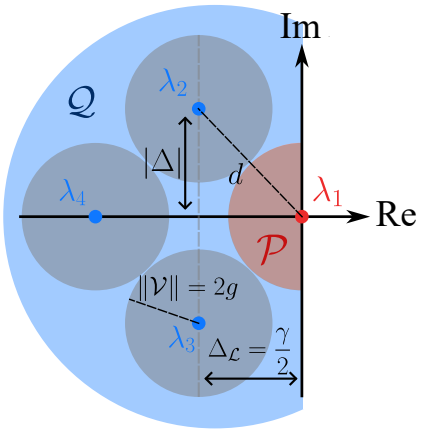

Figure 4.7: Qualitative illustration of the spectrum of $\mathcal{L}_0^{RF}$ defined in Eq. (4.56) under the perturbation $\mathcal{V}^{RF}$ given in Eq. (4.57). The gray disks indicate the possible displacement of the non-zero eigenvalues in the complex plane due to the perturbation. The red disk illustrates the corresponding displacement of the steady state and represents the perturbed slow space $\mathcal{P}$. Finally, the light blue region represents the fast subspace $\mathcal{Q}$, within which the non-zero eigenvalues should remain to stay in the complement of $\mathcal{P}$.

The parameters used in the simulations performed earlier do not necessarily fulfill condition (4.82). Indeed, in those simulations $d \simeq 10.0045 \simeq 10$, so that Eq. (4.82) imposes $g \lesssim 2.5$. Nevertheless, Figure 4.8 shows that the displacement of the eigenvalues of $\mathcal{L}_0$ induced by the perturbation $\mathcal{V}$ is of the order of the dispersive shift $\chi = g^2/\Delta$ introduced in Chapter 2, which is significantly smaller than the bound $\|\mathcal{V}\| = 2g$ predicted by Kessler's condition. The eigenvalues therefore remain well within the disk of radius $\|\mathcal{V}\| = 2g$, confirming that the spectral separation between the slow and fast subspaces is preserved in practice. Hence, the theoretical condition introduced in [7] should therefore be regarded as a worst-case estimate rather than an absolute condition that must be satisfied. Indeed, in the present case, the spectral separation between the slow and fast subspaces is well preserved even beyond this condition.

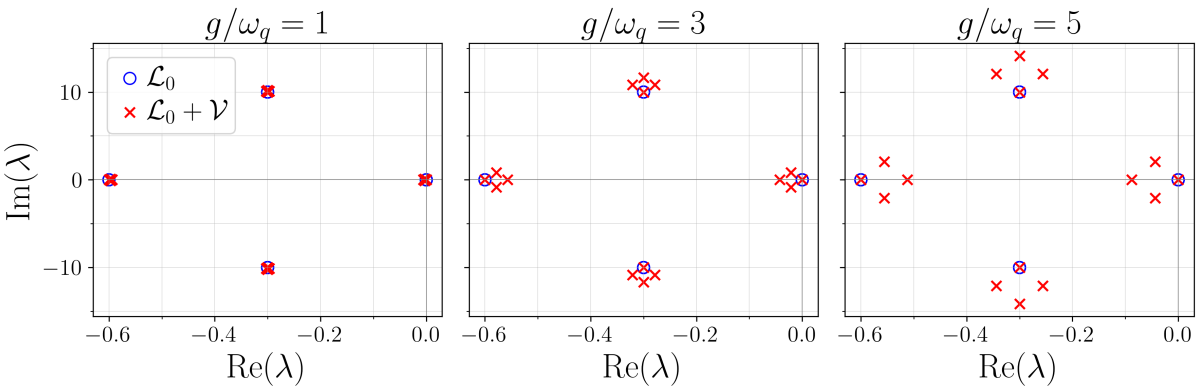

Figure 4.8: Comparison between the spectrum of $\mathcal{L}_0$ and $\mathcal{L}_0 + \mathcal{V}$ given in Eqs. (4.56) and (4.57) for different values of the coupling parameter g. Numerical parameters : $\omega_q = 1$ GHz, $\omega_r = \omega_d = 11$ GHz, $\gamma = 0.6$ GHz.

Summary 4. Application: a qubit coupled to a damped resonator

Chapter 4 presented the original contribution of this master thesis by applying the generalized Schrieffer-Wolff formalism to a qubit coupled to a damped resonator in the single-excitation subspace, governed by the Lindblad master equation

$$\dot{\rho} = -i[H, \rho] + \gamma \left(\sigma_-^{(r)} \rho \sigma_+^{(r)} - \frac{1}{2} \left\{ \sigma_+^{(r)} \sigma_-^{(r)}, \rho \right\} \right) \equiv \mathcal{L}[\rho].$$

First, an effective Redfield master equation for the qubit was derived by adiabatic elimination of the resonator, yielding

$$\dot{\rho}_q(t) = -i[H_0 + H_{\text{eff}}, \rho_q(t)] + \gamma_{\text{eff}} \left(\sigma_- \rho_q(t) \sigma_+ - \frac{1}{2} \{ \sigma_+ \sigma_-, \rho_q(t) \} \right),$$

where $H_{\text{eff}} = \omega_{\text{eff}} \sigma_+ \sigma_-$ is the Lamb-Shift Hamiltonian, and the effective frequency shift and decay rate are

$$\omega_{\text{eff}} = \frac{g^2 \Delta}{\left(\frac{\gamma}{2}\right)^2 + \Delta^2} \quad \text{and} \quad \gamma_{\text{eff}} = \frac{g^2 \gamma}{\left(\frac{\gamma}{2}\right)^2 + \Delta^2}.$$

The generalized Schrieffer-Wolff transformation was then applied by working in a suitable rotating frame defined by $R(t) = e^{-i\tilde{H}t}$ with $\tilde{H} = \frac{1}{2}\omega_q \left(\sigma_z^{(q)} + \sigma_z^{(r)} \right)$, in which $\mathcal{L}_0$ admits a fourfold degenerate zero eigenvalue in the full qubit-resonator space. The perturbation $\mathcal{V}$ depends solely on the coupling parameter g, ensuring a valid $\mathcal{L}_0 + \mathcal{V}$ separation.

The second-order effective Liouvillian was shown to reproduce exactly the Redfield result, confirming the consistency of the method.

Numerical simulations assessed higher-order corrections through the infidelity between the reduced qubit density matrix obtained from the n^{th}-order effective Liouvillian and the exact result obtained by tracing out the resonator. Higher-order terms systematically improve the fidelity, while increasing g degrades it, as expected from the perturbative nature of the expansion.

Finally, the validity condition of the expansion was refined from the original criterion $4g < \gamma$ to the tighter geometric condition

$$g < \frac{d}{2} \quad \text{with} \quad d = \sqrt{\left(\frac{\gamma}{2}\right)^2 + \Delta^2},$$

which accounts for the actual spectral separation between the slow and fast subspaces in the complex plane. However, it should be regarded as a worst case scenario since parameters beyond this condition still yields a valid expansion in the system analyzed here.

Chapter 5

Adding a Coherent Drive

The present chapter aims to place the work developed in Chapter 4 in a broader perspective by extending the model to include a coherent drive, as introduced in Section 2.2 through Eq. (2.23). This constitutes a step toward a more realistic description of the dispersive readout of superconducting qubits, where the resonator is typically driven by an external microwave field in order to probe the qubit state. Following the same approach as in Chapter 4, we derive an effective second-order master equation for the reduced density matrix of the qubit coupled to a damped and coherently driven resonator, by adiabatically eliminating the resonator degrees of freedom. This provides a starting point for understanding the more complex dynamics induced by the drive.

5.1 Master Equation

The master equation describing the dynamics of the qubit coupled to a driven cavity, which has been introduced in Section 2.2, is

$$\dot{\rho} = -i\,[H, \rho] + \mathcal{D}(a)\,[\rho]\,, \tag{5.1}$$

with

$$H = \frac{\omega_q}{2}\sigma_z + \omega_r a^\dagger a + g(\sigma_+ a + \sigma_- a^\dagger) + \epsilon a e^{i\omega_d t} + \epsilon^* a^\dagger e^{-i\omega_d t}, \tag{5.2}$$

and

$$\mathcal{D}(a)\,[\cdot] = \gamma\left(a \cdot a^\dagger - \frac{1}{2}\{a^\dagger a, \cdot\}\right). \tag{5.3}$$

In order to make the Liouvillian time-independent, lets us work in the rotating frame defined through $R(t) = e^{-i\omega_d t a^\dagger a}$, where the Hamiltonian becomes

$$H = \frac{\Delta_q}{2}\sigma_z + \Delta_r a^\dagger a + g(\sigma_+ a + \sigma_- a^\dagger) + \epsilon a + \epsilon^* a^\dagger, \tag{5.4}$$

with $\Delta_q = \omega_q - \omega_d$ and $\Delta_r = \omega_r - \omega_d$.
In analogy to the procedures followed in Section 4.2, we will need the Heisenberg equations for the operators of the isolated bath which is now driven. The adjoint master equation in this case leads to

$$\boxed{\dot{a}(t) = -i\Delta_r a(t) - \frac{\gamma}{2}a(t) - i\epsilon^*} \tag{5.5}$$

$$\boxed{\dot{a}^\dagger(t) = i\Delta_r a^\dagger(t) - \frac{\gamma}{2}a^\dagger(t) + i\epsilon.} \tag{5.6}$$

Comparing these with the case of the undriven cavity described by Eqs. (4.13a) and (4.13b), new terms depending on the drive intensity ϵ have appeared. As a consequence, the steady state of the cavity is no longer the vacuum. Indeed, in the stationary state where $\dot{a}(t) = \dot{a}^\dagger(t) = 0$,

we no longer have $a(t) = a^\dagger(t) = 0$. Instead, in the steady state, we have

$$a_{ss} = \frac{-i\epsilon^*}{i\Delta_r + \frac{\gamma}{2}}, \tag{5.7}$$

which yields the following expectation value

$$\boxed{\langle a \rangle_{ss} = \frac{-i\epsilon^*}{i\Delta_r + \frac{\gamma}{2}} \equiv \alpha.} \tag{5.8}$$

Furthermore, driving the cavity creates a coherent state[1] $|\alpha\rangle$, where α is a complex number such that $|\alpha|^2$ is the mean number of excitations in the cavity [39]. The drive rapidly becomes an issue when deriving a Redfield master equation in the same way as done in Section 4.2, because the bath correlation function does not decay to zero when the resonator is driven, it reaches a non-zero stationary value, thus preventing the use of the Born-Markov approximation. One way to address this problem consists in applying a displacement transformation to the cavity[2],

$$\boxed{a \to d + \alpha,} \tag{5.9}$$

where d corresponds to the mode of an undriven damped cavity associated with a vacuum steady state, while the expectation value α accounts for the coherent contribution created by the drive. Note that the operator d corresponds to the former operator a in the undriven case since they both describe a cavity decaying to the vacuum.
The displacement modifies the Hamiltonian Eq. (5.4) as follows

$$\begin{aligned} H' = \frac{\Delta_q}{2}\sigma_z + \Delta_r d^\dagger d + \Delta_r \alpha^* \alpha + \Delta_r(\alpha d^\dagger + \alpha^* d) \\ + g(\sigma_+ d + \sigma_- d^\dagger) + g(\sigma_+ \alpha + \sigma_- \alpha^*) \\ + \epsilon d + \epsilon^* d^\dagger + \epsilon\alpha + \epsilon^*\alpha^*. \end{aligned}$$

The terms $\Delta_r\alpha^*\alpha$, $\epsilon\alpha$ and $\epsilon^*\alpha^*$ are irrelevant constant contributions and may therefore be omitted from the Hamiltonian without consequence.
This displacement transformation also modifies the dissipator (5.3), leading to

$$\mathcal{D}(a)[\cdot] \to \mathcal{D}(d + \alpha)[\cdot]. \tag{5.10}$$

After calculations, we obtain

$$\mathcal{D}(d + \alpha)[\cdot] = \mathcal{D}(d)[\cdot] - i\frac{\gamma}{2}\left[i\left(\alpha^* d - \alpha d^\dagger\right), \cdot\right]. \tag{5.11}$$

A new unitary contribution appears, allowing for a new expression of the master equation as

$$\dot{\rho} = -i\left[H'', \rho\right] + \mathcal{D}(d)[\rho], \tag{5.12}$$

[1] A coherent state is a quantum state whose properties closely approximate those of a classical electromagnetic wave [39]. It plays a central role in quantum optics, since driving an optical cavity with a single-mode laser typically produces a coherent excitation of the cavity field.

[2] Formally, this transformation corresponds to the application of a displacement operator $D(\alpha) = \exp(\alpha a^\dagger - \alpha^* a)$ such that $D^\dagger(\alpha) a D(\alpha) = a + \alpha$ (we changed the notation to $d + \alpha$ to avoid confusion in this work) and $D(\alpha)|0\rangle = |\alpha\rangle$ [40].

where

$$H'' = \frac{\Delta_q}{2}\sigma_z + \Delta_r d^\dagger d + \Delta_r(\alpha d^\dagger + \alpha^* d) + g(\sigma_+ d + \sigma_- d^\dagger) + g(\sigma_+\alpha + \sigma_-\alpha^*) + \epsilon d + \epsilon^* d^\dagger + i\frac{\gamma}{2}\left(\alpha^* d - \alpha d^\dagger\right). \tag{5.13}$$

Furthermore, the definition (5.8) of α leads to $(\Delta_r - i\gamma/2)\,\alpha = \epsilon^*$ and the hermitian conjugate equality. Hence, the third term and last three terms of the Hamiltonian (5.13) cancel each other. Finally, the master equation after displacement of the cavity reads

Key Result 5.1. ME of a qubit readout system after displacement of the cavity

$$\dot{\rho} = -i\,[H, \rho] + \mathcal{D}(d)\,[\rho]\,, \tag{5.14}$$

with

$$H = \frac{\Delta_q}{2}\sigma_z + \Delta_r d^\dagger d + g(\sigma_+ d + \sigma_- d^\dagger) + g(\sigma_+\alpha + \sigma_-\alpha^*) \tag{5.15}$$

and

$$\mathcal{D}(d)\,[\cdot] = \gamma\left(d \cdot d^\dagger - \frac{1}{2}\{d^\dagger d, \cdot\}\right), \tag{5.16}$$

where the transformed Hamiltonian H given by Eq. (5.15), can be decomposed into three contributions: a system Hamiltonian $H_S = \frac{\Delta_q}{2}\sigma_z + g\,(\alpha\sigma_+ + \alpha^*\sigma_-)$ which depends only on qubit operators, a bath Hamiltonian $H_B = \Delta_r d^\dagger d$ describing the free resonator, and an interaction Hamiltonian $V = g\left(\sigma_+ d + \sigma_- d^\dagger\right)$. The words "system" and "bath" are chosen deliberately, as they anticipate the adiabatic elimination performed below.

5.2 Adiabatic elimination

Following the same approach as in Section 4.2, an effective master equation for the reduced density matrix of the qubit is derived by adiabatically eliminating the resonator degrees of freedom. To this end, the total Hamiltonian is decomposed as $H = H_S + H_B + V$, as introduced at the end of the previous section.

Interaction picture

We have, as previously, the following Redfield equation for the reduced density matrix of the qubit in the interaction picture:

$$\dot{\rho}_q(t) = -\int_0^{t\to\infty} \mathrm{Tr}_B\Big(\Big[V(t), [V(t-\tau), \rho_q(t)\otimes\rho_B]\Big]\Big)d\tau, \tag{5.17}$$

where the I subscripts referring to the interaction picture was omitted. In this case,

$$V = g\left(\sigma_+(t)d(t) + \sigma_-(t)d^\dagger(t)\right), \tag{5.18}$$

which depends on the time evolutions of the operators $\sigma_\pm(t)$ and $d(t)$, $d^\dagger(t)$ of the qubit and the displaced cavity, respectively. The operators $d(t)$ and $d^\dagger(t)$ obey the AME of the isolated cavity, leading to the corresponding Heisenberg equations. However, in order to get the time evolution of $\sigma_\pm(t)$, we need to compute (see Theoretical Concept 1.1)

$$\sigma_\pm(t) = e^{iH_0 t}\sigma_\pm e^{-iH_0 t}, \tag{5.19}$$

where $H_0 = H_S + H_B = \frac{\Delta_q}{2}\sigma_z + g(\sigma_+\alpha + \sigma_-\alpha^*) + \Delta_r d^\dagger d$.
To ease the calculations, H_S is expressed, without loss of generality, as

$$\boxed{H_S = \frac{\Delta_q}{2}\sigma_z + \frac{\Omega}{2}\sigma_x,} \tag{5.20}$$

with $\Omega = 2g|\alpha|$. Eq. (5.20) corresponds to the Hamiltonian of the quantum Rabi model, which describes a two-level system coupled to a single bosonic mode [41].

Proof. In order to express H_S as Eq. (5.20), the expectation value α is written in polar form, $\alpha = |\alpha|e^{i\phi}$. The system Hamiltonian then reads

$$H_S = \frac{\Delta_q}{2}\sigma_z + g|\alpha|(e^{i\phi}\sigma_+ + e^{-i\phi}\sigma_-). \tag{5.21}$$

Since $\sigma_x = \sigma_+ + \sigma_-$, choosing a reference frame in which the phase ϕ is absorbed into the qubit operators yields

$$H_S = \frac{\Delta_q}{2}\sigma_z + g|\alpha|\sigma_x. \tag{5.22}$$

Formally, this change of reference frame is implemented by the time-independent unitary transformation $U_\phi = e^{i\phi\sigma_z/2}$. Under this transformation, the qubit operators become

$$\sigma_{z,\phi} = U_\phi^\dagger \sigma_z U_\phi = \sigma_z \tag{5.23}$$
$$\sigma_{-,\phi} = U_\phi^\dagger \sigma_- U_\phi = e^{i\phi}\sigma_- \tag{5.24}$$
$$\sigma_{+,\phi} = U_\phi^\dagger \sigma_+ U_\phi = e^{-i\phi}\sigma_+, \tag{5.25}$$

using the BCH formula, as in the derivation of the interaction-picture time evolution of $\sigma_-(t)$ on page 47. Substituting Eqs. (5.23) to (5.25) into Eq. (5.21) gives Eq. (5.22).
However, the transformation U_ϕ also affects the interaction Hamiltonian V. In the transformed frame, one obtains

$$V = g\left(e^{-i\phi}\sigma_+(t)d(t) + e^{i\phi}\sigma_-(t)d^\dagger(t)\right). \tag{5.26}$$

Therefore, to recover the standard interaction term given in (5.18), the operators $d(t)$ and $d^\dagger(t)$ must be transformed as

$$d(t) \to e^{i\phi}d(t) \tag{5.27}$$
$$d^\dagger(t) \to e^{-i\phi}d^\dagger(t). \tag{5.28}$$

This is implemented by the additional time-independent unitary transformation $\bar{U}_\phi = e^{i\phi d^\dagger d}$.
Consequently, H_S can be written as (5.22), without loss of generality, since applying the time-independent unitary transformations U_ϕ and $\bar{U}_\phi$ merely correspond to a change of basis and therefore do not alter the physical content of the model. □

Physically, Eq. (5.20) is equivalent to describing a spin 1/2 subjected to an effective field $\mathbf{B_{eff}} = (\Omega, 0, \Delta_q)$. This becomes clear when writing

$$H_S = \frac{1}{2}\mathbf{B_{eff}} \cdot \sigma, \tag{5.29}$$

with $\sigma = (\sigma_x, \sigma_y, \sigma_z)$, the vector of Pauli matrices[3]. Diagonalizing the previous Hamiltonian greatly simplify the calculation of $\sigma_-(t)$. In other terms, one needs to align the effective field $\mathbf{B_{eff}}$ with the z-axis. With this in mind, the angle θ between $\mathbf{B_{eff}}$ and the z-axis is defined such that

$$\sin\theta = \frac{\Omega}{\Omega_{\text{eff}}} \tag{5.31}$$

$$\cos\theta = \frac{\Delta_q}{\Omega_{\text{eff}}}, \tag{5.32}$$

with $\Omega_{\text{eff}} = \sqrt{\Delta_q^2 + \Omega^2}$ [4] leading to

$$\boxed{H_S = \frac{\Omega_{\text{eff}}}{2}\left(\sin\theta\sigma_x + \cos\theta\sigma_z\right) \equiv \frac{\Omega_{\text{eff}}}{2}\tau_z,} \tag{5.33}$$

with the definition of $\tau_z \equiv \sin\theta\sigma_x + \cos\theta\sigma_z$. Introducing τ_x and τ_y accordingly, a basis in which H_S is diagonal, is given by

$$\begin{cases} \tau_x = \cos\theta\sigma_x - \sin\theta\sigma_z & \text{(5.34a)} \\ \tau_y = \sigma_y & \text{(5.34b)} \\ \tau_z = \sin\theta\sigma_x + \cos\theta\sigma_z, & \text{(5.34c)} \end{cases}$$

which is obtained by a rotation around the y-axis, i.e., $\tau_i = e^{i\sigma_y/2}\sigma_i e^{-i\sigma_y/2}$. The newly constructed matrices τ_i are referred to as *dressed* Pauli matrices [42]. The term *dressed* should be understood in contrast to the bare Pauli matrices, which correspond to the basis in which the Hamiltonian $\Delta_q\sigma_z/2$ of the isolated qubit is diagonal, with eigenvalues $\pm\Delta_q/2$. In the dressed basis, by contrast, the Hamiltonian $H_S = \Omega_{\text{eff}}\tau_z/2$ describing the qubit in the driven cavity system is diagonal, with shifted eigenvalues $\pm\Omega_{\text{eff}}/2$.

Inverting the system of Eqs. (5.34a) to (5.34c) yields

$$\begin{cases} \sigma_x = \cos\theta\tau_x + \sin\theta\tau_z & \text{(5.35a)} \\ \sigma_y = \tau_y & \text{(5.35b)} \\ \sigma_z = -\sin\theta\tau_x + \cos\theta\tau_z. & \text{(5.35c)} \end{cases}$$

Consequently, $\sigma_\pm = (\sigma_x \pm i\sigma_y)/2$ is expressed in the dressed basis as

$$\sigma_- = \frac{\sin\theta}{2}\tau_z + \frac{\cos\theta - 1}{2}\tau_+ \frac{\cos\theta + 1}{2}\tau_-, \tag{5.36}$$

with $\tau_\pm = (\tau_x \pm i\tau_y)/2$ (note that $\tau^\dagger = \tau_-$ holds).
Hence, one obtains

$$\sigma_-(t) = e^{iH_0t}\sigma_- e^{-iH_0t} = e^{iH_0t}\left(\frac{\sin\theta}{2}\tau_z + \frac{\cos\theta - 1}{2}\tau_+ + \frac{\cos\theta + 1}{2}\tau_-\right)e^{-iH_0t} \tag{5.37}$$

with

$$H_0 = \frac{\Omega_{\text{eff}}}{2}\tau_z + \Delta_r d^\dagger d. \tag{5.38}$$

[3]The Pauli matrices admits the following matrix representation

$$\sigma_x = \begin{pmatrix} 0 & 1 \\ 1 & 0 \end{pmatrix}, \quad \sigma_y = \begin{pmatrix} 0 & -i \\ i & 0 \end{pmatrix}, \quad \sigma_z = \begin{pmatrix} 1 & 0 \\ 0 & -1 \end{pmatrix}. \tag{5.30}$$

[4]The expression of Ω_{eff} comes from the condition $\cos^2\theta + \sin^2\theta = 1$

By linearity, Eq. (5.37) gives

$$\sigma_-(t) = e^{iH_0t}\frac{\sin\theta}{2}\tau_z e^{-iH_0t} + e^{iH_0t}\frac{\cos\theta-1}{2}\tau_+ e^{-iH_0t} + e^{iH_0t}\frac{\cos\theta+1}{2}\tau_- e^{-iH_0t}, \tag{5.39}$$

which, using the fact that τ_z commutes with H_0 and the BCH formula, yields

$$\boxed{\sigma_-(t) = S_0 + e^{i\Omega_{\text{eff}}t}S_{-\Omega} + e^{-i\Omega_{\text{eff}}t}S_{+\Omega},} \tag{5.40}$$

where we introduced the time-independent operators

$$\boxed{\begin{aligned} S_0 &= \frac{\sin\theta}{2}\tau_z && (5.41)\\ S_{-\Omega} &= \frac{\cos\theta-1}{2}\tau_+ && (5.42)\\ S_{+\Omega} &= \frac{\cos\theta+1}{2}\tau_-. && (5.43)\end{aligned}}$$

The choice of notation may appear counterintuitive at first, but its motivation will become clear in the following. Finally, since $\sigma_+(t) = \sigma_-^\dagger(t)$,

$$\boxed{\sigma_+(t) = S_0 + e^{-i\Omega_{\text{eff}}t}S_{-\Omega}^\dagger + e^{+i\Omega_{\text{eff}}t}S_{+\Omega}^\dagger.} \tag{5.44}$$

Note that $S_0 = S_0^\dagger$ since $\tau_z = \tau_z^\dagger$, but $S_{\pm\Omega_{\text{eff}}} = S_{\pm\Omega_{\text{eff}}}^\dagger$.

Bath correlation function

Expanding Eq. (5.17) yields

$$\begin{aligned}\dot\rho_q(t) = &\underbrace{-\int_0^{t\to\infty}\text{Tr}_B\Big(V(t)V(t-\tau)\rho_q(t)\otimes\rho_B\Big)d\tau}_{\text{I}} \underbrace{+\int_0^{t\to\infty}\text{Tr}_B\Big(V(t)\rho_q(t)\otimes\rho_B V(t-\tau)\Big)d\tau}_{\text{II}}\\ &\underbrace{+\int_0^{t\to\infty}\text{Tr}_B\Big(V(t-\tau)\rho_q(t)\otimes\rho_B V(t)\Big)d\tau}_{\text{III}} \underbrace{-\int_0^{t\to\infty}\text{Tr}_B\Big(\rho_q(t)\otimes\rho_B V(t-\tau)V(t)\Big)d\tau}_{\text{IV}}.\end{aligned} \tag{5.45}$$

To determine the bath correlation functions needed for the computation of these integrals, the time evolution of the displaced bath operators $d(t)$ and $d^\dagger(t)$ is obtained from the AME of the isolated damped harmonic oscillator. Both the dissipator and the bath Hamiltonian are the same as in the undriven case (see Key Result 5.1), except they involve the displaced operators d and $d^\dagger$ instead of a and $a^\dagger$. Hence the AME yields exactly the same results:

$$\boxed{\begin{aligned} d(t) &= e^{-i\omega_r t-\frac{\gamma}{2}t}d && (5.46)\\ d^\dagger(t) &= e^{i\omega_r t-\frac{\gamma}{2}t}d. && (5.47)\end{aligned}}$$

Thus, the bath correlation functions are the ones of an isolated damped harmonic oscillator and take the same form as in Section 4.2. For instance, in analogy with Eq. (4.23), we have

$$\boxed{\langle d(t)d^\dagger(t-\tau)\rangle = \langle d(\tau)d^\dagger(0)\rangle = e^{\left(-i\Delta_r-\frac{\gamma}{2}\right)\tau},} \tag{5.48}$$

where the displaced resonator is assumed to be initially prepared in the state $\rho_B = |0\rangle\langle 0|$, where $|0\rangle$ denotes the vacuum state of the displaced cavity.

Secularized master equation

Having established the BCFs and time evolution of the qubit operators, term I of Eq. (5.45),

$$\int_0^{t\to\infty} \mathrm{Tr}_B\Big(V(t)V(t-\tau)\rho_q(t)\otimes\rho_B\Big)d\tau = -g^2\int_0^{t\to\infty}\langle d(t)d^\dagger(t-\tau)\rangle\sigma_+(t)\sigma_-(t-\tau)\rho_q(t)\,d\tau, \tag{5.49}$$

requires the evaluation of the product $\sigma_+(t)\sigma_-(t-\tau)$ which is computed using Eqs. (5.40) and (5.44). Applying the secular approximation, Eq. (5.49) ultimately leads to

$$-\sum_{\nu\in\{0,\pm\Omega_{\mathrm{eff}}\}}\frac{g^2}{-i\left(\Delta_r-\nu\right)-\frac{\gamma}{2}}S_\nu S_\nu^\dagger\rho_S, \tag{5.50}$$

where $S_\nu = S_{\pm\Omega}$ for $\nu = \pm\Omega_{\mathrm{eff}}$, justifying the previous choice of sign notation for $S_{\pm\Omega}$.

Proof. The computation of Eq. (5.49) requires to know the expression of $\sigma_+(t)\sigma_-(t-\tau)$. Eqs. (5.40) and (5.44) yield

$$\begin{aligned}\sigma_+(t)\sigma_-(t-\tau) &= \left(S_0+e^{i\Omega_{\mathrm{eff}}t}S_+ + e^{-i\Omega_{\mathrm{eff}}t}S_-\right)\left(S_0+e^{-i\Omega_{\mathrm{eff}}(t-\tau)}S_+^\dagger + e^{i\Omega_{\mathrm{eff}}(t-\tau)}S_-^\dagger\right) &(5.51)\\ &= S_0^2 + e^{-i\Omega_{\mathrm{eff}}(t-\tau)}S_0S_+^\dagger + e^{i\Omega_{\mathrm{eff}}(t-\tau)}S_0S_-^\dagger\\ &\quad + e^{i\Omega_{\mathrm{eff}}t}S_+S_0 + e^{i\Omega_{\mathrm{eff}}\tau}S_+S_+^\dagger + e^{2i\Omega_{\mathrm{eff}}t-i\Omega_{\mathrm{eff}}\tau}S_+S_-^\dagger\\ &\quad + e^{-i\Omega_{\mathrm{eff}}t}S_-S_0 + e^{-2i\Omega_{\mathrm{eff}}t+i\Omega_{\mathrm{eff}}\tau}S_-S_+^\dagger + S_-S_-^\dagger e^{-e^{2i\Omega_{\mathrm{eff}}\tau}}, &(5.52)\end{aligned}$$

where we used the simplified notation $S_\pm \equiv S_{\pm\Omega}$ for readability. In contradiction to the undriven case, this product still contains time-dependent terms. However, as seen in Section 1.3, the secular approximation (valid under the condition that the relaxation time of the bath τ_R is larger than the typical intrinsic timescale of the system τ_S) can be performed and considers those terms to oscillate rapidly hence averaging to zero over time. Consequently, the only surviving terms are the one highlighted in green and

$$\sigma_+(t)\sigma_-(t-\tau) \simeq S_0^2 + e^{i\Omega_{\mathrm{eff}}\tau}S_+S_+^\dagger + e^{-i\Omega_{\mathrm{eff}}\tau}S_-S_-^\dagger, \tag{5.53}$$

which injected into Eq. (5.49) and using the expression of the BCF given by Eq. (5.48) yields

$$\begin{aligned}I &= -g^2\int_0^{t\to\infty} e^{\left(-i\Delta_r-\frac{\gamma}{2}\right)\tau}\left(S_0^2 + e^{i\Omega_{\mathrm{eff}}\tau}S_+S_+^\dagger + e^{-i\Omega_{\mathrm{eff}}\tau}S_-S_-^\dagger\right)\rho_q(t)\,d\tau &(5.54)\\ &= -g^2\sum_\nu \frac{1}{-i\left(\Delta_r-\nu\right)-\frac{\gamma}{2}}S_\nu S_\nu^\dagger\rho_q(t). &(5.55)\end{aligned}$$

□

Terms II, III and IV are evaluated similarly and Eq. (5.45) becomes

$$\dot{\rho}_q(t) = \underbrace{-\sum_\nu \frac{g^2}{-i\left(\Delta_r-\nu\right)-\frac{\gamma}{2}} S_\nu S_\nu^\dagger \rho_q(t)}_{\text{I}} \underbrace{+\sum_\nu \frac{g^2}{i\left(\Delta_r-\nu\right)-\frac{\gamma}{2}} S_\nu \rho_q(t) S_\nu^\dagger}_{\text{II}} \\ \underbrace{+\sum_\nu \frac{g^2}{-i\left(\Delta_r-\nu\right)-\frac{\gamma}{2}} S_\nu \rho_q(t) S_\nu^\dagger}_{\text{III}} \underbrace{-\sum_\nu \frac{g^2}{i\left(\Delta_r-\nu\right)-\frac{\gamma}{2}} \rho_q(t) S_\nu S_\nu^\dagger}_{\text{IV}}. \tag{5.56}$$

The careful reader may observe a close resemblance to Eq. (4.27). Hence proceeding as in the previous chapter, the fractions are written with a common denominator and a detuning $\Delta_{r\nu} = \Delta_r - \nu$ is defined.
Finally, the effective master equation for the reduced density matrix of the qubit in the interaction picture reads

$$\boxed{\dot{\rho}_q(t) = -i\sum_\nu \zeta_\nu \left[S_\nu S_\nu^\dagger, \rho_q(t)\right] + \Gamma_\nu \left(S_\nu \rho_q S_\nu^\dagger - \frac{1}{2}\left\{S_\nu S_\nu^\dagger, \rho_q(t)\right\}\right)} \tag{5.57}$$

with

$$\boxed{\zeta_\nu = \frac{g^2\gamma}{\left(\frac{\gamma}{2}\right)^2 + \Delta_{r\nu}^2}} \tag{5.58}$$

and

$$\boxed{\Gamma_\nu = \frac{g^2\Delta_{r\nu}}{\left(\frac{\gamma}{2}\right)^2 + \Delta_{r\nu}^2}.} \tag{5.59}$$

Back to the initial frame

Going back to the initial frame, rotating at the drive frequency, which was the starting point of the chapter, only adds the system Hamiltonian $H_S = \Omega_{\text{eff}}\tau_z/2$ in the unitary contribution. Finally, Eq. (5.57) becomes

$$\dot{\rho}_q(t) = -i\sum_\nu \left[\frac{\Omega_{\text{eff}}}{2}\tau_z + \zeta_\nu S_\nu S_\nu^\dagger, \rho_q(t)\right] + \Gamma_\nu \left(S_\nu \rho_q S_\nu^\dagger - \frac{1}{2}\left\{S_\nu S_\nu^\dagger, \rho_q(t)\right\}\right), \tag{5.60}$$

which admits the following explicit form

Key Result 5.2. Reduced effective master equation for the qubit coupled to a driven cavity

$$\begin{aligned}\dot{\rho}_q(t) = &-i\left[\frac{\Omega_{\text{eff}}+\delta_{LS}}{2}\tau_z, \rho_q(t)\right] \\ &+ \Gamma_{+\Omega}\left(\frac{1+\cos\theta}{2}\right)^2 \mathcal{D}(\tau_-)\left[\rho_q(t)\right] \\ &+ \Gamma_{-\Omega}\left(\frac{1-\cos\theta}{2}\right)^2 \mathcal{D}(\tau_+)\left[\rho_q(t)\right] \\ &+ \Gamma_0 \frac{\sin^2\theta}{2}\mathcal{D}(\tau_z)\left[\rho_q(t)\right]\end{aligned} \tag{5.61}$$

with

$$\Omega_{\text{eff}} = \sqrt{\Delta_q^2 + (2g|\alpha|)^2} \tag{5.62}$$

$$\delta_{LS} = \zeta_{+\Omega} \left(\frac{1+\cos\theta}{2} \right)^2 - \zeta_{-\Omega} \left(\frac{1-\cos\theta}{2} \right)^2 \tag{5.63}$$

$$\zeta_{-\Omega} = \frac{g^2\gamma}{\left(\frac{\gamma}{2}\right)^2 + (\Delta_r - \Omega_{\text{eff}})^2} \tag{5.64}$$

$$\zeta_{+\Omega} = \frac{g^2\gamma}{\left(\frac{\gamma}{2}\right)^2 + (\Delta_r + \Omega_{\text{eff}})^2} \tag{5.65}$$

$$\Gamma_{+\Omega} = \frac{g^2(\Delta_r - \Omega_{\text{eff}})}{\left(\frac{\gamma}{2}\right)^2 + (\Delta_r - \Omega_{\text{eff}})^2} \tag{5.66}$$

$$\Gamma_{-\Omega} = \frac{g^2(\Delta_r + \Omega_{\text{eff}})}{\left(\frac{\gamma}{2}\right)^2 + (\Delta_r + \Omega_{\text{eff}})^2} \tag{5.67}$$

$$\Gamma_0 = \frac{g^2\Delta_r}{\left(\frac{\gamma}{2}\right)^2 + \Delta_r^2}. \tag{5.68}$$

Finally, the effective master equation for a qubit coupled to a coherently driven cavity, in the dressed basis and the frame rotating at the drive frequency, contains a unitary contribution and three distinct dissipators, each governed by its own rate and associated with a specific physical process.

The Hamiltonian contribution $\delta_{LS}\tau_z/2$ corresponds to the Lamb-Shift and is given by

$$\sum_\nu \zeta_\nu S_\nu S_\nu^\dagger = \zeta_0 S_0^2 + \zeta_+ S_+ S_+^\dagger + \zeta_- S_- S_-^\dagger, \tag{5.69}$$

where

$$\zeta_0 S_0^2 = \zeta_0 \frac{\sin^2\theta}{4}\tau_z^2 = \zeta_0 \frac{\sin^2\theta}{4}\mathbb{1} \tag{5.70}$$

constitutes an irrelevant constant to the Hamiltonian and can thus be omitted. Moreover, the last two terms are proportional to $\tau_-\tau_+$ and $\tau_+\tau_-$, respectively. Hence, using the identities $\tau_-\tau_+ = (\mathbb{1}-\tau_z)/2$ and $\tau_+\tau_- = (\mathbb{1}+\tau_z)/2$ straightforwardly leads to the expression $\delta_{LS}\tau_z/2$ with δ_{LS} given by Eq. (5.63).

The first dissipator, proportional to $\Gamma_{+\Omega}$, describes the relaxation of the dressed qubit, that is, the decay from the upper to the lower dressed state, induced by its interaction with the resonator.

The second dissipator, proportional to $\Gamma_{-\Omega}$, describes the reverse process, namely the excitation of the dressed qubit from the lower to the upper dressed state, again mediated by the resonator.

The third dissipator, proportional to Γ_0 and acting through $\mathcal{D}(\tau_z)$, is of a different nature than the previous two. Indeed, this term corresponds to pure dephasing, meaning that rather than inducing transitions between the dressed states, it solely acts on the off-diagonal elements of the density matrix, destroying the coherences of the qubit without any associated population transfer.

Theoretical Concept 5.1. Pure dephasing

Pure dephasing is a phenomenon where the populations of the qubit density matrix are left unchanged, while the coherences decay, hence pure dephasing degrades the coherences of the qubit without inducing any transition between its energy levels [11].

When $\theta = 0$, the dressed and bare bases coincide and the second and third dissipators vanish. Indeed, for $\theta = 0$, Eq. (5.31) implies $\Omega = 2g|\alpha| = 0$ thus corresponding to the absence of a drive. In this limit, one recovers the dynamics of a qubit coupled to an undriven resonator, which involves only the relaxation channel derived in Chapter 4. The vanishing of the excitation and pure dephasing channels is therefore consistent with this expectation.

The three rates $\Gamma_{+\Omega}$, $\Gamma_{-\Omega}$, and Γ_0 each take the form of a Lorentzian evaluated at a specific frequency ν

$$\Gamma_\nu = \frac{g^2 \Delta_{r\nu}}{\left(\frac{\gamma}{2}\right)^2 + \Delta_{r\nu}^2}. \tag{5.71}$$

This Lorentzian structure shows that each dissipative process is most efficient when the relevant frequency ν matches the cavity resonance Δ_r.

Note that this three-dissipator structure is reminiscent of the Mollow triplet in quantum optics [42], where a strongly driven two-level atom undergoes transitions at three distinct frequencies: the drive frequency and two frequencies symmetrically displaced.

From the perspective of dispersive readout of superconducting qubits, this result carries practical implications. The three dissipative channels and their associated rates depend on the system parameters, in particular the drive amplitude through $\Omega_{\text{eff}} = \sqrt{\Delta_q^2 + (2g|\alpha|)^2}$. This suggests that a judicious choice of parameters could allow one to selectively suppress or enhance specific dissipative processes. More broadly, the effective master equation derived here provides a solid basis for future work, in particular for identifying the parameter regimes in which the driven "qubit + resonator" system operates most favorably for high-fidelity dispersive readout.

Summary 5. Adding a coherent drive

Chapter 5 extended the model studied in Chapter 4 by including a coherent drive on the resonator, placing this work in the broader context of realistic dispersive readout of superconducting qubits. This chapter is intended as a perspective, opening directions for future developments.
Starting from the full Lindblad master equation

$$\dot{\rho} = -i[H, \rho] + \mathcal{D}(a)[\rho], \quad H = \frac{\Delta_q}{2}\sigma_z + \Delta_r a^\dagger a + g(\sigma_+ a + \sigma_- a^\dagger) + \epsilon a + \epsilon^* a^\dagger,$$

a displacement transformation was applied to restore a vacuum steady state for the resonator, enabling the use of the Born-Markov approximation.

After diagonalizing the driven qubit Hamiltonian $H_S = \Delta_q\sigma_z/2 + g(\alpha\sigma_+ + \alpha^*\sigma_-)$ through the introduction of dressed Pauli matrices $\{\tau_i\}$ and performing a secular approximation, the adiabatic elimination of the resonator yielded the following effective master equation for the qubit in the dressed basis:

$$\begin{aligned}\dot{\rho}_q(t) = &- i\left[\frac{\Omega_{\text{eff}} + \delta_{LS}}{2}\tau_z,\, \rho_q(t)\right] + \Gamma_{+\Omega}\left(\frac{1+\cos\theta}{2}\right)^2 \mathcal{D}(\tau_-)[\rho_q(t)] \\ &+ \Gamma_{-\Omega}\left(\frac{1-\cos\theta}{2}\right)^2 \mathcal{D}(\tau_+)[\rho_q(t)] + \Gamma_0\,\frac{\sin^2\theta}{2}\,\mathcal{D}(\tau_z)[\rho_q(t)],\end{aligned}$$

with

$$\Omega_{\text{eff}} = \sqrt{\Delta_q^2 + (2g|\alpha|)^2} \quad \text{and} \quad \Gamma_\nu = \frac{g^2\Delta_{r\nu}}{\left(\frac{\gamma}{2}\right)^2 + \Delta_{r\nu}^2}.$$

The three dissipators correspond to distinct physical processes: $\mathcal{D}(\tau_-)$ and $\mathcal{D}(\tau_+)$ describe relaxation and excitation of the dressed qubit mediated by the resonator, while $\mathcal{D}(\tau_z)$ induces pure dephasing.

This effective master equation constitutes a starting point for the optimization of dispersive readout protocols. In particular, it allows for the identification of parameter regimes in which specific dissipative channels can be suppressed or enhanced.

Conclusion

The aim of this master's thesis was to develop a more accurate framework for describing the reduced dynamics of a superconducting qubit during readout. More specifically, the central objective was to apply the generalized Schrieffer-Wolff method to systematically derive effective master equations beyond second order, providing an increasingly precise description of the reduced qubit dynamics.

Chapter 1 first introduced the theoretical foundations of open quantum systems, establishing the density operator formalism together with the Redfield and Lindblad master equations. The vectorization procedure was then introduced, before concluding with a discussion of the spectral properties of Liouvillians and the adjoint master equation.

Then, Chapter 2 motivated the research by presenting the physical architecture underlying dispersive readout of superconducting qubits. The transmon was introduced as an effective two-level system, and the dispersive readout architecture was presented where the qubit state is inferred by probing a coupled microwave resonator whose interaction with the qubit is described by the Jaynes-Cummings Hamiltonian. The limitations of the dispersive approximation were then highlighted, motivating the development of an approach going beyond the standard treatment.

Subsequently, Chapter 3 presented the generalized Schrieffer-Wolff formalism for dissipative systems, as originally introduced by Kessler [7]. The method consists in a systematic perturbative expansion of the Liouvillian, obtained by applying a similarity transformation that renders it block-diagonal, thereby decoupling the slow and fast subspaces and allowing for the definition of an effective Liouvillian governing the slow dynamics, whose second-order expansion reproduces the result of adiabatic elimination.

Building on this, Chapter 4 constitutes the original contribution of this thesis. The generalized Schrieffer-Wolff formalism was applied to a qubit coupled to a damped resonator within the single-excitation subspace. After identifying a rotating frame that yields a proper $\mathcal{L}_0 + \mathcal{V}$ separation, the second-order effective Liouvillian was shown to exactly reproduce the adiabatic elimination result, independently derived as a Redfield master equation at the beginning of the chapter. Higher-order corrections were then computed numerically and assessed through fidelity comparisons against the exact dynamics, confirming that each additional order systematically improves the accuracy of the reduced description. Finally, the validity conditions of the expansion were refined beyond those originally proposed by Kessler [7].

Lastly, Chapter 5 opened a first perspective toward a more realistic readout model by extending the framework to include a coherent drive on the resonator. Through a displacement transformation restoring a vacuum steady state, followed by a dressed-basis diagonalization and a secular approximation, an effective master equation for the driven qubit was derived, providing a starting point for the optimization of dispersive readout by determining favorable parameter regimes.

A logical first perspective of this work would be to compare the master equation derived in Chapter 5 to high-order reduced qubit descriptions obtained via the generalized Schrieffer-Wolff method, in the same spirit as the comparison made in Chapter 4. More broadly, the systematic nature of the Schrieffer-Wolff expansion makes it well-suited for more complex architectures, and natural directions include additional dissipative mechanisms acting directly on the qubit or adding multiple harmonic oscillators to model Purcell filters in order to bring the theoretical framework closer to current experimental implementations, where achieving fast, high-fidelity quantum non-demolition readout remains one of the central challenges of superconducting quantum computing. In this context, another interesting direction would be to derive quantum trajectory approaches based on the unraveling of high-order Schrieffer-Wolff qubit reduced descriptions. This would provide a bridge between effective master-equation descriptions and single-run measurement records, and could help clarify how higher-order corrections affect measurement back-action and information extraction.

Bibliography

[1] R. Au-Yeung, B. Camino, O. Rathore, and V. Kendon, "Quantum algorithms for scientific computing," *Reports on Progress in Physics*, vol. 87, no. 11, p. 116 001, Oct. 2024. DOI: 10.1088/1361-6633/ad85f0.

[2] Y.-Y. Jiang et al., "Advancements in superconducting quantum computing," *National Science Review*, vol. 12, no. 8, Aug. 1, 2025. DOI: 10.1093/nsr/nwaf246.

[3] A. Blais, A. L. Grimsmo, S. M. Girvin, and A. Wallraff, "Circuit Quantum Electrodynamics," *Reviews of Modern Physics*, vol. 93, no. 2, p. 025 005, May 19, 2021. DOI: 10.1103/RevModPhys.93.025005.

[4] P. Krantz, M. Kjaergaard, F. Yan, T. P. Orlando, S. Gustavsson, and W. D. Oliver, "A quantum engineer's guide to superconducting qubits," *Applied Physics Reviews*, vol. 6, no. 2, p. 021 318, Jun. 2019. DOI: 10.1063/1.5089550.

[5] E. A. Sete, J. M. Gambetta, and A. N. Korotkov, "Purcell effect with microwave drive: Suppression of qubit relaxation rate," *Physical Review B*, vol. 89, no. 10, p. 104 516, Mar. 21, 2014. DOI: 10.1103/PhysRevB.89.104516.

[6] R. Palacino and J. Keeling, "Atom-only theories for u(1) symmetric cavity-qed models," *Phys. Rev. Res.*, vol. 3, p. L032016, 3 Jul. 2021. DOI: 10.1103/PhysRevResearch.3.L032016.

[7] E. M. Kessler, "Generalized Schrieffer-Wolff formalism for dissipative systems," *Physical Review A: Atomic, Molecular, and Optical Physics*, vol. 86, no. 1, p. 012 126, Jul. 2012. DOI: 10.1103/PhysRevA.86.012126.

[8] M. A. Nielsen and I. L. Chuang, *Quantum Computation and Quantum Information*. Cambridge University Press, 2000.

[9] M. Le Bellac, *Physique quantique*. Les Ulis, Paris: EDP Sciences ; CNRS Editions, 2003, ISBN: 978-2-86883-655-7.

[10] J. J. Sakurai and J. Napolitano, *Modern Quantum Mechanics*, 3rd ed. Cambridge University Press, Sep. 17, 2020, ISBN: 978-1-108-58728-0 978-1-108-47322-4. DOI: 10.1017/9781108587280.

[11] H.-P. Breuer and F. Petruccione, *The Theory of Open Quantum Systems*. Oxford ; New York: Oxford University Press, 2002, 625 pp., ISBN: 978-0-19-852063-4.

[12] A. G. Redfield, "On the Theory of Relaxation Processes," *IBM Journal of Research and Development*, vol. 1, no. 1, pp. 19–31, Jan. 1957. DOI: 10.1147/rd.11.0019.

[13] F. Damanet, *Dynamique quantique dissipative et application à la superradiance, Travail de fin d'études présenté dans le cadre de l'obtention du grade de Maître en sciences physiques*. Université de Liège, 2012.

[14] G. Lindblad, "On the generators of quantum dynamical semigroups," *Communications in Mathematical Physics*, vol. 48, no. 2, pp. 119–130, Jun. 1976. DOI: 10.1007/BF01608499.

[15] V. Gorini, A. Kossakowski, and E. C. G. Sudarshan, "Completely positive dynamical semigroups of N-level systems," *Journal of Mathematical Physics*, vol. 17, no. 5, pp. 821–825, May 1, 1976. DOI: 10.1063/1.522979.

[16] T. C. Ralph, "Howard Wiseman and Gerard Milburn: Quantum measurement and control," *Quantum Information Processing*, vol. 11, no. 1, pp. 313–315, Feb. 1, 2012. DOI: 10.1007/s11128-011-0277-3.

[17] J. A. Gyamfi, "Fundamentals of Quantum Mechanics in Liouville Space," *European Journal of Physics*, vol. 41, no. 6, p. 063 002, Nov. 1, 2020. DOI: 10.1088/1361-6404/ab9fdd.

[18] V. Jagadish and F. Petruccione, "An Invitation to Quantum Channels," *Quanta*, vol. 7, pp. 54–67, Jul. 26, 2018. DOI: 10.12743/quanta.v7i1.77.

[19] M.-D. Choi, "Completely positive linear maps on complex matrices," *Linear Algebra and its Applications*, vol. 10, no. 3, pp. 285–290, Jun. 1, 1975. DOI: 10.1016/0024-3795(75)90075-0.

[20] A. Jamiołkowski, "Linear transformations which preserve trace and positive semidefiniteness of operators," *Reports on Mathematical Physics*, vol. 3, no. 4, pp. 275–278, Dec. 1, 1972. DOI: 10.1016/0034-4877(72)90011-0.

[21] F. W. Byron Jr. and R. W. Fuller, *Mathematics of Classical and Quantum Physics* (Addison-Wesley Series in Advanced Physics), 2 vols. Reading, MA: Addison-Wesley, 1969.

[22] R. R. Puri, *Mathematical Methods of Quantum Optics* (Springer Series in Optical Sciences), W. T. Rhodes, red. Berlin, Heidelberg: Springer Berlin Heidelberg, 2001, vol. 79, ISBN: 978-3-642-08732-5 978-3-540-44953-9.

[23] R. A. Horn and C. R. Johnson, *Matrix Analysis*. Cambridge: Cambridge University Press, 1985. DOI: 10.1017/CBO9780511810817.

[24] À. Rivas and S. F. Huelga, *Open Quantum Systems: An Introduction* (SpringerBriefs in Physics). Berlin, Heidelberg: Springer Berlin Heidelberg, 2012, ISBN: 978-3-642-23353-1 978-3-642-23354-8. DOI: 10.1007/978-3-642-23354-8.

[25] N. Shibata and H. Katsura, "Quantum Ising chain with boundary dephasing," *Progress of Theoretical and Experimental Physics*, vol. 2020, no. 12, 12A108, Dec. 15, 2020. DOI: 10.1093/ptep/ptaa131.

[26] A. Machado Lacerda, "Quantum Thermodynamics with Nonequilibrium Steady States," Ph.D. dissertation, School of Physics, Physics, Trinity College Dublin, 2026.

[27] H. Ibach and H. Lüth, *Solid-State Physics: An Introduction to Principles of Materials Science*. Berlin, Heidelberg: Springer Berlin Heidelberg, 2009, ISBN: 978-3-540-93803-3 978-3-540-93804-0. DOI: 10.1007/978-3-540-93804-0.

[28] J. Koch et al., "Charge-insensitive qubit design derived from the Cooper pair box," *Physical Review A*, vol. 76, no. 4, p. 042 319, Oct. 12, 2007. DOI: 10.1103/PhysRevA.76.042319.

[29] C. Cohen-Tannoudji, B. Diu, F. Laloë, and S. R. Hemley, *Quantum mechanics* (A Wiley-Interscience publication). New York, NY: Wiley, 1977, ; ISBN: 9780471569527.

[30] C. Kittel, *Introduction to Solid State Physics*, 8th ed. Hoboken, NJ: John Wiley & Sons, 2004, ISBN: 978-0-471-41526-8.

[31] Z. Minev. "Introduction to Quantum Computing and Quantum Hardware," YouTube.

[32] G. S. Agarwal, *Quantum Optics*. Cambridge University Press, 2012.

[33] M. Scala, "Microscopic derivation of the Jaynes-Cummings model with cavity losses," *Physical Review A*, vol. 75, no. 1, 2007. DOI: 10.1103/PhysRevA.75.013811.

[34] S. M. Girvin, "Circuit QED: Superconducting qubits coupled to microwave photons," in *Quantum Machines: Measurement and Control of Engineered Quantum Systems*, M. Devoret, B. Huard, R. Schoelkopf, and L. F. Cugliandolo, Eds., 1st ed., Oxford University PressOxford, Jun. 12, 2014, pp. 113–256, ISBN: 978-0-19-968118-1 978-0-19-176145-4. DOI: 10.1093/acprof:oso/9780199681181.003.0003.

[35] B. C. Hall, *Lie Groups, Lie Algebras, and Representations: An Elementary Introduction* (Graduate Texts in Mathematics). Cham: Springer International Publishing, 2015, vol. 222.

[36] S. Bravyi, D. DiVincenzo, and D. Loss, "Schrieffer-Wolff transformation for quantum many-body systems," *Annals of Physics*, vol. 326, no. 10, pp. 2793–2826, Oct. 2011. DOI: 10.1016/j.aop.2011.06.004.

[37] M. Tokieda and A. Riva, "Time-convolutionless master equation applied to adiabatic elimination," *Physical Review A*, vol. 111, no. 5, p. 052 206, May 8, 2025. DOI: 10.1103/PhysRevA.111.052206.

[38] F. Damanet, "Cooperative spontaneous emission with quantized atomic motion," Ph.D. dissertation, Université de Liège, Liège, Belgium, 2017.

[39] R. Loudon, *The Quantum Theory of Light*. Oxford University Press, 2010.

[40] C. Gerry and P. Knight, *Introductory Quantum Optics*. Cambridge University Press, 2004.

[41] Q. Xie, H. Zhong, M. T. Batchelor, and C. Lee, "The quantum Rabi model: Solution and dynamics," *Journal of Physics A: Mathematical and Theoretical*, vol. 50, no. 11, p. 113 001, Feb. 2017. DOI: 10.1088/1751-8121/aa5a65.

[42] L. Mandel and E. Wolf, *Optical Coherence and Quantum Optics*. Cambridge, UK: Cambridge University Press, 1995, ISBN: 978-0521417112.